The Trend of Wind Speed over the United States during 1998 – 2011

MASSACHUSETTS INSTITUTE OF TECHNOLOGY
SEP 26 2017
LIBRARIES
ARCHIVES

by

Tao Feng

B.S. Environmental Science, Peking University (2015)

B.S. Economics (dual degree), Peking University (2015)

Submitted to the Department of Earth, Atmospheric, and Planetary Science

in partial fulfillment of the requirements for the degree of

Master of Science in Atmospheric Science

at the

MASSACHUSETTS INSTITUTE OF TECHNOLOGY

September 2017

© Massachusetts Institute of Technology 2017. All rights reserved.

Author ..... Signature redacted .....

Department of Earth, Atmospheric, and Planetary Science
August 31, 2017

Certified by..... Signature redacted .....

Paul A. O'Gorman
Associate Professor of Atmospheric Science
Thesis Supervisor

Signature redacted

Accepted by..... .....

Robert D. van der Hilst
Schlumberger Professor of Earth and Planetary Sciences
Head, Department of Earth, Atmospheric, and Planetary Science

The Trend of Wind Speed over the United States during 1998 – 2011

by

Tao Feng

Submitted to the Department of Earth, Atmospheric, and Planetary Science
on August 31, 2017, in partial fulfillment of the
requirements for the degree of
Master of Science in Atmospheric Science

Abstract

Through the analysis of the high-resolution radiosonde measurements over the U.S., we identified a decreasing trend near the surface and an increasing trend at the upper levels, which is consistent with previous studies. The decreasing trend of near-surface wind speed is statistically significant ($p<0.01$). However, the statistical significance of the decreasing trend drops with increases in altitude. We identified a largest negative trend in wind speed close to the surface. The magnitude of this largest negative trend is up to 15 times of the values reported in the previous studies. This might be due to the higher resolution in the vertical than data used in the previous studies, but it could also be a short-term phenomenon due to the shorter record considered as compared with the previous work. We also found a relationship between the elevation of the sites and the trend of near-surface wind and wind aloft. We identified a statistically negative relation between the magnitude of the decreasing trend and the elevation of the stations. The height of the planetary boundary layer (PBL) is estimated using three different methods. For non-elevated sites, a decreasing trend is seldom found for wind above the PBL, suggesting an important role for the land surface in determining the trend of wind speed. For elevated sites such as those in the mountainous west of the US, a decreasing trend is found for both the near-surface wind and the wind aloft, indicating that the changes in free-tropospheric circulation may also exert influence on changes in surface wind speeds for these sites.

Thesis Supervisor: Paul A. O'Gorman
Title: Associate Professor of Atmospheric Science

Acknowledgments

I would like to thank my thesis advisor Professor Paul O'Gorman, for his guidance, patience and support. Whenever I have a question, Paul is always there to help me. I have learned a great deal from him through discussion and in the classroom.

I would like to thank Professor Susan Solomon for drawing my attention to the fascinating topic of stilling of the winds and introducing me the U.S. high resolution radiosonde dataset without which this study would not be possible.

I am also grateful to my academic adviser Professor Noelle Selin. Without her help and support, my study at MIT may not be possible.

I am particularly lucky to have a great family. It is the unconditional love of my family members that enables me to overcome the difficulties. I always feel encouraged whenever I think of my Mom, for her courage and perseverance.

Contents

Acknowledgments 5

Table of Contents 6

1 Introduction **19**

2 Data and Methods **25**

2.1 Radiosonde Data 25

2.2 Methods of Trend Calculation 26

2.2.1 Interpolation and vertical coordinates 26

2.2.2 Calculation of the trend in wind speed 28

2.3 Methods of PBL Height Calculation 33

3 Results and Discussion **36**

3.1 Vertical Profile of Wind Speed Trend 36

3.2 The Relation between the Level of Largest Negative Trend and the PBL Top . . . 42

3.3 Vertical profile of Trends in Wind Speed over Different Time Zones 44

3.4 Spatial Distribution of Wind Speed Trend 52

3.5 The Influence of the Measuring Frequency on the Trends 59

4 Conclusions and Future Work **67**

Appendix **70**

A1 Distributions of the 6-Second Data and the 1-Second Data 70

A2 Ratio between the Annual Mean to the Corresponding Standard Deviation 71

A3 Spatial Distribution of the Trends in Wind Speed 73

A4 Spatial Distribution of the Trend Index 76

Bibliography 81

List of Figures

1-1 Measured daily $PM_{2.5}$ concentration ($\mu g/m^3$) and wind speed (m/s) at 15m bove the ground. No measurements of $PM_{2.5}$ were taken during 03/07/2014-03/06/2014. Red dashed circle marked the inverse relation between $PM_{2.5}$ concentration and wind speed. Data is obtained from College of Environmental Sciences and Engineering, Peking University. Refer to Wu et al., (2007) for detailed information about the station where the measurements were taken..... 21

1-2 Vertical profile of mean wind speed trend in Vautard et al. (2010). The right-hand panel shows the normalized wind speed trend in the unit of 'per decade'. The normalized trend equals absolute trend (m/s per decade) divided by the grand mean of wind speed (m/s) at the corresponding pressure level. Reprinted by permission from Macmillan Publishers Ltd: [Nature Geoscience] (Vautard et al., 2010), copyright (2010) 22

2-1 U.S. high resolution radiosonde measurements stations: red color denotes the stations belonging to U.S., blue color denotes the stations belonging to other countries, dot denotes the stations included in this study, square denotes the stations excluded from this study; blue rectangle indicates the same geographical range of North America used in Vautard et al., (2010) 26

2-2 Illustration of two soundings launched at different time at the same station. Black solid line denotes the land surface of the station. Black dashed denotes the level which the radiosonde measures. The number in red shows the altitude of the levels that the radiosonde measures. The blue solid line denotes the level to be interpolated from the measurements 27

2-3 The elevation of the 94 stations included in the high resolution radionsode dataset. The color of the dots represents the elevation with darker color indicating higher elevation 28

2-4 Illustration of comparisons between the original sounding and the interpolated sounding. The measurements were taken at 0 UTC on 1998/01/01 at Santa Teresa, NM (site # 03020). The original sounding is shown in blue and the interpolated sounding is shown in green. The right-hand panel shows the results using A.G.L. coordinate. The interpolation range is 0m-15000m. The left-hand panel shows the results using pressure coordinate. The interpolation range is 1000hPa – 100hPa. Note that sounding in the left-hand panel starts above 1000hPa indicating that this station is elevated 29

2-5 Calculation of the trend in wind speed of 100hPa constant pressure surface at Santa Teresa, NM and (a) 90% confidence interval of the trend, (b) 95% confidence interval of the trend, and (c) 99% confidence interval of the trend. The bands indicate the confidence intervals. 'ws' is short for 'wind speed', 'Ucmp' is short for *U* component (i.e. zonal component) of wind speed, and 'Vcmp' is short for *V* component (i.e. meridional component) of wind speed 31

2-6 Vertical profile of trends in wind speed with pressure vertical coordinate for Station Elko, NV. The upper panel (a) shows the (absolute) trends (m/s per decade) in wind speed (ws), zonal wind (Ucmp), and meridional wind (Vcmp) calculated based the 7-year criterion. The lower panel (b) shows the same trends calculated based on the 10-year criterion. The dashed green circles mark the difference between the two types of trends 31

2-7 Vertical profile of the 95% confidence interval (CI) of trends in wind speed with pressure vertical coordinate for Station Elko, NV. The panel (a) shows CI of the (absolute) trends (m/s per decade) in wind speed (ws), zonal wind (Ucmp), and meridional wind (Vcmp) calculated based the 7-year criterion. The lower panel (b) shows the same things calculated based on the 10-year criterion. The dashed green circles mark the difference between the two types of trends 32

3-1 Vertical profile of trends in wind speed with pressure vertical coordinate. The upper panel (a) shows the (absolute) trends (m/s per decade) in wind speed (ws), zonal wind (Ucmp), and meridional wind (Vcmp). The lower panel (b) shows the corresponding normalized trends (per decade) 38

3-2 Vertical profile of trends in wind speed with A.G.L. vertical coordinate. The upper panel (a) shows the (absolute) trends (m/s per decade) in wind speed (ws), zonal wind (Ucmp), and meridional wind (Vcmp). The lower panel (b) shows the corresponding normalized trends (per decade) 38

3-3 Lower part (0m-1000m) of the vertical profile of trends in wind speed with A.G.L. vertical coordinate. The upper panel (a) shows the (absolute) trends (m/s per decade) in wind speed (ws), zonal wind (Ucmp), and meridional wind (Vcmp). The lower panel (b) shows the corresponding normalized trends (per decade) 39

3-4 Vertical profile of 95% confidence interval (CI) of the normalized trends in wind speed with A.G.L. vertical coordinate. The upper panel (a) shows the 95% CI of the normalized trends (per decade) in wind speed (ws), zonal wind (Ucmp), and meridional wind (Vcmp) at 0 UTC. The lower panel (b) shows the normalized trends (per decade) at 12 UTC 39

3-5 Vertical profile of trends in wind speed calculated based on the median, with pressure vertical coordinate. The upper panel (a) shows the (absolute) trends (m/s per decade) in wind speed (ws), zonal wind (Ucmp), and meridional wind (Vcmp). The lower panel (b) shows the corresponding normalized trends (per decade) 40

3-6 Vertical profile of trends in wind speed calculated based on the median, with A.G.L. vertical coordinate. The upper panel (a) shows the (absolute) trends (m/s per decade) in wind speed (ws), zonal wind (Ucmp), and meridional wind (Vcmp). The lower panel (b) shows the corresponding normalized trends (per decade) 40

3-7 Lower part (0m–1000m) of the vertical profile of trends in wind speed calculated based on the median, with A.G.L. vertical coordinate. The upper panel (a) shows the (absolute) trends (m/s per decade) in wind speed (ws), zonal wind (Ucmp), and meridional wind (Vcmp). The lower panel (b) shows the corresponding normalized trends (per decade) 41

3-8 Lower part of the vertical profile of trends in wind speed (calculated based on the mean), with A.G.L. vertical coordinate and its relation to the PBL height. The panel (a) shows the (absolute) trends (m/s per decade) in wind speed (ws), zonal wind (Ucmp), and meridional wind (Vcmp) and its relation to the PBL (at 12 UTC) calculated using the bulk Richardson number method. The panel (b) shows the same trends and its relation to the PBL (at 12 UTC) calculated using the air parcel method. The panel (c) shows the same trends and its relation to the PBL (at both 0 and 12 UTC) calculated using the elevated inversion method. The dashed line indicates the 95% confidence interval of the PBL estimates 43

3-9 65 stations over the contiguous U.S.. The color of the dots represents the elevation with darker color indicating higher elevation 44

3-10 Vertical profile of trends in wind speed calculated based on the median, with A.G.L. vertical coordinate for stations located within 80°W-70°W (9 stations). The upper panel (a) shows the (absolute) trends (m/s per decade) in wind speed (ws), zonal wind (Ucmp), and meridional wind (Vcmp). The lower panel (b) shows the corresponding normalized trends (per decade) 45

3-11 Vertical profile of trends in wind speed calculated based on the median, with A.G.L. vertical coordinate for stations located within 90°W-80°W (15 stations). The upper panel (a) shows the (absolute) trends (m/s per decade) in wind speed (ws), zonal wind (Ucmp), and meridional wind (Vcmp). The lower panel (b) shows the corresponding normalized trends (per decade) 46

3-12 Vertical profile of trends in wind speed calculated based on the median, with A.G.L. vertical coordinate for stations located within 100°W-90°W (14 stations). Panel (a) shows the (absolute) trends (m/s per decade) in wind speed (ws), zonal

wind (Ucmp), and meridional wind (Vcmp). Panel (b) shows the corresponding normalized trends (per decade) 46

3-13 Vertical profile of trends in wind speed calculated based on the median, with A.G.L. vertical coordinate for stations located within 110°W-100°W (13 stations). Panel (a) shows the (absolute) trends (m/s per decade) in wind speed (ws), zonal wind (Ucmp), and meridional wind (Vcmp). Panel (b) shows the corresponding normalized trends (per decade) 47

3-14 Vertical profile of trends in wind speed calculated based on the median, with A.G.L. vertical coordinate for stations located within 120°W-110°W (10 stations). Panel (a) shows the (absolute) trends (m/s per decade) in wind speed (ws), zonal wind (Ucmp), and meridional wind (Vcmp). Panel (b) shows the corresponding normalized trends (per decade) 47

3-15 Vertical profile of trends in wind speed calculated based on the median, with A.G.L. vertical coordinate for stations located within 130°W-120°W (4 stations). Panel (a) shows the (absolute) trends (m/s per decade) in wind speed (ws), zonal wind (Ucmp), and meridional wind (Vcmp). Panel (b) shows the corresponding normalized trends (per decade) 48

3-16 Lower part (0m-1000m) of the profile shown in **Figure 3-10**, 80°W-70°W. Panel (a) shows the (absolute) trends (m/s per decade) in wind speed (ws), zonal wind (Ucmp), and meridional wind (Vcmp). Panel (b) shows the corresponding normalized trends (per decade) 48

3-17 Lower part (0m-1000m) of the profile shown in **Figure 3-11**, 90°W-80°W. Panel (a) shows the (absolute) trends (m/s per decade) in wind speed (ws), zonal wind (Ucmp), and meridional wind (Vcmp). Panel (b) shows the corresponding normalized trends (per decade) 49

3-18 Lower part (0m-1000m) of the profile shown in **Figure 3-12**, 100°W-90°W. Panel (a) shows the (absolute) trends (m/s per decade) in wind speed (ws), zonal wind (Ucmp), and meridional wind (Vcmp). Panel (b) shows the corresponding normalized trends (per decade) 49

3-19 Lower part (0m-1000m) of the profile shown in **Figure 3-13**, 110°W-100°W. Panel (a) shows the (absolute) trends (m/s per decade) in wind speed (ws), zonal wind (Ucmp), and meridional wind (Vcmp). Panel (b) shows the corresponding normalized trends (per decade) 50

3-20 Lower part (0m-1000m) of the profile shown in **Figure 3-14**, 120°W-110°W. Panel (a) shows the (absolute) trends (m/s per decade) in wind speed (ws), zonal wind (Ucmp), and meridional wind (Vcmp). Panel (b) shows the corresponding normalized trends (per decade) 50

3-21 Lower part (0m-1000m) of the profile shown in **Figure 3-15**, 130°W-120°W. Panel (a) shows the (absolute) trends (m/s per decade) in wind speed (ws), zonal wind (Ucmp), and meridional wind (Vcmp). Panel (b) shows the corresponding normalized trends (per decade) 51

3-22 Spatial distribution of the trend in wind speed (m/s per decade) at 0 UTC averaged vertically over (a) 200m, (b) 500m, (c) 900m, and (d) 1500m above the surface of each station 55

3-23 Relations between the trends in the wind speed (m/s per decade) averaged vertically over (a) 200m, (b) 500m, (c) 900m, and (d) 1500m above the surface of each station and the elevation of the stations 56

3-24 Spatial distribution of the trend in wind speed (m/s per decade) at 0 UTC at (a) 4800m A.G.L., (b) 6000m A.G.L., (c) 700hPa constant pressure surface, and (d) 500hPa constant pressure surface. The square denotes the stations with statistically significant (p<0.05) decreasing trend at the corresponding level 58

3-25 37 stations whose measuring frequency does not change. The color of the dots represents the elevation with darker color indicating higher elevation. Stations in the blue rectangle are included in the calculation of trends 59

3-26 For 26 stations whose measuring frequency does not change. Vertical profile of trends in wind speed with A.G.L. vertical coordinate. The upper panel (a) shows the (absolute) trends (m/s per decade) in wind speed (ws), zonal wind

(Ucmp), and meridional wind (Vcmp). The lower panel (b) shows the corresponding normalized trends (per decade) 60

3-27 For 26 stations whose measuring frequency does not change. Lower part (0m-1000m) of the vertical profile of trends in wind speed with A.G.L. vertical coordinate. Panel (a) shows the (absolute) trends (m/s per decade) in wind speed (ws), zonal wind (Ucmp), and meridional wind (Vcmp). Panel (b) shows the corresponding normalized trends (per decade) 61

3-28 52 stations whose measuring frequency changes. The color of the dots represents the elevation with darker color indicating higher elevation. Stations in the blue rectangle are included in the calculation of trends 61

3-29 For 52 stations whose measuring frequency changes. Vertical profile of trends in wind speed with A.G.L. vertical coordinate. The upper panel (a) shows the (absolute) trends (m/s per decade) in wind speed (ws), zonal wind (Ucmp), and meridional wind (Vcmp). The lower panel (b) shows the corresponding normalized trends (per decade) 62

3-30 For 52 stations whose measuring frequency changes. Lower part (0m-1000m) vertical profile of trends in wind speed with A.G.L. vertical coordinate. Panel (a) shows the (absolute) trends (m/s per decade) in wind speed (ws), zonal wind (Ucmp), and meridional wind (Vcmp). Panel (b) shows the corresponding normalized trends (per decade) 63

3-31 Stations out of the 52 stations described above with elevation lower than **200m**. Lower part (0m-1000m) vertical profile of trends in wind speed with A.G.L. vertical coordinate. Panel (a) shows the (absolute) trends (m/s per decade) in wind speed (ws), zonal wind (Ucmp), and meridional wind (Vcmp). Panel (b) shows the corresponding normalized trends (per decade) 63

3-32 Stations among the 52 stations described above with elevation higher than **1000m**. Lower part (0m-1000m) vertical profile of trends in wind speed with A.G.L. vertical coordinate. Panel (a) shows the (absolute) trends (m/s per decade)

in wind speed (ws), zonal wind (Ucmp), and meridional wind (Vcmp). Panel (b) shows the corresponding normalized trends (per decade) 64

3-33 Stations among the 52 stations described above with elevation lower than **1000m** but higher than 200m. Lower part (0m-1000m) vertical profile of trends in wind speed with A.G.L. vertical coordinate. Panel (a) shows the (absolute) trends (m/s per decade). Panel (b) shows the normalized trends (per decade) 64

3-34 For the 52 stations described above, but utilize the 6-second data available at these stations Lower part (0m-1000m) vertical profile of trends in wind speed with A.G.L. vertical coordinate. Panel (a) shows the (absolute) trends (m/s per decade). Panel (b) shows the normalized trends (per decade) 65

A1 Station Elko, NV. Distribution wind speed data at the selected pressure level. rrs = 0 denotes the distribution of the 6-second data, and rrs = 1 denotes the distribution of the 1-second data. The pressure on the left panel is 100hPa, 300hPa, and 500hPa, and that on the right is 700hPa, 850hPa and 1000hPa 70

A2 Station Elko, NV. Ratio between annual mean to the corresponding standard deviation of the wind speed data at the selected pressure level. rrs = 0 denotes the ratio corresponding to the 6-second data, and rrs = 1 denotes the ratio corresponding to the 1-second data. The pressure levels are (a) 100hPa, 300 hPa, and 500 hPa; and (b) 700 hPa, 850 hPa and 1000 hPa. 72

A3 Spatial distribution of the trend in wind speed (m/s per decade) at 12 UTC averaged vertically over (a) 200m, (b) 500m, (c) 900m, and (d) 1500m above the surface of each station 75

A4-1 Trend index at 00:00 UTC 78

A4-2 Relations between the trend index and the elevation of stations (the band of the fitted curve represents the 95% confidence interval of the slope) 79

A4-3 Trend index for layers below PBL and layers above PBL 80

List of Tables

3-1 Number of stations and local time at 0 UTC/12 UTC in the 6 time zones 44

3-2 Magnitudes of the trends in wind speed at the surface and the largest negative trend of each time zone. 'Absolute trend' refers to the values retrieved from Panel (a) from Figure 3-16 to Figure 3-21. 'Normalized trend' refers to the values retrieved from Panel (b) from Figure 3-16 to Figure 3-21 51

Chapter 1

Introduction

Wind stilling refers to the decreasing trend found for surface wind speed. The decline of surface wind is observed in many regions of the world and is a potential concern for various fields.

Indeed, near-surface wind speed are of great importance indicating possible impacts of global climate change (Pryor et al., 2009). The decline of surface wind has been shown to be the main cause for the decreasing pan evaporation, which has a strong impact on global hydrological cycle (McVicar et al., 2012; Roderick et al., 2007). In China, a significant inverse relationship (see **Figure 1-1**) is observed between the level of particulate matter pollution and surface wind speed, that the sharp decrease in $PM_{2.5}$ concentration is accompanied with an almost simultaneous strong increase in the surface wind speed, indicating the importance of strong wind for the diffusion of high level particulate pollutants in the city of Beijing. Similar results suggesting the influence of wind stilling on the formation of particulate matter pollution in Beijing and eastern part of China are reported by Guo et al., (2014) and Liang et al., (2015).

Stilling surface winds have been found in China (Xu et al., 2006), Netherlands (Smits et al., 2005), Australia (McVicar et al., 2008), and the contiguous United States (Pryor et al., 2009). Over China, wind decline was attributed to north-south warming gradient in winter, and to sunlight dimming caused by air pollution in summer (Xu et al., 2006). Vautard et al. (2010) reported that between 1979 and 2008 surface wind speeds have declined by 5-15% over almost all continental areas in the northern hemisphere mid-latitudes, based on observational records

of 822 sites in the study regions. McVicar et al. (2012) performed a meta-analysis over the 148 regional terrestrial (based on observational records) studies by calculating the mean trend for surface wind speed. They found that the average trend was -0.014m s^{-1} a^{-1} for studies with more than 30 sites observing data for more than 30 years. Moreover, McVicar et al. (2012) suggested that declines in surface wind speed are geographically widespread, with declines being reported in the tropics and mid-latitudes of both hemispheres, and increases reported at high-latitudes (latitude greater than ~ 70°).

The stilling surface winds can be due to (1) changes in mean circulation and/or to the decrease of synoptic weather system intensity, both of which are a consequence of climate change, (2) changes in near-surface wind due to increasing surface roughness in the near field of each station, (3) instrumental drifts or measurements artefacts. [10] Among them, (3) is not likely. This is because independent pan evaporation trends have been modeled using forcing meteorological (including surface wind speed) data in both northern and southern hemisphere. The modeled pan evaporation rate trends were in general agreement with observed pan evaporation rate trends, and in several studies the pan evaporation rate reductions have been primarily attributed to declining surface wind speed. [2] This general agreement between observations and model outputs of pan evaporation suggests that even if there are measurements artefacts in wind speed data, they are not likely to lead significant biases in the wind speed trend.

Vautard et al. (2010) attributed the decline in surface wind to the increase of surface roughness. It is estimated that surface roughness increase could explain 25-60% of the stilling. Here, the magnitude of changes in surface roughness is estimated from increases in biomass and land-use change in Eurasia. This conclusion is drawn from the comparison between the surface wind speed and upper-level wind speed (850hPa and above) measured by radiosonde. They found that the trend of wind speed is negative near the surface for all of the four study regions (Europe, Central Asia, East Asia and North America), whereas the trend turns to positive aloft. For altitude above 500hPa, the trend of wind speed is positive for all study regions (see **Figure 1-2**), indicating that the upper-level wind is increasing instead of decreasing between 1979 and 2008. Moreover, the decreasing trend of surface wind is not fully captured by reanalysis products. National Center for Environmental Prediction/National Center

of Atmospheric Research (NCEP/NCAR) reanalysis does not exhibit any trend in surface (10m) winds over land (Vautard et la., 2010). European Center for Medium-range Weather Forecast (ECMWF) ERA-interim reanalysis only partially capture the decreasing trend geographically. The potential explanation for this is that reanalyses do not take land use changes into account, therefore, this discrepancies between observations and reanalysis supports the argument of Vautard et al. (2010).

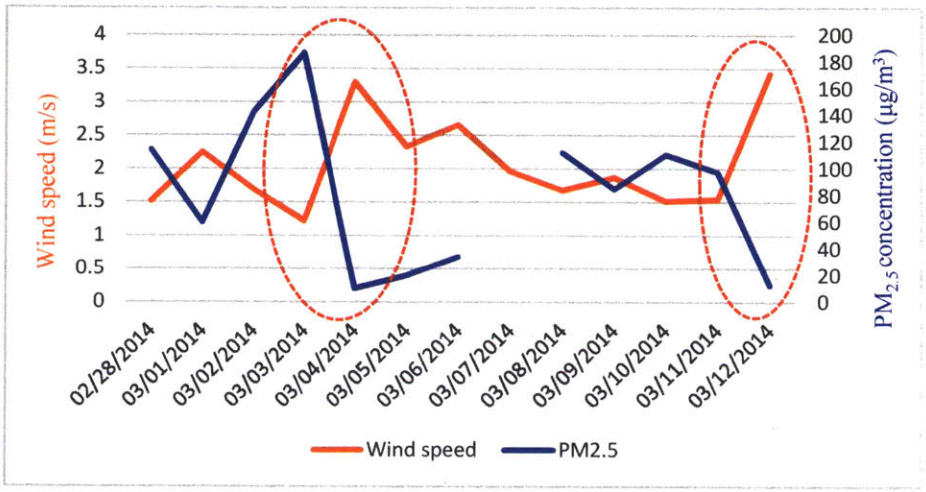

Figure 1-1: Measured daily $PM_{2.5}$ concentration ($\mu g/m^3$) and wind speed (m/s) at 15m above the ground. No measurements of $PM_{2.5}$ were taken during 03/07/2014-03/06/2014. Red dashed circle marked the inverse relation between $PM_{2.5}$ concentration and wind speed. Data is obtained from College of Environmental Sciences and Engineering, Peking University. Refer to Wu et al., (2007) for detailed information about the station where the measurements were taken.

There are some additional evidence that makes the argument of Vautard et al. (2010) more plausible. Surface wind speed over the ocean has been reported to have an increasing trend by several studies using the *in situ* observational systems (Flohn and Kapala, 1989; Cardone, Greenwood and Cane, 1990; Thomas et al., 2008) and satellite remotely sensed observational systems (Young et al., 2011). Young et al., (2011) shows that wind speeds over the majority of the world's oceans have increased by at least 0.25-0.5% per year. The trend is stronger in the southern hemisphere than the northern hemisphere. However, the causes for this increasing trend are unknown. Griffin et al., (2010) showed that the continental surface wind speed indicates a significant decreasing trend while the trend of the coastal wind is quite unclear. They suggested that this is because the coastal wind is under the influence of both continental wind and oceanic wind which have opposite trend patterns. This comparison indicated that the

interactions with the underlying surface (e.g. land, ocean) may have significant influences on wind speed trend.

Despite the evidence supporting the argument of Vautard et al., (2010), there are controversial results for the trend of upper-level wind speed. Vautard et al., (2010), based on observations, suggested an increasing trend in the upper-level wind speed. In contrast, Coumou et al., (2015) showed a decreasing trend of upper-level zonal wind in the mid-latitudes in summer from 1979 – 2013 based on NCEP/NCAR and ERA-interim reanalysis. Moreover, McVicar et al., (2012) studied the trend in surface wind speed in Australia using both gridded data and observations from stations. They found that the trends of wind speed calculated from both datasets agree with each other, indicating that the preceding discrepancy between Vautard et al., (2010) and Coumou et al., (2015) is not likely to be caused by whether the data is gridded or not.

On the other hand, the discrete plots of the upper-level wind speed trend (see **Figure 1-2**) suggest that the resolution of upper-level wind speed is relatively low (5 measurements in total from 1000hPa to 200hPa) in Vautard et al., (2010). With this low-resolution data, some vertical variations of wind speed trend might be missing. Even without the contradictory results with Coumou et al., (2015), it still requires a higher resolution vertical wind profile to draw relevant conclusions about the trend in upper-level wind speed.

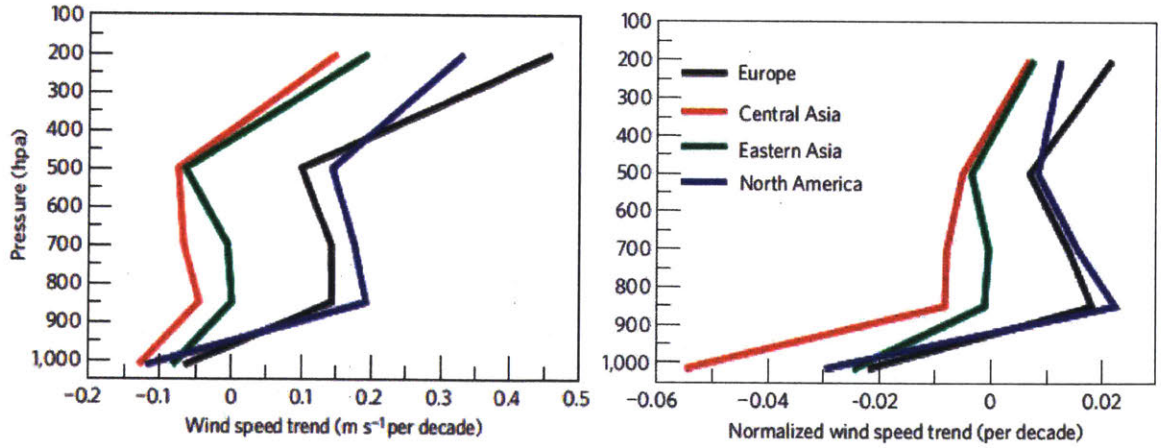

Figure 1-2: Vertical profile of mean wind speed trend in Vautard et al. (2010). The right-hand panel shows the normalized wind speed trend in the unit of 'per decade'. The normalized trend equals absolute trend (m/s per decade) divided by the grand mean of wind speed (m/s) at the corresponding pressure level. Reprinted by permission from Macmillan Publishers Ltd: [Nature Geoscience] (Vautard et al., 2010), copyright (2010).

For this reason, we propose to use a high-resolution wind speed dataset (details in Chapter 2) to study the trend of wind speed. To study the influence of land surface on vertical wind speed trend, we also calculate the planetary boundary height (PBL). We compare the calculated PBL height with the vertical wind speed trend profile. We also study the role of elevation of time of day when the measurements are taken in determining the trends. The following chapters are organized in this way. We discuss the wind speed dataset and methods used in the calculation in Chapter 2. The calculated wind speed trend profiles are discussed in Chapter 3. Relevant conclusions and implications are addressed in Chapter 4.

Chapter 2

Data and Methods

2.1 Radiosonde Data

We used the US high vertical Resolution Radiosonde Data measured by National Oceanic and Atmospheric Administration (NOAA) and maintained by the Stratospheric Processes and their Role in Climate Data Center (Wang and Marvin, 2003).

It includes data for the period of 1998 – 2011 for 94 US operated stations. Two soundings are launched per day, one at 00:00 UTC, and the other at 12:00 UTC. The locations of the stations are displayed in **Figure 2-1**. Among them, the sounding records of 5 sites (denoted with square) are too short to calculate the trend (see Section 2.2.2 for the criteria used in the calculation of trends), so they are not included in the analysis. The dataset spans a period during which NOAA progressively upgraded their upper air stations from the MicroART radiotheodolite tracking system to the Radiosonde Replacement System (RRS) which utilizes GPS tracking. Consequently, each station dataset transitions from the 6-second (~30 meter) resolution MicroART format to the 1-second (~5 meter) resolution RRS format at a specific date between 2005 and 2011. To obtain longer records, we use both 6-second data and 1-second data in this study. To examine whether this change of measuring frequency affects the wind speed data, we performed three types of tests (1) comparing the shapes of the distribution of the wind speed data measured by the two types of devices; (2) calculating of the ratio of annual mean wind speed to the corresponding standard deviation; (3) calculating the trend in wind

speed by including the 6-second data only. Among them, (2) is based on the assumption that, for a given site and whatever the height or exposure of the measurement station, the ratio between mean and standard deviation should remain almost constant and be a characteristic of the meso-scale environment (Verkaik, 2000). The results of (1) are listed in Appendix 1. It suggests that the distribution of 1-second data is similar to that of the 6-second data for the selected pressure levels. Test (2) suggests for each of the 94 stations although the mean-to-standard-deviation ration varies between different pressure levels, within in each pressure level the ratio of 1-second data generally falls into the range of that of the 6-second data. For this reason, no significant differences are brought by the change of measurement resolution as shown by Test (2). An example of the calculate mean-to-standard-deviation ratio is shown in Appendix 2. This results corresponds to Station located at Elko, NV (47.87°, -115.73 °). The results of test (3) are discussed in Section 3.5.

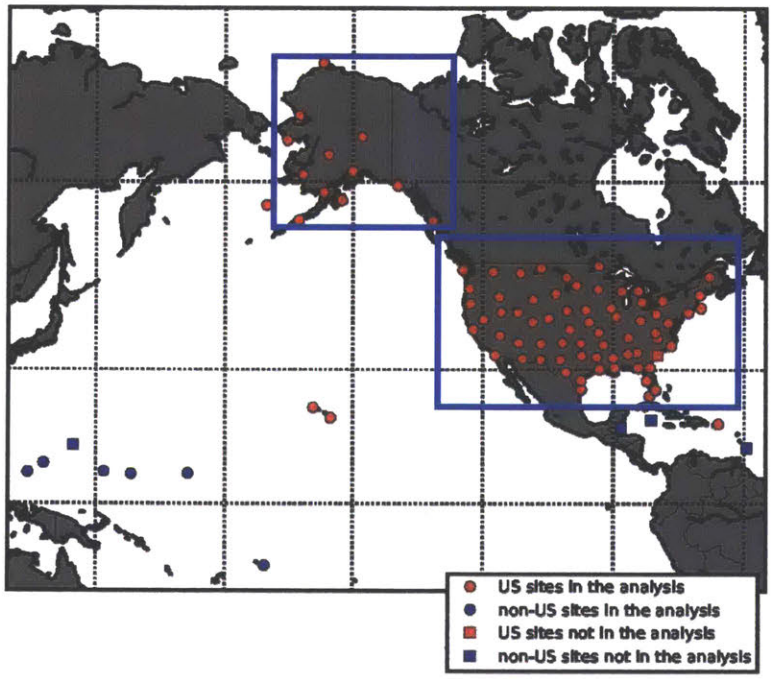

Figure 2-1: US high resolution radiosonde measurements stations: red color denotes the stations belong to US, blue color denotes the stations belong to other countries, dot denotes the stations included in this study, square denotes the stations excluded from this study; blue rectangle indicates the same geographical range of North America used in Vautard et al., (2010).

2. 2 Methods of trend calculation

2.2.1 Interpolation and vertical coordinates

For each individual sounding at the same station, it may measure wind speed at different levels after the same time after launching. As illustrated in **Figure 2-2**, consider two soundings launched at the same station but at different time (e.g. 0 UTC and 12UTC). For sounding 1, it measures wind speed at 30.5m after 6s departing the surface and wind speed at 62m after 12s departing the surface. However, since sounding 2 is launched at a different time and the atmospheric conditions changes, it may measures wind speed at 29.5m and 61m after 6s and 12s departing the surface, respectively. Given the fixed measuring frequency (6s or 1s), the spatial position of the corresponding measurements can be different across soundings event at the same station. On the other hand, the elevation of the stations varies substantially from one to another. **Figure 2-3** shows that the elevation of the 94 stations ranges from 2m to 2179m above the sea level. Therefore, the level which the radiosonde measures after the same departing time can be completely different across stations.

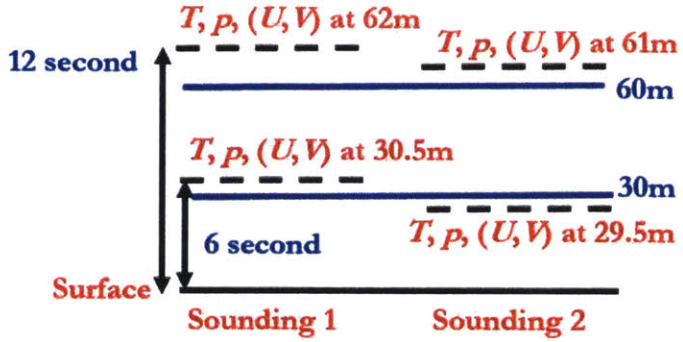

Figure 2-2: Illustration of two sounding launched at different time at the same station. Black solid line denotes the land surface of the station. Black dashed denotes the level which the radiosonde measures. The number in red shows the altitude of the levels that the radiosonde measures. The blue solid line denotes the level to be interpolated from the measurements.

For these reasons, in order to implement analysis across time and stations, it is necessary to interpolate the real measurements of the radionsonde to some standard levels measured in either pressure or altitude. As shown in **Figure 2-2**, the measurements taken by the two soundings are both interpolated to 30m and 60m. Here we used both pressure and altitude above ground (A.G.L.) as the vertical coordinate to interpolate between levels of measurements. Between the two levels of measurements, linear interpolation is implemented to calculate the wind speed at the desired standard levels. For pressure coordinate, we interpolate the

measurements within the range of 1000hPa – 100hPa at a step of 2hPa, that is to say, standard levels to which we interpolate are 1000hPa, 998hPa, 996hPa,…, 102hPa, 100hPa. As for A.G.L. coordinate, we interpolate the measurements within the range of 0m-15000m at a step of 30m, which means that the standard levels after interpolation are 0m, 30m, 60m,…, 14970m, 15000m. **Figure 2-4** shows the comparison between the original sounding and interpolated sounding in terms of wind speed at one station. It suggests that the interpolated sounding agreed well with the original sounding.

It should be noted that more than 1/3 stations are located above 100m higher than the sea level, therefore, there are much fewer measurements near the surface in the pressure coordinate system than in the A.G.L. system, so the A.G.L. coordinate system is better at characterizing the interactions between wind and the land surface. For this reason, we only use the plots with pressure coordinates to compare with **Figure 1-2**, and use the A.G.L. system for the rest of the analyses.

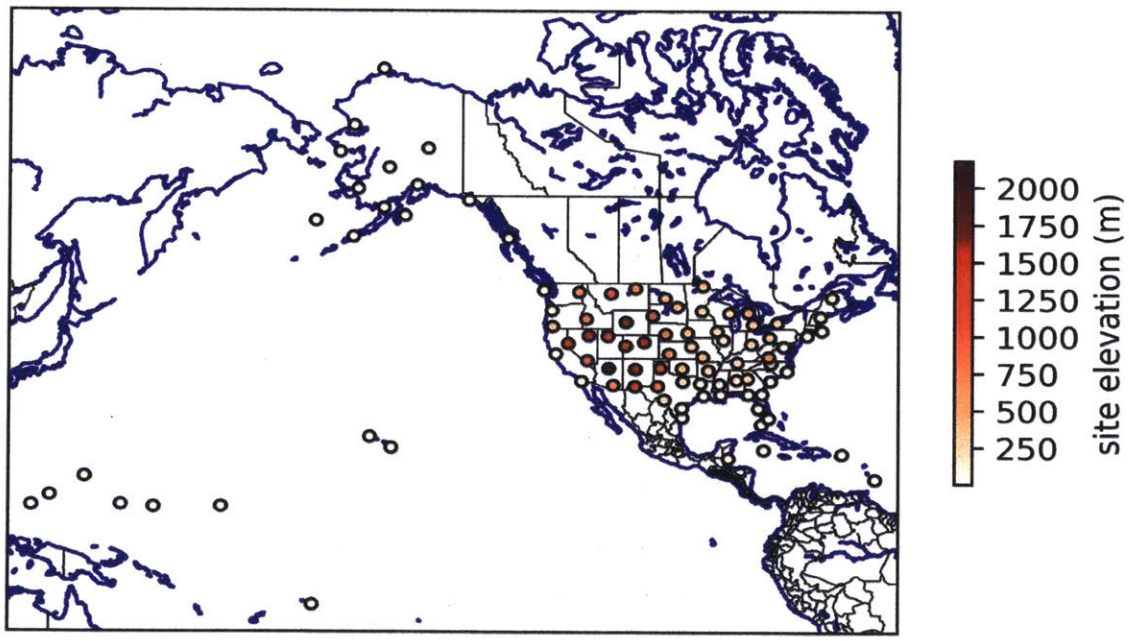

Figure 2-3: The elevation of the 94 stations included in the high resolution radionsode dataset. The color of the dots represents the elevation with darker color indicating higher elevation.

2.2.2 Calculation of the trend in wind speed

Before the calculation of the trend in wind speed, outliers were filtered using the same filtering

method used by Vautard et al. (2010). The filtering process is based on data of a single vertical layer (measured in either pressure or A.G.L. coordinate) of a single month for each station. Wind speeds that lie outside the range [*mean*-3×*std*, *mean*+3×*std*] are removed from the analysis, where std is the standard deviation of the data of that month and vertical layer.

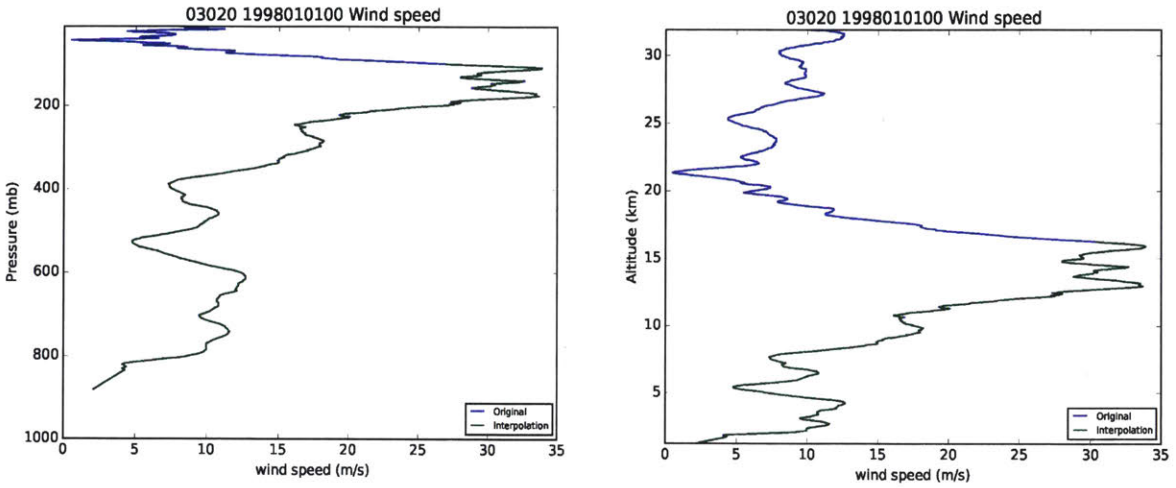

Figure 2-4: Illustration of comparisons between the original sounding and the interpolated sounding. The measurements were taken at 0 UTC on 1998/01/01 at Santa Teresa, NM (site # 03020). The original sounding is shown in blue and the interpolated sounding is shown in green. The right-hand panel shows the results using A.G.L. coordinate. The interpolation range is 0m-15000m. The left-hand panel shows the results using pressure coordinate. The interpolation range is 1000hPa – 100hPa. Note that sounding in the left-hand panel starts above 1000hPa, indicating that this station is elevated.

We require (1) at least 50% of data presented in one month/season/year; and (2) no consecutive gap larger than 1/3 of the timespan used to calculate the mean values exists. For each vertical layer (measured in either pressure or A.G.L.), the wind speed trend (m/s per year) is obtained by taking an ordinary least square (OLS) linear fit over the annual mean wind speed. We also calculate the 90%, 95%, and 99% confidence intervals of the slope in order to test if the trend is statistically significant. To better understand the trend in wind speed in terms of atmospheric dynamics, we also calculated the trend in zonal (U) and meridional wind (V), and displayed them together with the trend of wind speed. **Figure 2-5** shows one of the linear fits over the annual mean wind speed data as an example. It suggests that the trend in wind speed at 100hPa constant pressure surface at Santa Teresa, NM is decreasing, however, it is not

statistically significant (p<0.1). Note that the trend calculated in this way is in the unit of m/s per year. In order to better compare with the results of Vautard et al. (2010) which is in the unit of m/s per decade, the results calculated here were multiplied by 10 and are therefore measured in m/s per decade.

To eliminate the influence of the absolute value of wind speed on the trend and its associated uncertainties, we normalized the trend with the grand mean as Vautard et al. (2010) did in **Figure 1-2**. A rule that "at least 7 years' (half of the time span of the dataset) of data is present" is applied when calculating the slope. In order to test whether the results are affected by the minimum number of years required to calculate the trend, we applied a more stringent rule that "at least 10 years' of data is required to calculate the trend" in the sensitivity analysis. It turns out that the trends calculated for each vertical layer at each site using the two criteria are almost identical. For example, **Figure 2-6** and **Figure 2-7** show the vertical profile of the trends calculated using both criteria for the station located at Elko, NV (40.87°, -115.73°). As marked with the green dashed circle in the figure, only a slight difference is observed over the surface layer of the meridional wind. Similar conditions also applies to other stations, therefore, the 7-year criterion and the 10-year criterion result in almost identical outcome, so we used the 7-year criterion for the rest of the analysis in this thesis.

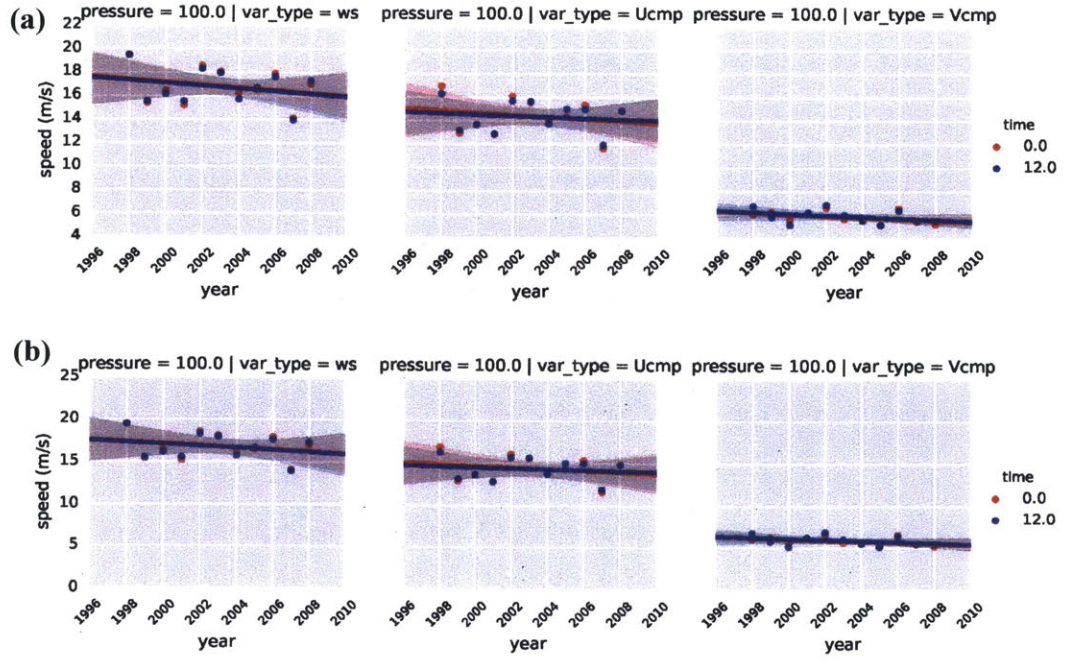

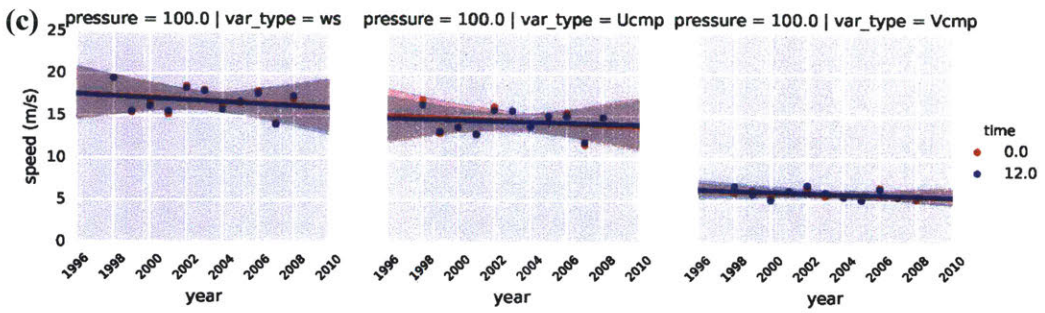

Figure 2-5: Calculation of the trend in wind speed of 100hPa constant pressure surface at Santa Teresa, NM and (a) 90% confidence interval of the trend, (b) 95% confidence interval of the trend, and (c) 99% confidence interval of the trend. The bands indicate the confidence intervals. 'ws' is short for 'wind speed', 'Ucmp' is short for *U* component (i.e. zonal component) of wind speed, and 'Vcmp' is short for *V* component (i.e. meridional component) of wind speed.

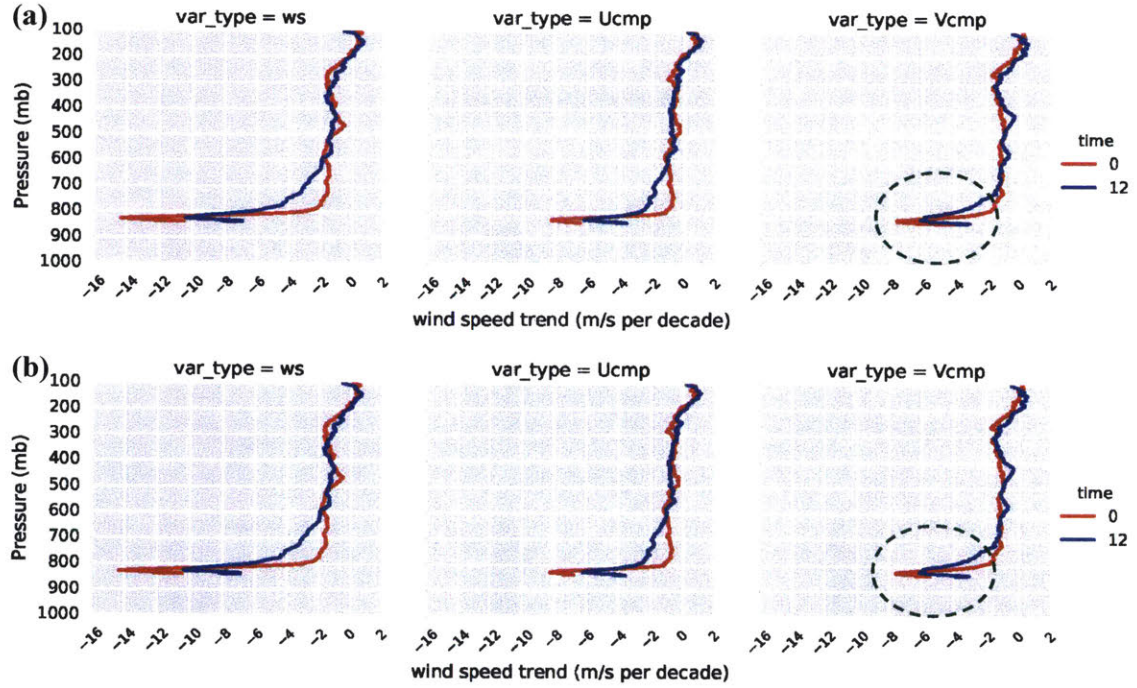

Figure 2-6: Vertical profile of trends in wind speed with pressure vertical coordinate for Station Elko, NV. The upper panel (a) shows the (absolute) trends (m/s per decade) in wind speed (ws), zonal wind (Ucmp), and meridional wind (Vcmp) calculated based the 7-year criterion. The lower panel (b) shows the same trends calculated based on the 10-year criterion. The dashed green circles mark the difference between the two types of trends.

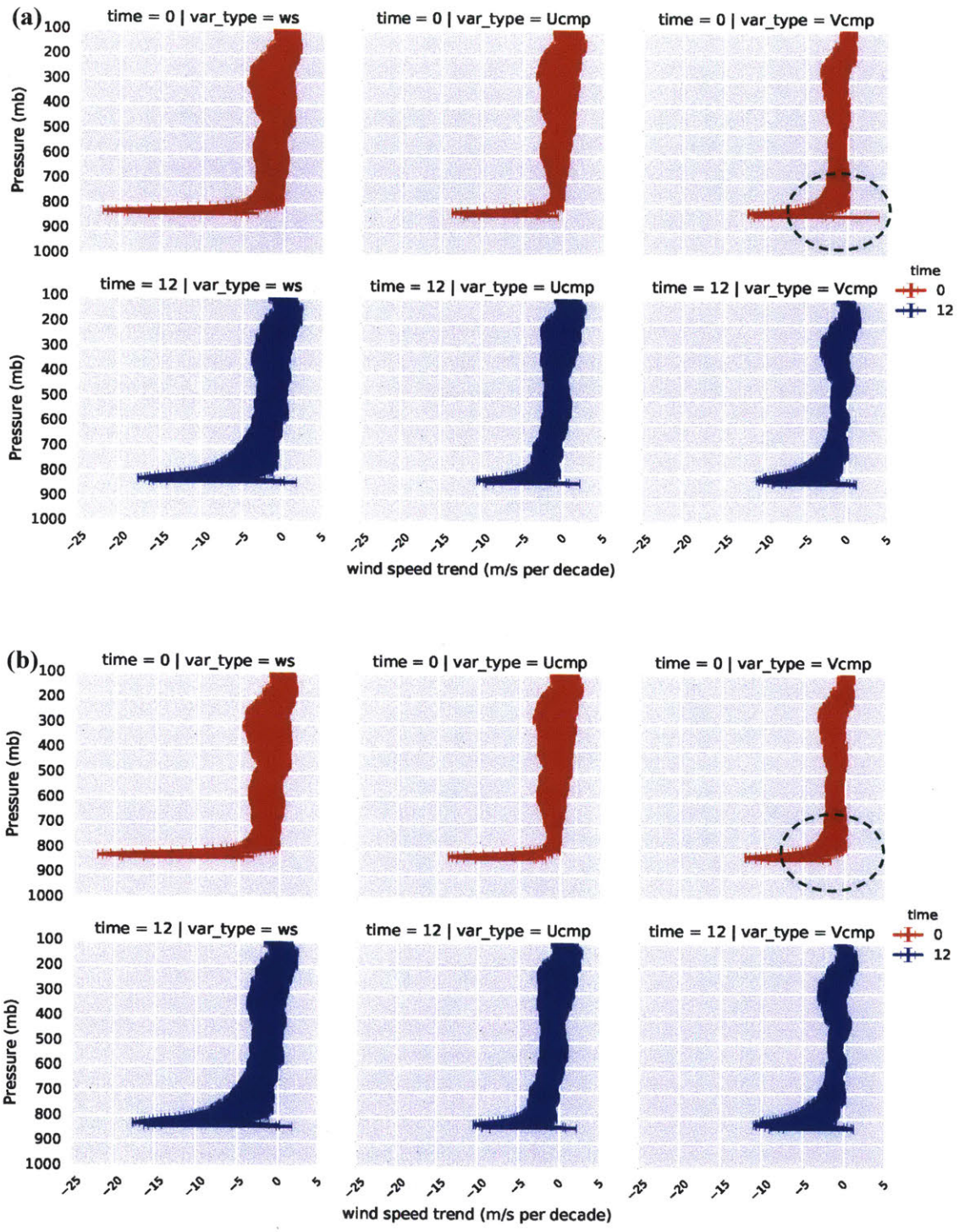

Figure 2-7: Vertical profile of the 95% confidence interval (CI) of trends in wind speed with pressure vertical coordinate for Station Elko, NV. The panel (a) shows CI of the (absolute) trends (m/s per decade) in wind speed (ws), zonal wind (Ucmp), and meridional wind (Vcmp) calculated based the 7-year criterion. The lower panel (b) shows the same things calculated based on the 10-year criterion. The dashed green circles mark the difference between the two types of trends.

2.3 Calculation of PBL height

When calculating PBL height, we deliberately avoided the Artic regions (e.g. Alaska) where the PBL often exhibits surface-based inversion, tropical regions (e.g. Hawaii), which we would frequently experience deep convection and thus ill-defined PBL heights. Therefore, we only calculate PBL height using data of the 65 stations located over the contiguous United States. We employed three methods to calculate the PBL height.

First, we use the bulk Richardson number (*Ri*, the dimensionless ratio of suppression of turbulence by buoyancy to production of turbulence by wind shear) method. The bulk Richardson number method is regarded as the best method for calculating the climatological PBL height (Seidel et al., 2012), because it is suitable for both stable and convective boundary layers, identifies a nonnegative height in all cases, and is not strongly dependent on sounding vertical resolution.

Ri is defined as

$$Ri(z) = \frac{(g/\theta_{vs})(\theta_{vz} - \theta_{vs})(z - z_s)}{(u_z - u_s)^2 + (v_z - v_s)^2 + (bu_*^2)} \tag{2.1}$$

where z is the height, and s denotes the surface, g is the acceleration of gravity, θ_v is the virtual potential temperature (excluding condensate loading, r_L=0), u and v are component wind speeds, b is a constant, and u_* is the surface friction velocity. The virtual potential temperature is

$$\theta_v = \theta(1 + 0.61r - r_L) \tag{2.2}$$

Since u_* is not known from radiosonde data, according to Seidel et al. (2012), we set b = 0, and thus ignore surface frictional effects, which is much smaller than the bulk shear terms in the denominator, and is not significant in stable conditions. Based on Vogelzang et al. (1996), PBL height is the lowest level z at which interpolated *Ri* crosses the critical value of 0.25, $z(\mathrm{Ri}_{0.25})$.

Although the bulk Richardson number method is regarded the best fit for PBL calculation based on radiosonde measurements, we also include the other two methods i.e. (1) elevated inversion method which identifies PBL height as the height of the base of an elevated temperature inversion; (2) air parcel method which identifies PBL height based on hypothetical

vertical displacement of a parcel of air from the surface and characterization of the height at which virtual potential temperature is equal to the surface value (Seidel, Ao, and Kun, 2010). This is because the bulk *Ri* method incorporates wind speed (u, and v) into the calculation, therefore, may bring underlying association with the wind speed profile, which makes it harder to detect the relation between the trend in wind speed and PBL height. For this reason, PBL heights calculated from these three methods are compared in later analysis to identify a better estimate of PBL height.

Chapter 3

Results and Discussion

3.1 Vertical profile of trends in wind speed

To compare with the results of Vautard et al. (2010) over the same geographical range in North America as shown in **Figure 1-2**, we calculate the trend in wind speed over the 79 stations located in North America. To do this, we first calculate the average annual mean wind speed over the 79 stations and then calculate the trends based on the annual mean. The geographical range of these stations are shown within the blue rectangles in **Figure 2-1. Figure 3-1** shows the results using pressure as the vertical coordinate. The upper panel (a) shows the trend in wind speed (ws), zonal wind (Ucmp), and meridional wind (Vcmp) and the lower panel (b) shows the normalized trend. The trend in wind speed in **Figure 3-1** is similar to that in **Figure 1-2**, with a negative trend near the surface and a positive trend higher up. Vautard et al. (2010) shows that the trend in wind speed over North America turns from negative to positive at 950hPa. However, **Figure 3-1 (a) and (b)** suggests that trends do not become positive until ~550hPa. This difference may be due to the higher vertical resolution of the dataset used in this study than that used in Vautard et al. (2010), as the higher resolution data captures more variations of trends in wind speed in the vertical. But it could also be due a short-term variability as a result of the shorter time span (1998-2011) of this study as compared to that (1979-2008) in Vautard et al. (2010). In **Figure 3-1 (b)**, the normalized trend is -0.05 per decade (i.e. -5% per decade) at 1000hPa, indicating that near-surface wind declines 5% per

decade in terms of the climatological mean. This is value is comparable to the value (-3% per decade) reported in Vautard et al. (2010) for North America. **Figure 3-1** also shows that the decreasing trends in wind speed peak at certain levels above 1000hPa, however, these levels do not align in the vertical in the pressure coordinate system. Another feature of the profiles of trend in wind speed is that the profile becomes 'smoother' above ~800hPa, whereas, it shows a 'jagged' pattern between 1000hPa -- 800hPa.

Figure 3-2 shows the vertical profile of trends in wind speed (ws), zonal wind (Ucmp), and meridional wind (Vmcp) with the A.G.L. vertical coordinate. The 'jagged' pattern near the surface (1000hPa-800hPa) shown in **Figure 3-1** no longer exists in **Figure 3-2**. Instead, **Figure 3-2** shows a largest negative trend in wind speed, zonal wind, and meridional wind close to the surface. **Figure 3-3** shows the lower part (0m-1000m) of the profile shown in **Figure 3-2**. **Figure 3-3** suggests that the largest negative trend is roughly 50-80m above the surface. The normalized trend in wind speed shown in **Figure 3-3 (b)** indicates that the largest negative trend is close to -0.5 per decade, which means that winds at this level declines nearly 50% per decade in terms of the climatological mean. Note that this value is 10 times of the value reported in Vautard et al. (2010) for 1000hPa. The normalized trend in wind speed at the surface is -0.14 per decade which is three times the value at 1000hPa shown in **Figure 3-1**. The negative trends in wind speed do not turn positive until ~5000m.

Figure 3-4 shows the 95% confidence interval of the trends in wind speed, zonal wind, and meridional wind. It suggests that the negative trend in wind speed at the surface and the largest negative trend are both statistically significant ($p<0.05$). The significance of the negative trend drops with altitude and the trends above ~2000m are not statistically significant ($p<0.05$) although the mean value of the trend does not become positive until 4000m.

In order to test if the calculated trends are sensitive to the statistical metric used in the calculation, we also calculated the trend in wind speed, zonal wind, and meridional wind based on the median instead of the mean. For each vertical layer measured in pressure or A.G.L., the average trend of that layer is calculated as the median of the trends of all available stations. Unlike the trend calculation based on the linear fit over the annual mean which involves the number of stations directly into the calculation, linear fit over the median is less affected by the number of available stations in a certain layer.

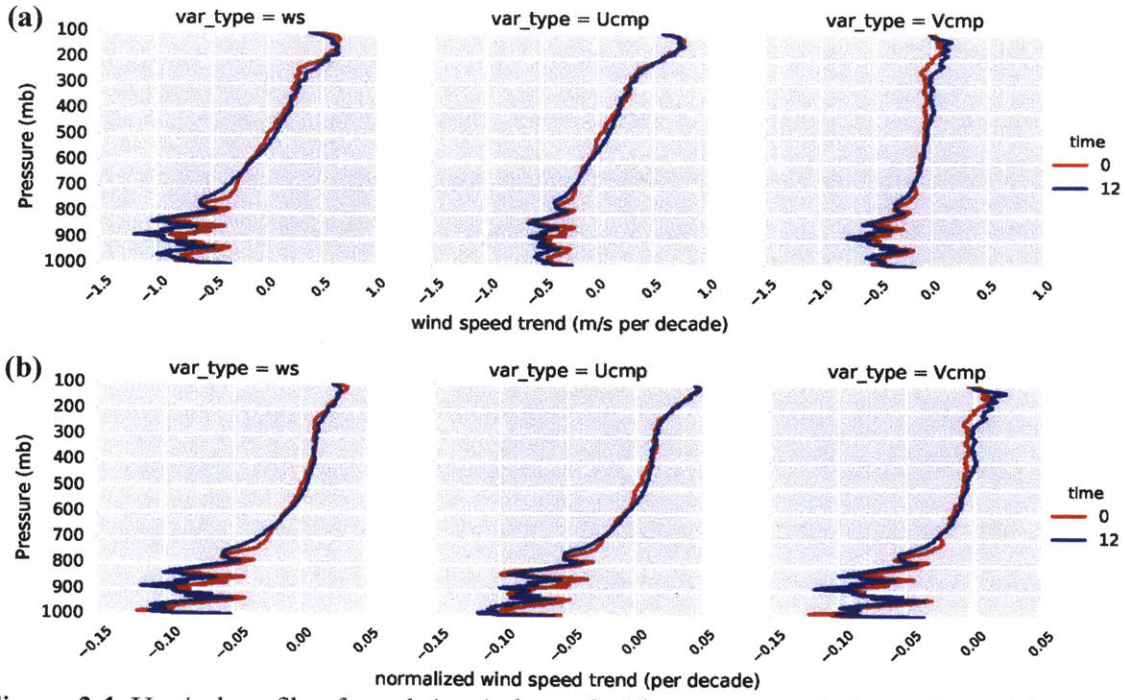

Figure 3-1: Vertical profile of trends in wind speed with pressure vertical coordinate. The upper panel (a) shows the (absolute) trends (m/s per decade) in wind speed (ws), zonal wind (Ucmp), and meridional wind (Vcmp). The lower panel (b) shows the corresponding normalized trends (per decade).

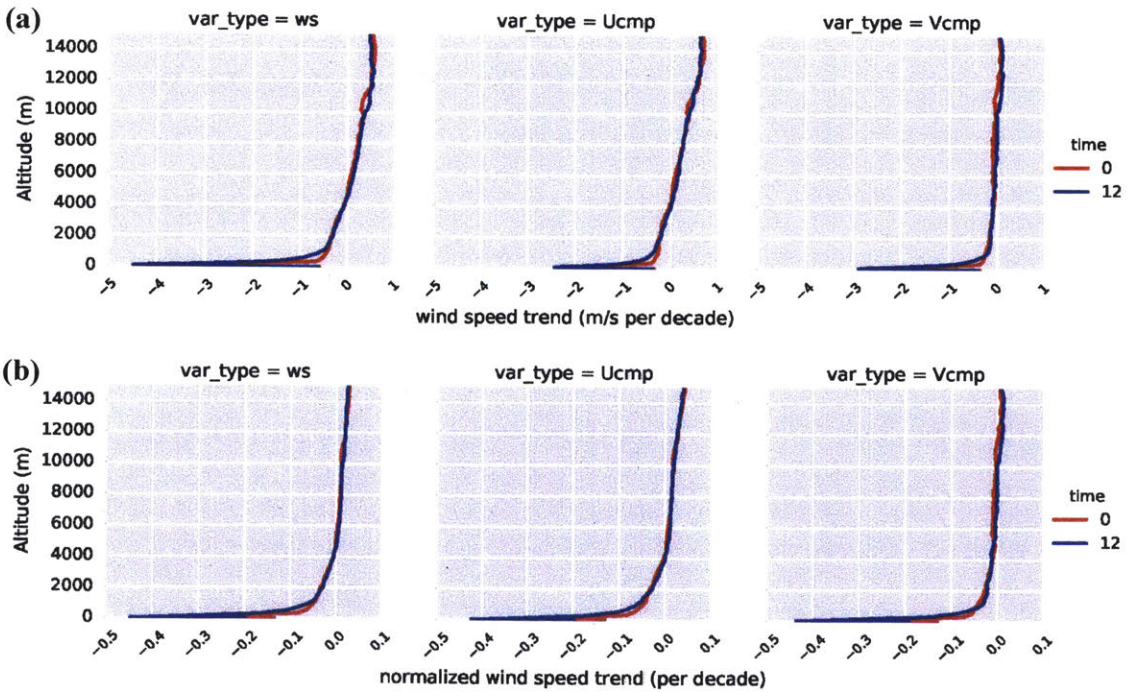

Figure 3-2: Vertical profile of trends in wind speed with A.G.L. vertical coordinate. The upper panel (a) shows the (absolute) trends (m/s per decade) in wind speed (ws), zonal wind (Ucmp), and meridional wind (Vcmp). The lower panel (b) shows the corresponding normalized trends (per decade).

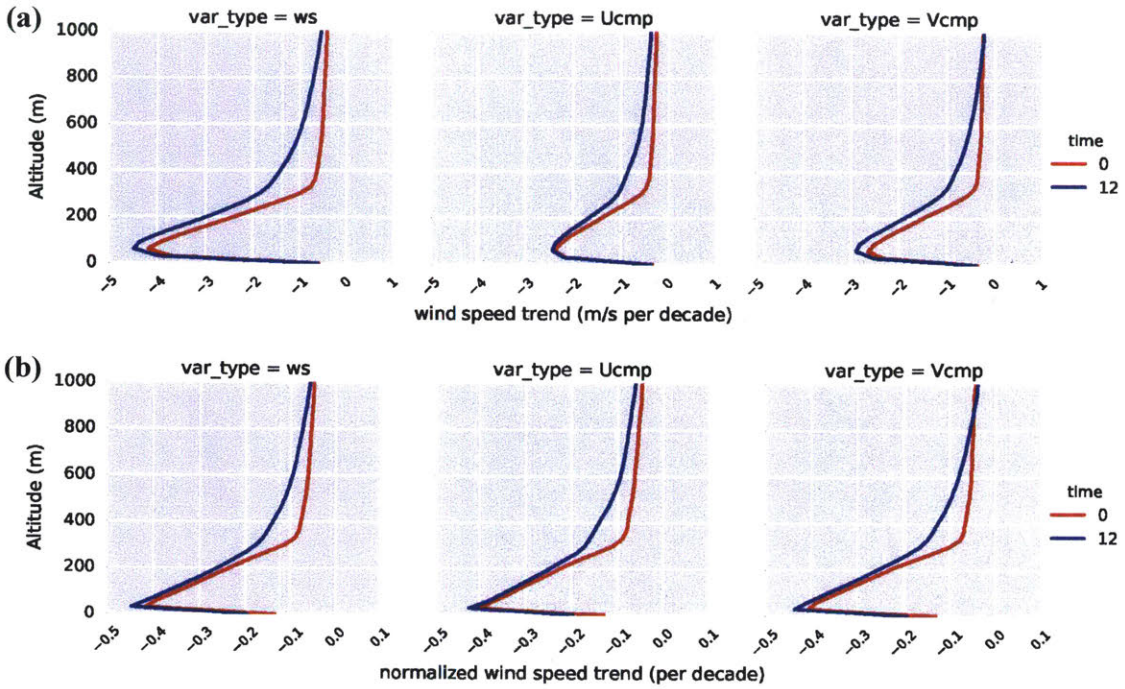

Figure 3-3: Lower part (0m-1000m) of the vertical profile of trends in wind speed with A.G.L. vertical coordinate. The upper panel (a) shows the (absolute) trends (m/s per decade) in wind speed (ws), zonal wind (Ucmp), and meridional wind (Vcmp). The lower panel (b) shows the corresponding normalized trends (per decade).

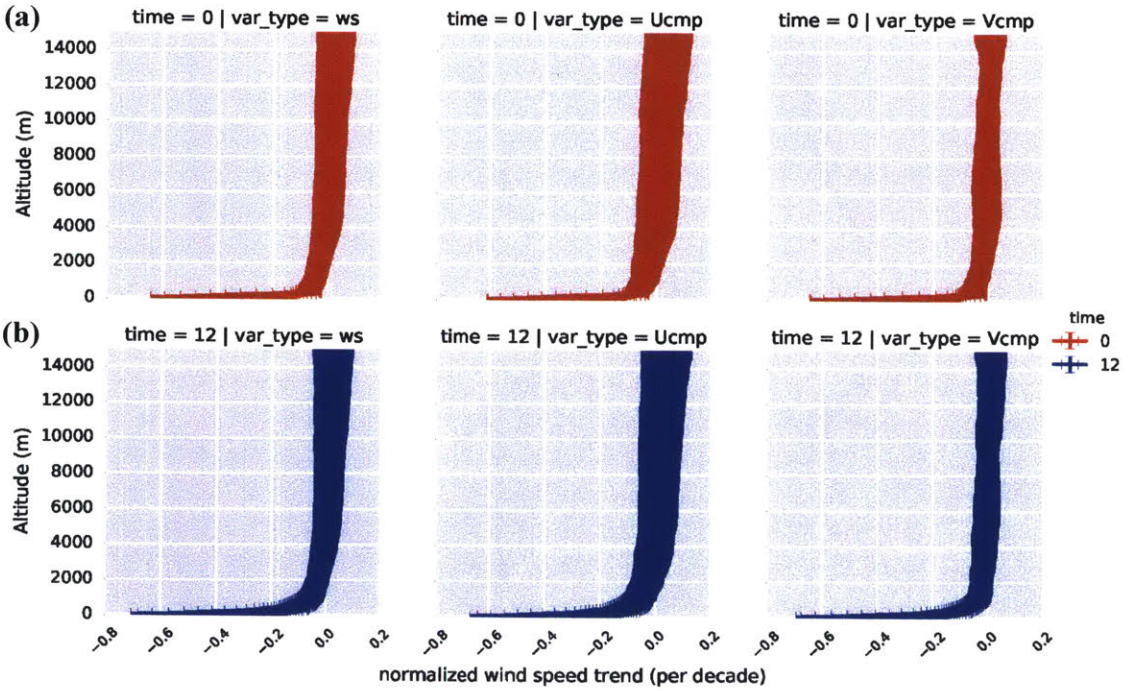

Figure 3-4: Vertical profile of 95% confidence interval (CI) of the normalized trends in wind speed with A.G.L. vertical coordinate. The upper panel (a) shows the 95% CI of the normalized trends (per decade) in wind speed (ws), zonal wind (Ucmp), and meridional wind (Vcmp) at 0 UTC. The lower panel (b) shows the normalized trends (per decade) at 12 UTC.

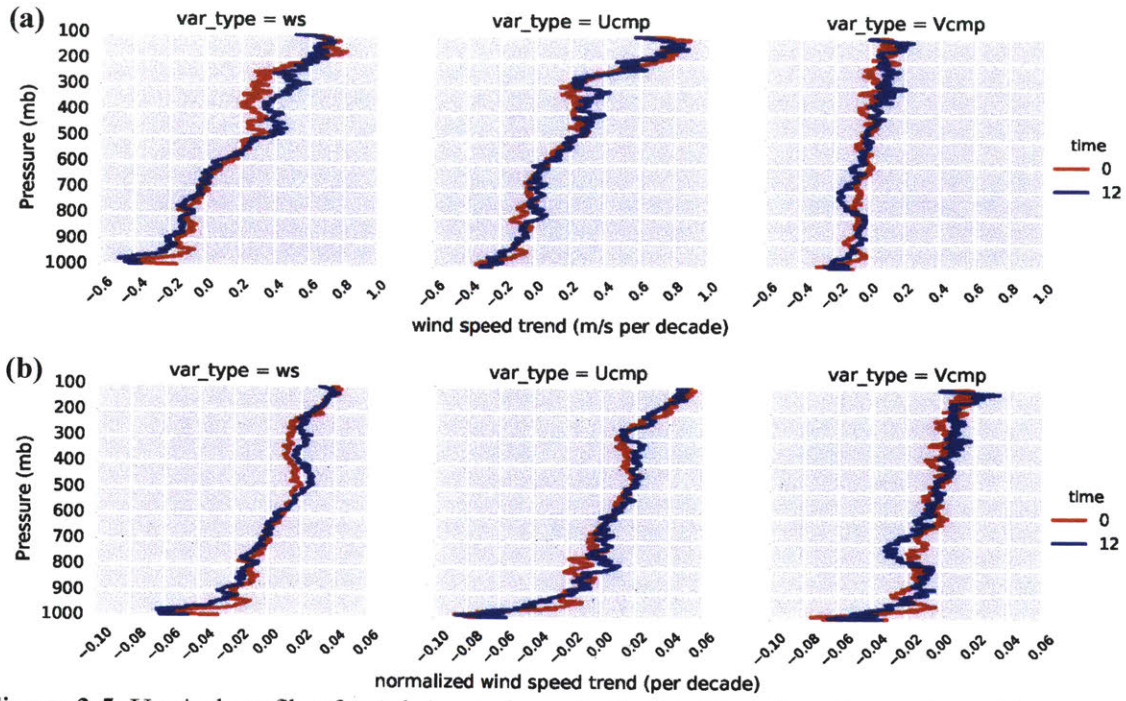

Figure 3-5: Vertical profile of trends in wind speed calculated based on the median, with pressure vertical coordinate. The upper panel (a) shows the (absolute) trends (m/s per decade) in wind speed (ws), zonal wind (Ucmp), and meridional wind (Vcmp). The lower panel (b) shows the corresponding normalized trends (per decade).

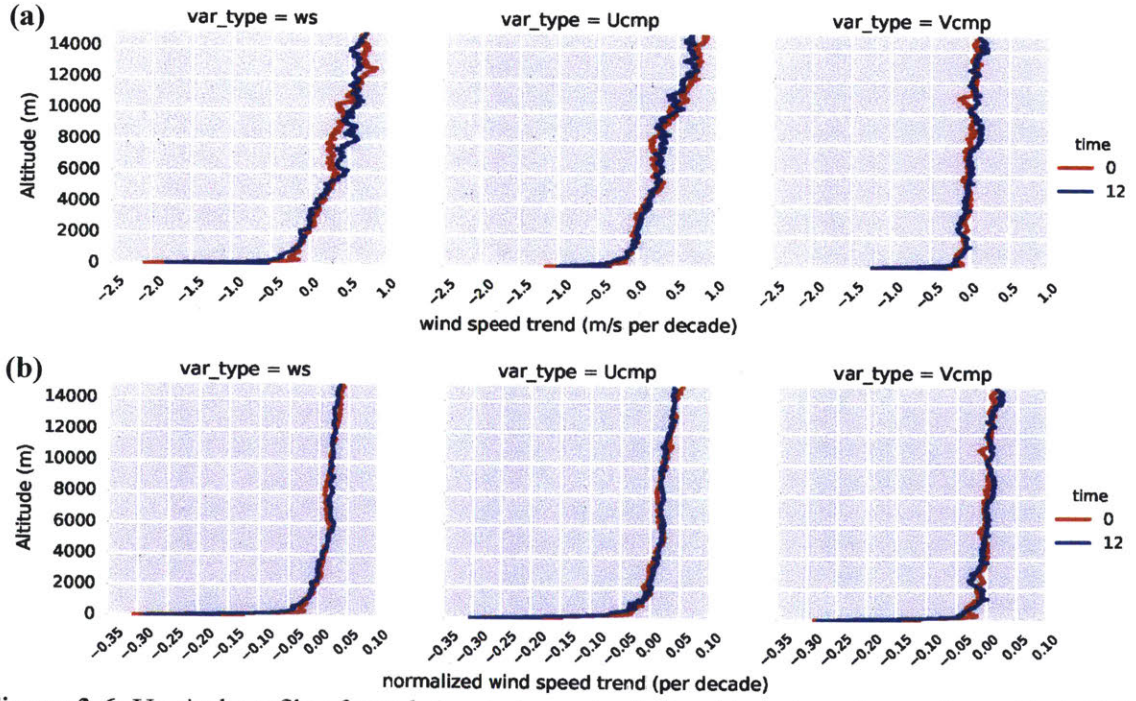

Figure 3-6: Vertical profile of trends in wind speed calculated based on the median, with A.G.L. vertical coordinate. The upper panel (a) shows the (absolute) trends (m/s per decade) in wind speed (ws), zonal wind (Ucmp), and meridional wind (Vcmp). The lower panel (b) shows the corresponding normalized trends (per decade).

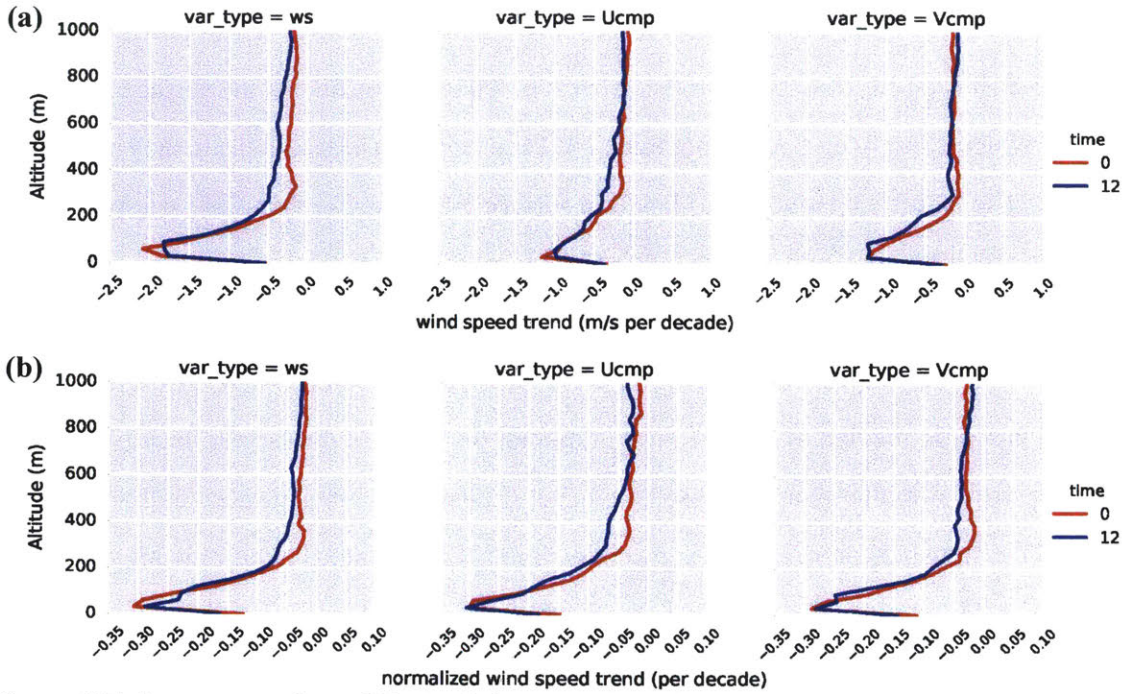

Figure 3-7: Lower part (0m–1000m) of the vertical profile of trends in wind speed calculated based on the median, with A.G.L. vertical coordinate. The upper panel (a) shows the (absolute) trends (m/s per decade) in wind speed (ws), zonal wind (Ucmp), and meridional wind (Vcmp). The lower panel (b) shows the corresponding normalized trends (per decade).

Figure 3-5 and **Figure 3-6** show the trends calculated based on the median with pressure coordinate and A.G.L. coordinate, respectively. **Figure 3-5** shows similar pattern to **Figure 3-1**. The trends in wind speed do not turn positive until close to 600hPa which is much higher than the level reported in Vautard et al. (2010). Moreover, the normalized trend in wind speed at 1000hP is -0.05 per decade which is the same as the one shown in **Figure 3-1**. One difference between **Figure 3-5** and **Figure 3-1** is that the near-surface part of **Figure 3-5** does not show the 'jagged pattern' indicated in **Figure 3-1**. This is because the 'jagged pattern' shown in **Figure 3-1** reflects the largest negative trend of stations with different elevation. Although the value of the largest negative trend is much greater than the trends at other levels, the number of stations showing the largest negative trend for a given pressure level is limited, therefore, this largest negative trend and the resultant 'jagged' pattern cannot be reflected in the trends calculated based on the median.

As for the trend based on the median with A.G.L. coordinate shown in **Figure 3-5**, it also shows similar pattern to **Figure 3-2**. The negative trends do not turn positive until close to 4000m. Both the (absolute) trends and the normalized trends indicate a largest negative trend

close to the surface. **Figure 3-6** shows the lower part (0m-1000m) of the vertical profile shown in **Figure 3-5**. It suggests that the normalized trend based on the median at the surface is -0.13 per decade which close to corresponding trend (-0.14 per decade) based on the mean shown in **Figure 3-2**. The largest negative trend shown in **Figure 3-5** is smaller than the corresponding value in **Figure 3-2**, which may be due to the difference in the statistical metrics.

The similar patterns of the trends based on the mean and trends based on the median suggests that (1) the largest negative trend close to the surface still exists in the case of calculation based on median instead of mean although the value of the largest negative trend based on median is smaller than that based on mean; (2) the trend in wind speed at the surface is robust to the statistical metrics used in the calculation. The estimated trend in wind speed at the surface is 5% per decade with pressure coordinate and 14% per decade with A.G.L. coordinate. The former value is also comparable with that reported in Vautard et al. (2010). It should be noted that the largest negative trend (-0.45 per decade) is 15 times of the normalized trend (-0.03 per decade) in wind speed at 1000hPa reported in Vautard et al. (2010). As shown in **Figure 3-3**, this largest negative trend is 50-80m above the surface. To the best knowledge of the author, this is the first-time that the largest negative trend is reported. It may be due to the high-vertical-resolution data used in this study as previous work like Vautard et al. (2010) mainly looked at radiosonde data with records at the significant levels only. It is also possible that this largest negative trend only reflects a short-term variability of the wind speed since only 14-year data (1998-2011) is used in the calculation of the trend. Therefore, for future work, it is necessary to implement similar analysis on other high-resolution radiosonde data with longer timespan to test if the largest negative trend is statistically robust.

3.2 The relation between the largest negative trend and PBL

To examine the structure of the wind speed trend close to the surface and in particular detect the relation between the largest negative trend and PBL, we calculate the wind speed trend for the 65 sites located over the contiguous US and focus on the trend below the altitude of 1000m.

Figure 3-8 shows the trends with A.G.L. coordinate and the PBL height calculated using the three methods. Note that **Figure 3-8 (a)** and **(b)** only show the PBL height at 12 UTC. The

convective boundary is much higher and significantly affected by surface heating and convection

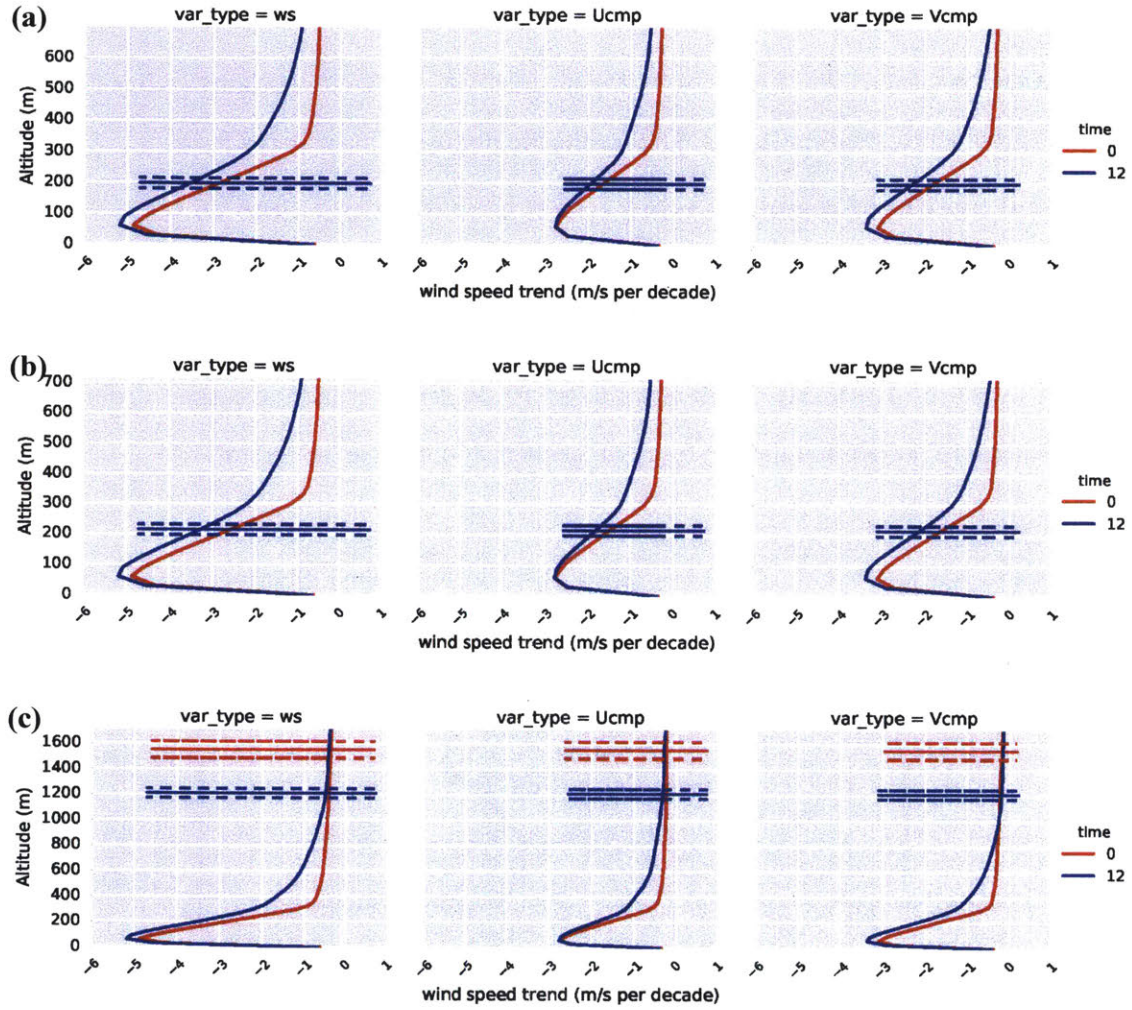

Figure 3-8: Lower part of the vertical profile of trends in wind speed (calculated based on the mean), with A.G.L. vertical coordinate and its relation to the PBL height. The panel (a) shows the (absolute) trends (m/s per decade) in wind speed (ws), zonal wind (Ucmp), and meridional wind (Vcmp) and its relation to the PBL (at 12 UTC) calculated using the bulk Richardson number method. The panel (b) shows the same trends and its relation to the PBL (at 12 UTC) calculated using the air parcel method. The panel (c) shows the same trends and its relation to the PBL (at both 0 and 12 UTC) calculated using the elevated inversion method. The dashed line indicates the 95% confidence interval of the PBL estimates.

Figure 3-8 (a) and **(b)** suggests that the PBL height estimates using bulk *Ri* method and air parcel method are similar, however, elevated inversion method generated a much higher PBL height. This comparison also suggests that the association between wind speed trend and PBL height calculated using bulk *Ri* method is not likely to be biased by the incorporation of

wind speed into PBL height calculation. **Figure 3-8** indicates that the largest negative trend is within the PBL. Note that the contiguous U.S. spans three time-zone from the western coast to the eastern coast, therefore, the different stations at 0 UTC and 12 UTC may reflect different surface heating conditions. For this reason, it is necessary to carry out the same analysis over the stations grouped by the time-zones. The results are discussed in section 3.3.

3.3 Vertical profile of trends in wind speed over different time zones

Figure 3-9 shows the 65 stations over the contiguous US. We grouped the stations by longitude with each group spanning 10 degree longitude therefore, there are 6 groups from the west to the east as shown in **Table 3-1**. With a width of 10 degree longitude, the time difference between the eastern border and the western border of each time zone is ~30min.

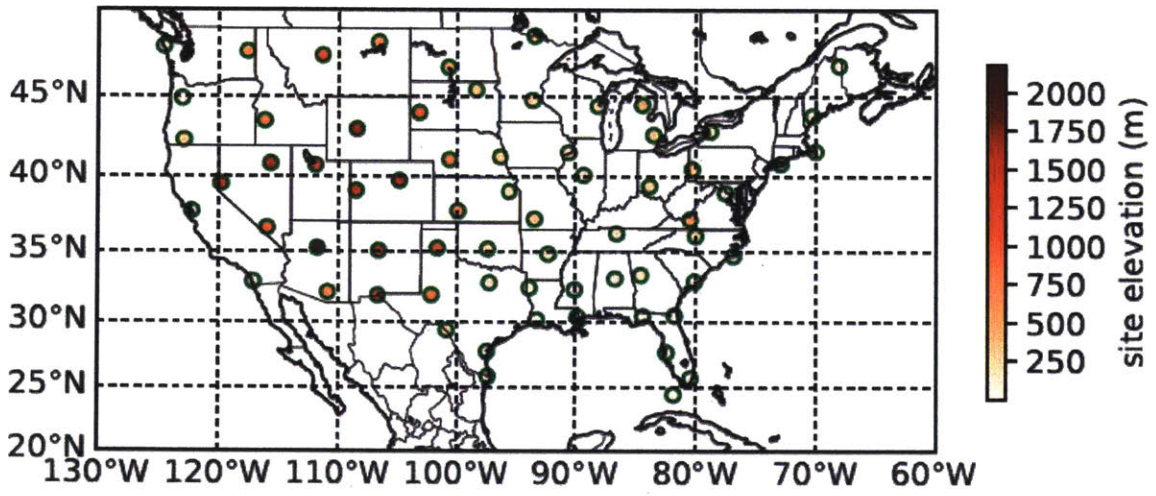

Figure 3-9: 65 stations over the contiguous US. The color of the dots represents the elevation with darker color indicating higher elevation.

Table 3-1: Number of stations and local time at 0 UTC/12 UTC in the 6 time zones

Time zone	Local time at 0 UTC	Local time at 12 UTC	Number of stations (#)
80°W – 70°W	6 - 6:30 pm	6 - 6:30 am	9
90°W – 80°W	5:30 – 6 pm	5:30 – 6 am	15
100°W – 90°W	5 – 5:30 pm	5:30 – 6 am	14
110°W – 100°W	4:30 – 5 pm	4:30 – 5 am	13
120°W – 110°W	4 – 4:30 pm	4 – 4:30 am	10
130°W – 120°W	3:30 – 4 pm	3:30 – 4 am	4

As shown in **Table 3-1**, the number of stations in each time zone differs much. In order to reduce the influence of number of stations on the results, we calculate the vertical profile of trends in wind speed based on the median instead of the mean (as discussed in section 3.1). As shown from **Figure 3-10** to **Figure 3-15**, the vertical profile of the trends calculated based on the median of all 6 time zones all indicate the largest negative trend near the surface. **Figure 3-16** to **Figure 3-21** show the lowest 1000 meters of the profiles shown in **Figure 3-10** to **Figure 3-15**. They suggest that the vertical profiles of wind speed trends of 90°W-80°W, 110°W-100°W, 120°W-110°W, and 130°W-120°W indicate a diurnal difference. The largest negative trend peaks at nighttime in 90°W-80°W, 110°W-100°W, 130°W-120°W, however, the largest negative trend peaks at day time in 120°W-110°W. Moreover, the largest negative trend exist even without a diurnal difference. This evidence suggests that the observed largest negative trend is not directly related nighttime phenomena such as the nocturnal jet.

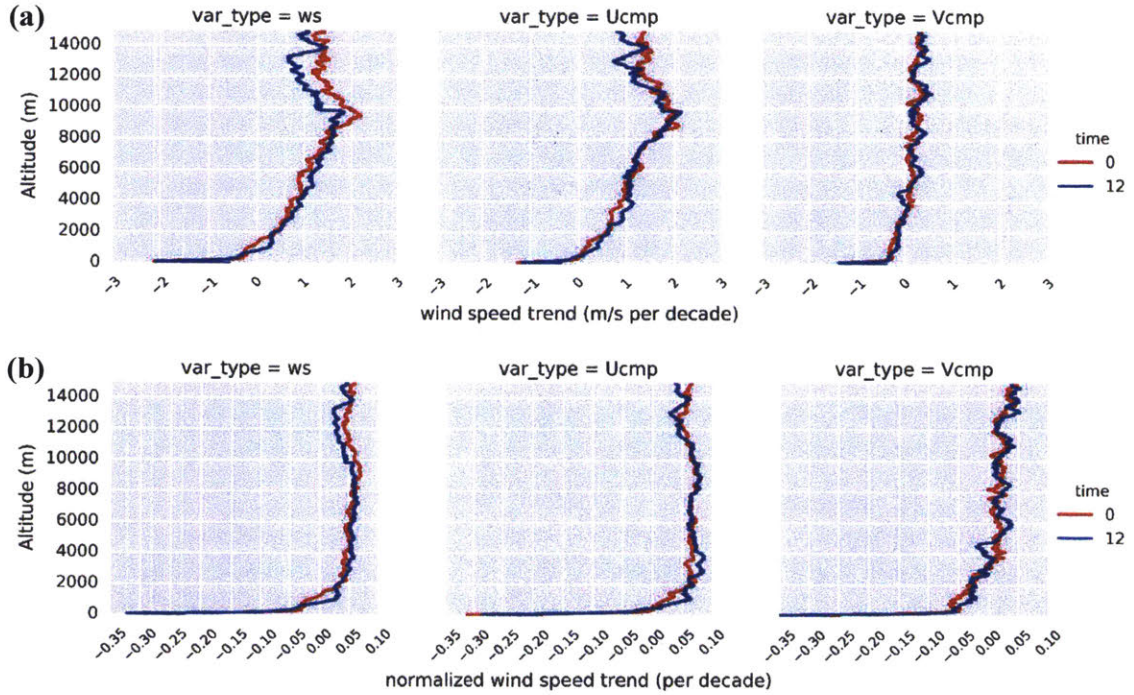

Figure 3-10: Vertical profile of trends in wind speed calculated based on the median, with A.G.L. vertical coordinate for stations located within 80°W-70°W (9 stations). The upper panel (a) shows the (absolute) trends (m/s per decade) in wind speed (ws), zonal wind (Ucmp), and meridional wind (Vcmp). The lower panel (b) shows the corresponding normalized trends (per decade).

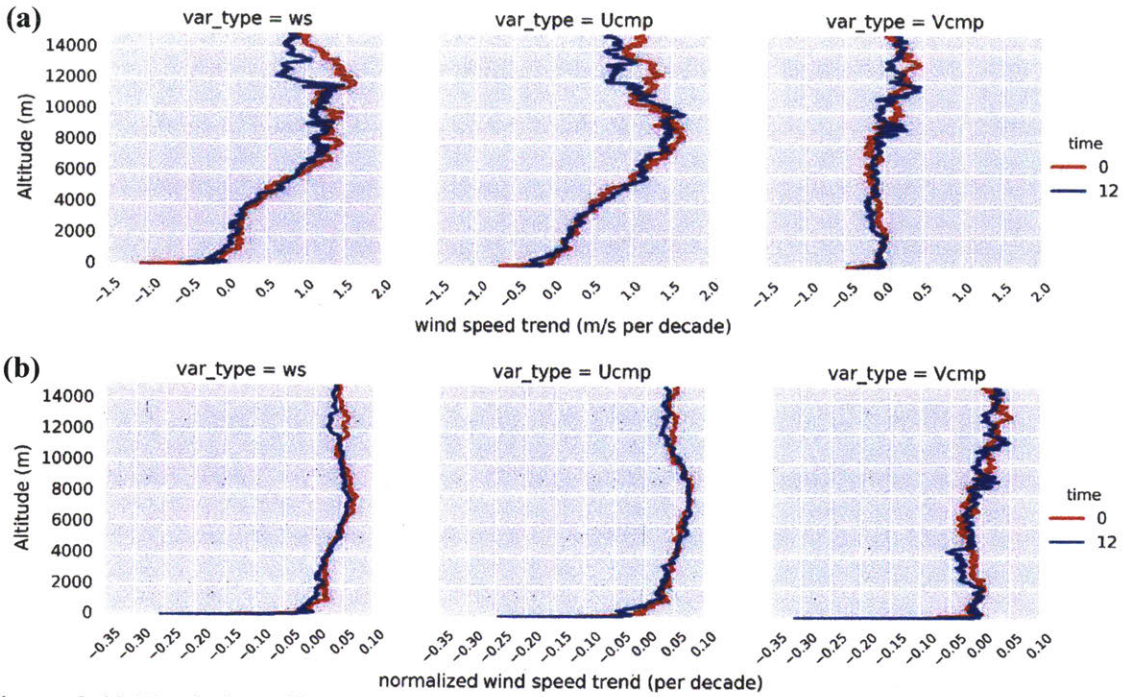

Figure 3-11: Vertical profile of trends in wind speed calculated based on the median, with A.G.L. vertical coordinate for stations located within 90°W-80°W (15 stations). The upper panel (a) shows the (absolute) trends (m/s per decade) in wind speed (ws), zonal wind (Ucmp), and meridional wind (Vcmp). The lower panel (b) shows the corresponding normalized trends (per decade).

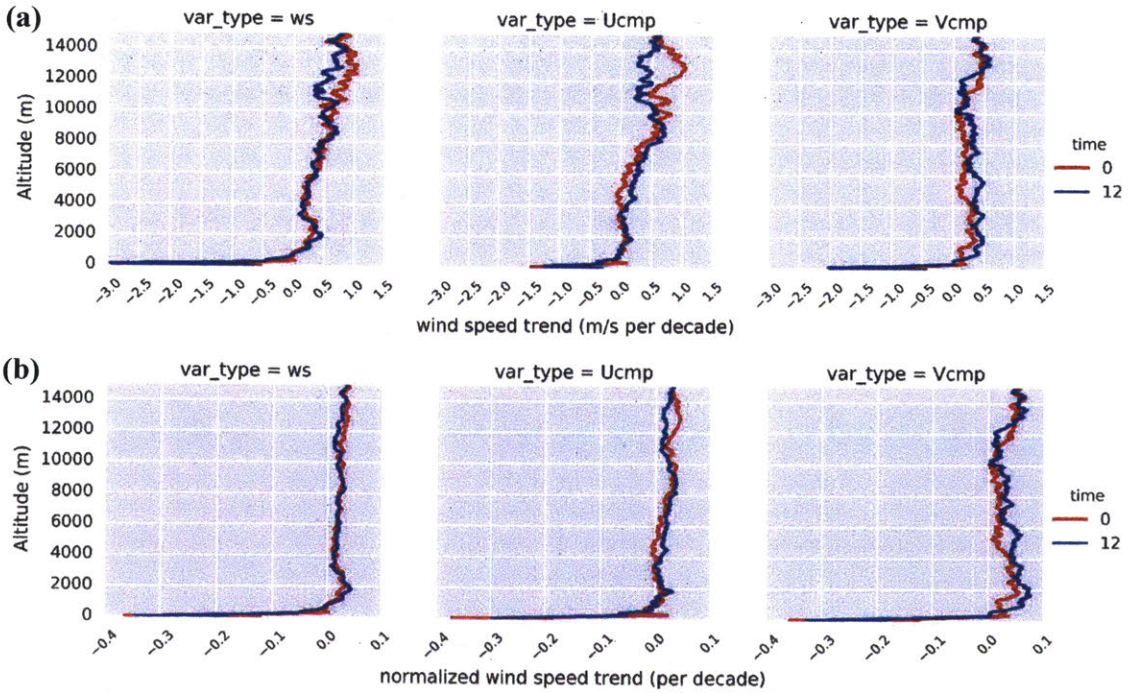

Figure 3-12: Vertical profile of trends in wind speed calculated based on the median, with A.G.L. vertical coordinate for stations located within 100°W-90°W (14 stations). Panel (a) shows the (absolute) trends (m/s per decade) in wind speed (ws), zonal wind (Ucmp), and meridional wind (Vcmp). Panel (b) shows the corresponding normalized trends (per decade).

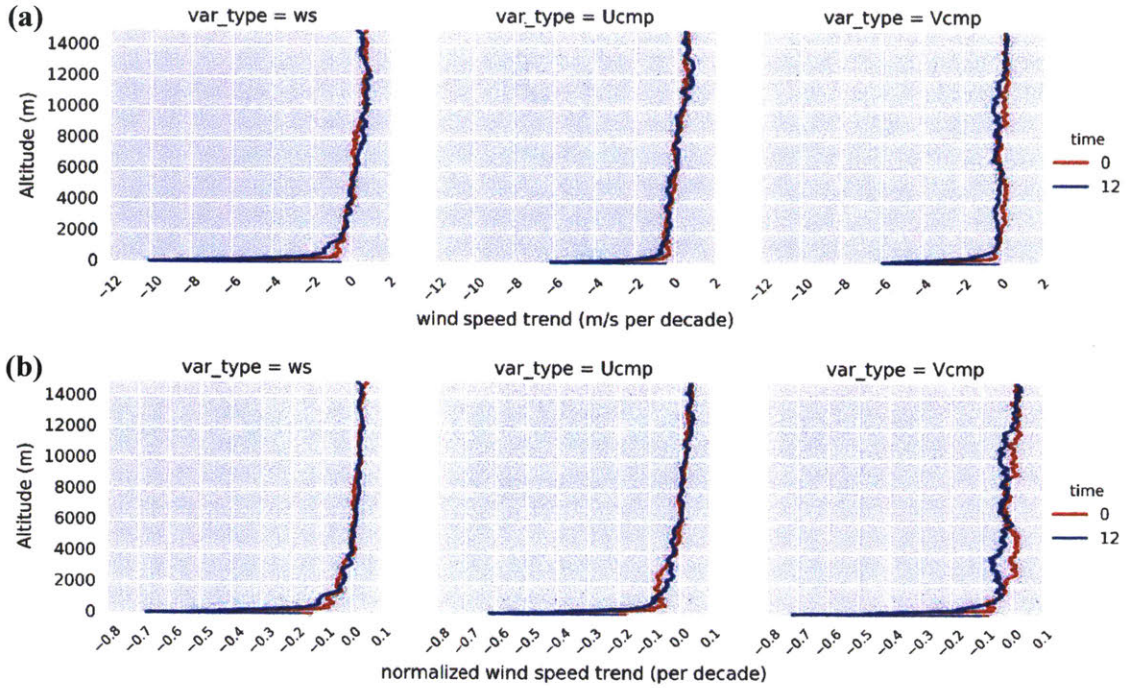

Figure 3-13: Vertical profile of trends in wind speed calculated based on the median, with A.G.L. vertical coordinate for stations located within 110°W-100°W (13 stations). Panel (a) shows the (absolute) trends (m/s per decade) in wind speed (ws), zonal wind (Ucmp), and meridional wind (Vcmp). Panel (b) shows the corresponding normalized trends (per decade).

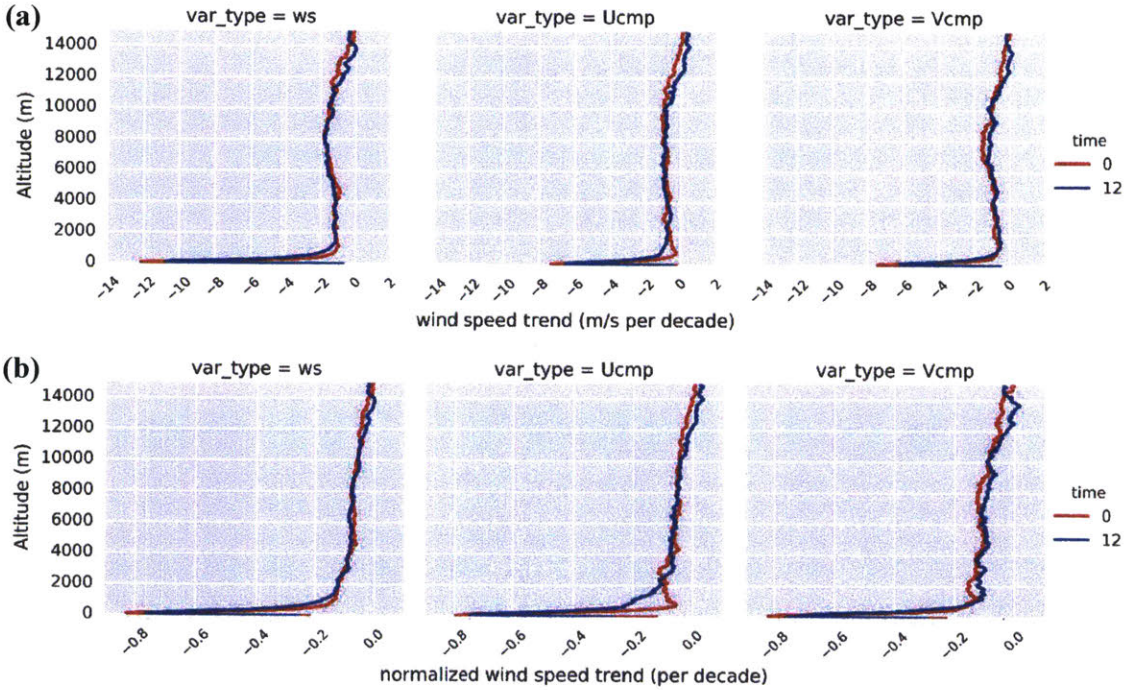

Figure 3-14: Vertical profile of trends in wind speed calculated based on the median, with A.G.L. vertical coordinate for stations located within 120°W-110°W (10 stations). Panel (a) shows the (absolute) trends (m/s per decade) in wind speed (ws), zonal wind (Ucmp), and meridional wind (Vcmp). Panel (b) shows the corresponding normalized trends (per decade).

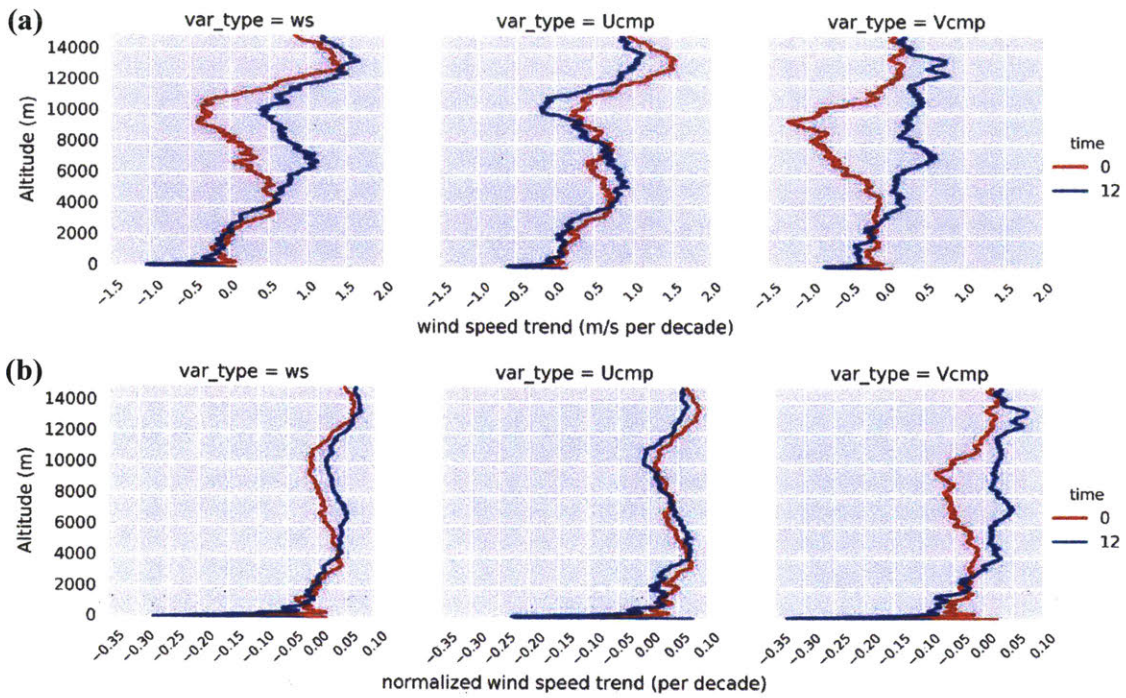

Figure 3-15: Vertical profile of trends in wind speed calculated based on the median, with A.G.L. vertical coordinate for stations located within 130°W-120°W (4 stations). Panel (a) shows the (absolute) trends (m/s per decade) in wind speed (ws), zonal wind (Ucmp), and meridional wind (Vcmp). Panel (b) shows the corresponding normalized trends (per decade).

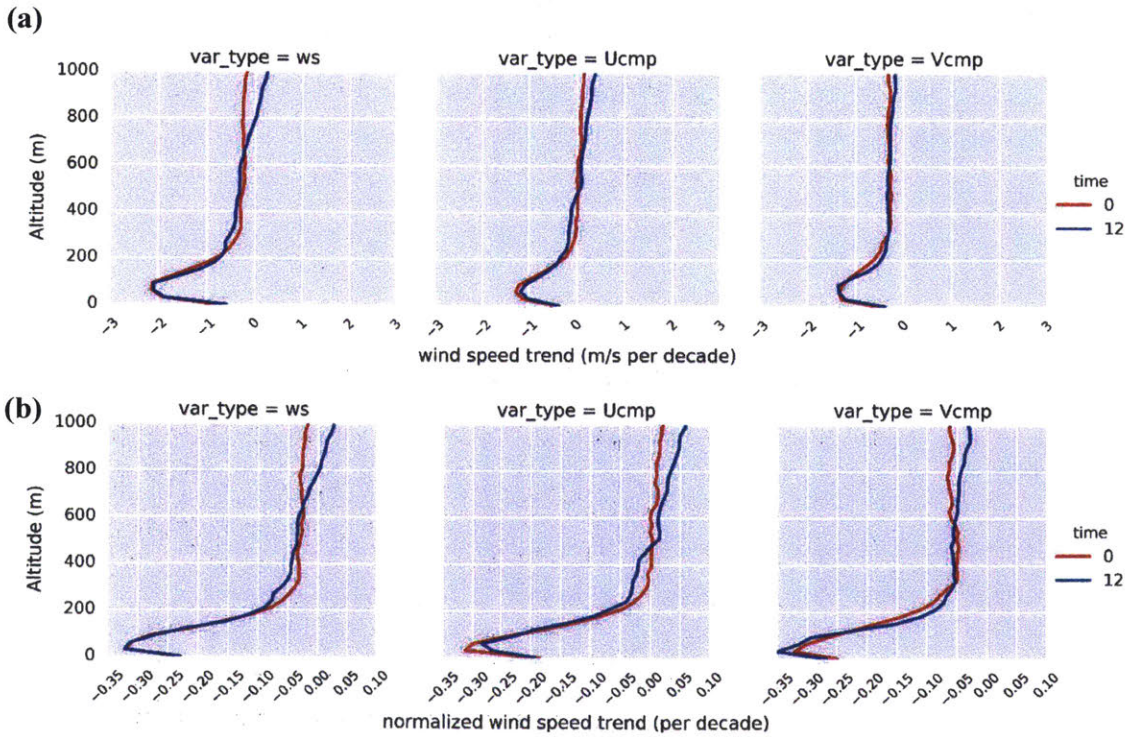

Figure 3-16: Lower part (0m-1000m) of the profile shown in **Figure 3-10**, 80°W-70°W. Panel (a) shows the (absolute) trends (m/s per decade) in wind speed (ws), zonal wind (Ucmp), and meridional wind (Vcmp). Panel (b) shows the corresponding normalized trends (per decade).

The lower part of the vertical profiles in **Figure 3-10** to **Figure 3-15** are shown in **Figure 3-16** to **Figure 3-21**.

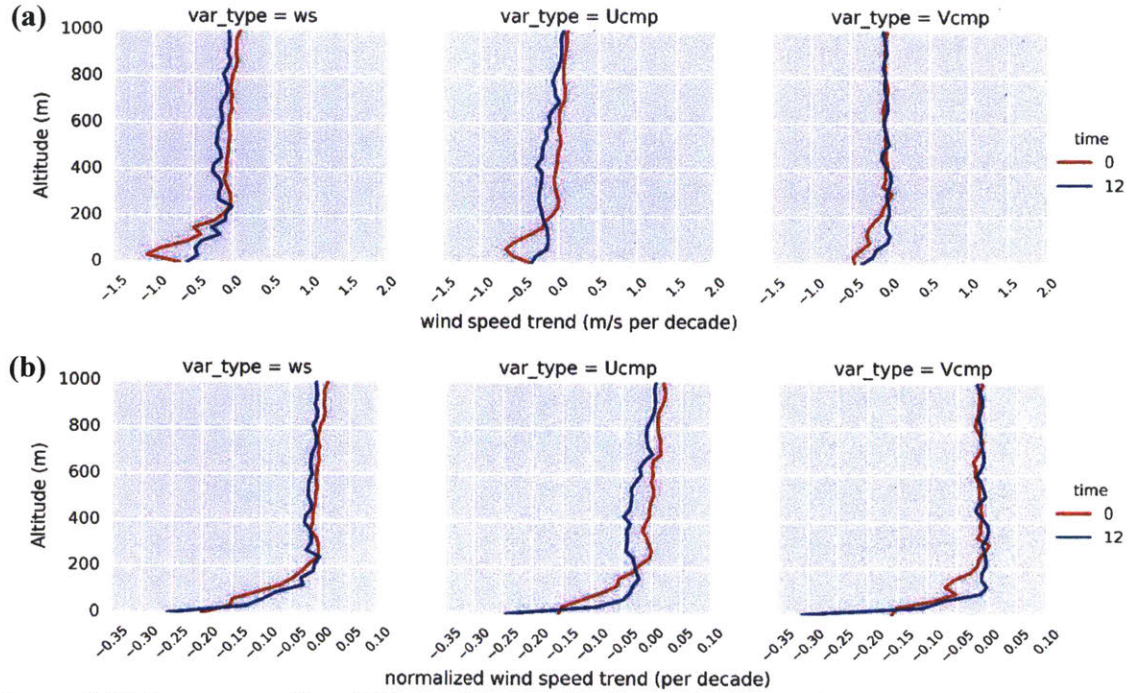

Figure 3-17: Lower part (0m-1000m) of the profile shown in **Figure 3-11**, 90°W-80°W. Panel (a) shows the (absolute) trends (m/s per decade) in wind speed (ws), zonal wind (Ucmp), and meridional wind (Vcmp). Panel (b) shows the corresponding normalized trends (per decade).

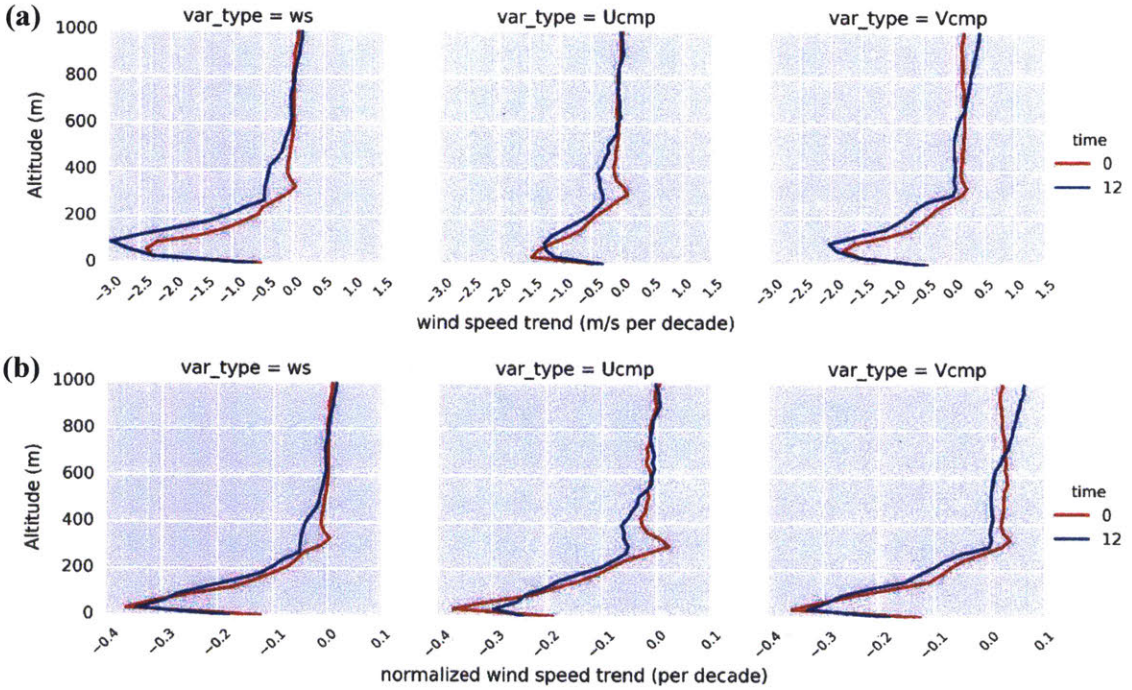

Figure 3-18: Lower part (0m-1000m) of the profile shown in **Figure 3-12**, 100°W-90°W. Panel (a) shows the (absolute) trends (m/s per decade) in wind speed (ws), zonal wind (Ucmp), and meridional wind (Vcmp). Panel (b) shows the corresponding normalized trends (per decade).

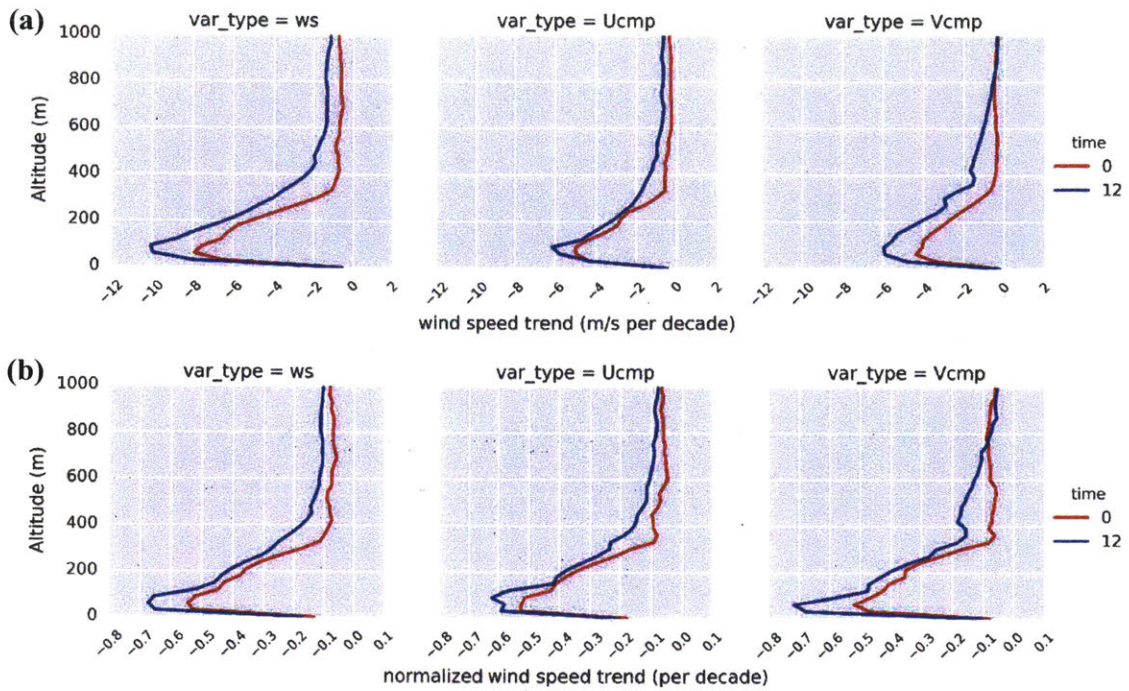

Figure 3-19: Lower part (0m-1000m) of the profile shown in **Figure 3-13**, 110°W-100°W. Panel (a) shows the (absolute) trends (m/s per decade) in wind speed (ws), zonal wind (Ucmp), and meridional wind (Vcmp). Panel (b) shows the corresponding normalized trends (per decade).

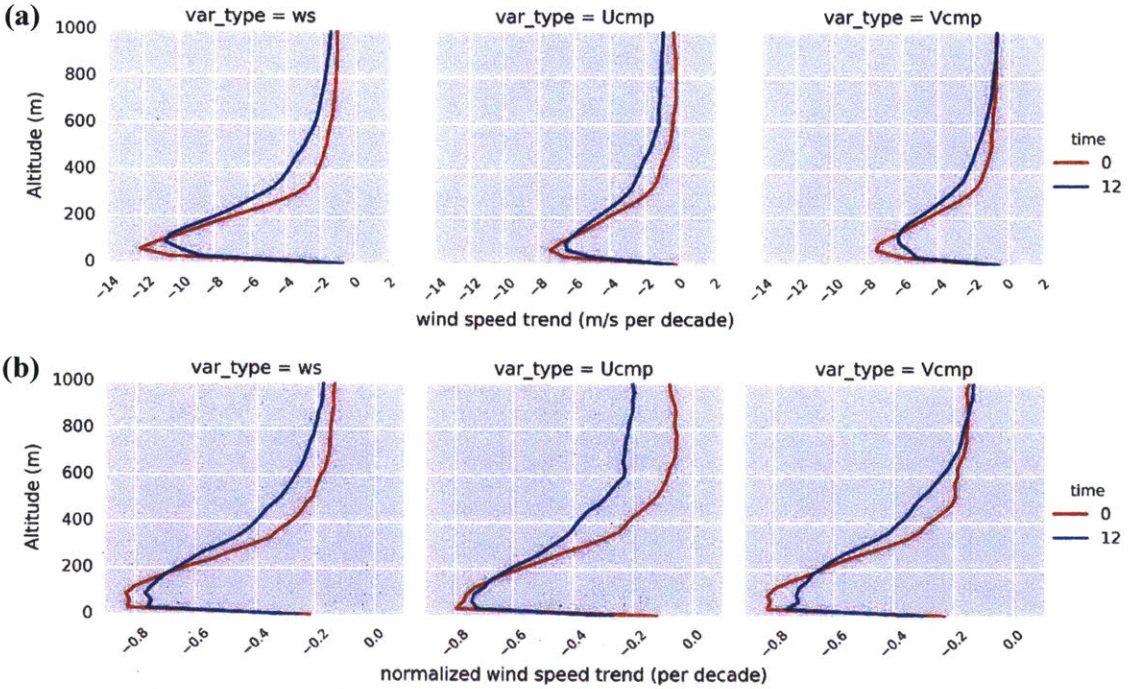

Figure 3-20: Lower part (0m-1000m) of the profile shown in **Figure 3-14**, 120°W-110°W. Panel (a) shows the (absolute) trends (m/s per decade) in wind speed (ws), zonal wind (Ucmp), and meridional wind (Vcmp). Panel (b) shows the corresponding normalized trends (per decade).

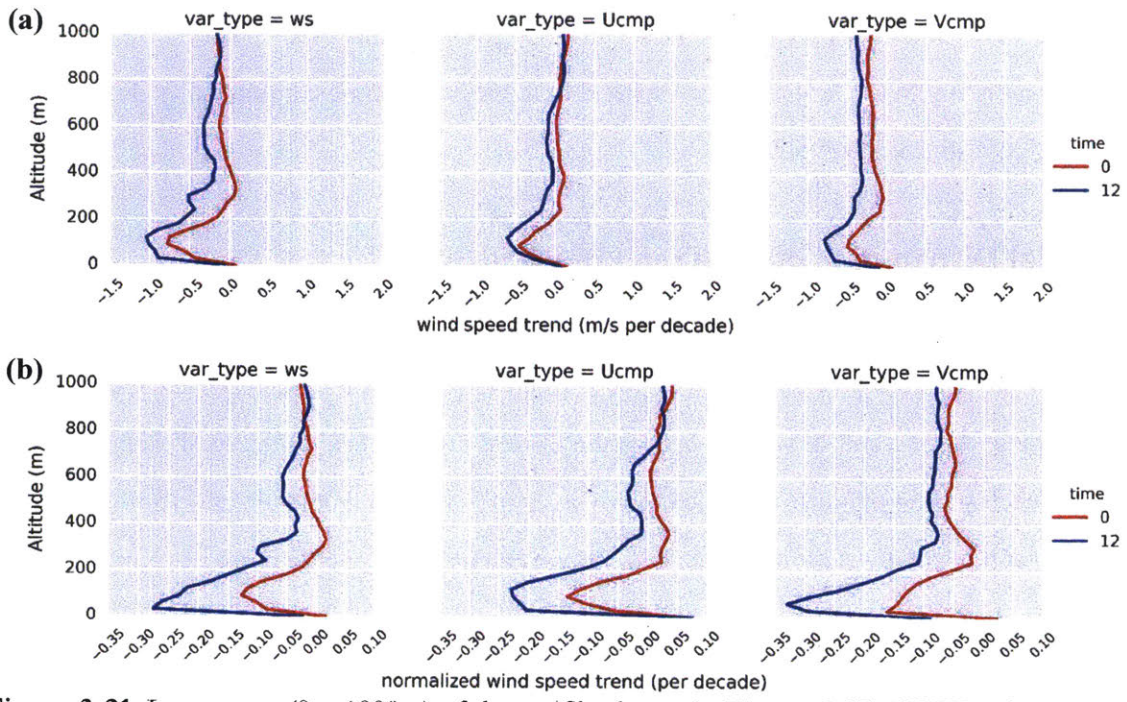

Figure 3-21: Lower part (0m-1000m) of the profile shown in **Figure 3-15**, 130°W-120°W. Panel (a) shows the (absolute) trends (m/s per decade) in wind speed (ws), zonal wind (Ucmp), and meridional wind (Vcmp). Panel (b) shows the corresponding normalized trends (per decade).

Table 3-2: Magnitudes of the trends in wind speed at the surface (0m) and the largest negative trend of each time zone. 'Absolute trend' refers to the values retrieved from Panel (a) from Figure 3-16 to Figure 3-21. 'Normalized trend' refers to the values retrieved from Panel (b) from Figure 3-16 to Figure 3-21.

Time zone	Number of stations	Absolute trend, surface (m/s per decade)	Absolute trend, largest negative trend (m/s per decade)	normalized trend, surface (per decade)	Normalized trend, largest negative trend (per decade)
80°W-70°W	9	-0.60	-2.1	-0.23	-0.33
90°W-80°W	15	-0.60	-1.1	-0.23	-0.23
100°W-90°W	14	-0.5	-3.0	-0.13	-0.37
110°W-100°W	13	-0.80	-10	-0.15	-0.65
120°W-110°W	10	-0.90	-12	-0.20	-0.80
130°W-120°W	4	-0.10	-1.0	-0.010	-0.28

The magnitudes of the trend in wind speed at the surface and the largest negative trend of each time zone are recorded in **Table 3-2**. Except the 4 stations in zone 130°W-120°W, the rest of the regions all indicate comparable normalized trend in wind speed for the surface (~20%). However, the largest negative trend in different regions varies largely from each other. Time zone 120°W-100°W indicates the biggest value in terms of the largest negative trend with

normalized trend equaling up to 70%. This value suggests that the wind speed in the vertical layer corresponding to the largest negative trend in the region declines dramatically during the time period investigated (1998-2011).

3.4 Spatial Distribution of the Trend in Wind Speed

Table 3-2 indicates that the magnitude of the largest negative trend peaks in the region between 120°W-100°W. To further examine the spatial distribution of the trend in wins speed, we calculate the average trend in wind speed of the closest layer to the surface with height of X meters for each station of North America. The values of X are 200, 500, 900, and 1500. That is to say, for each of the 89 stations in this dataset, we calculate the average trend in wind speed of the layers closest to the surface of each station. The height of these layers ranges from 200m, 500m, 900m, and 1500m.

Figure 3-22 shows results of the calculation described above. Only trends at 0 UTC are shown in **Figure 3-22**. The spatial distribution of the trends at 12 UTC which is similar to that at 0 UTC is listed in Appendix 3. **Figure 3-22** (a) shows the trend in the wind speed (m/s per decade) averaged vertically 200m above the surface of each station at 0 UTC. It suggests that for almost every one of the 79 sites in North America, the trend in wind speed is negative i.e. wind speed is decreasing near the surface over North America. Furthermore, for the contiguous US, the stations that shows smaller decreasing trend are concentrated in the eastern part of the US, while stations in the western US especially those located in the mountainous region shows a larger decreasing trend. **Figure 3-22 (b) – (d)** show similar trends averaged vertically over 500m, 900m, and 1500m above the surface of each station, respectively. They suggests that the magnitudes of the average trends become smaller as the height of the layer increases, which is in consistent with the previous finding that the largest negative trend is close to the surface (50 - 80m above the surface).

On the other hand, **Figure 3-22 (b) – (d)** show similar spatial pattern as **Figure 3-22 (a)** that the decreasing trend in wind speed is larger at sites located in the mountainous region. As shown in **Figure 2-3**, these stations in the mountainous west are characterized by the high elevation from the sea level. This finding is consistent with the "elevation-dependent" wind speed trend previously reported for the Tibetan Plateau (Lin et al., 2013) and Alps (McVicar

et al., 2010) which describes that the near surface wind speed over the elevated region experiences more significant decreases than lower regions.

Figure 3-23 shows the relations between the trend corresponding to the layer of X meters (X=200, 500, 900, and 1500) and the elevation of the station. It suggest that magnitude of the decreasing trend is positively associated with the elevation of the stations i.e. stations with higher elevation are associated with larger magnitude of decrease in its near-surface wind speed. This finding is in support of the preceding elevation-dependence of relation.

Another characteristic of the stations with higher elevation is that the decreasing trend in wind speed extends to much higher altitude than the non-elevated stations. **Figure 3-24** shows the spatial distribution of the trend in wins speed of each station at constant height surface above the ground of each station (A.G.L. 4800m, 6000m) and constant pressure surface (700hPa, 500hPa). It shows that the trends in wind speed at the stations with high elevation are still negative at these upper level, while the trends of the non-elevated are positive at these levels. Moreover, the negative trends of these elevated stations are statistically significant (p<0.05). Since the influence of the surface is indirect at these levels, such pattern suggests that the decreasing trend of wind speed of the elevated sites is not dominated by the changes in land roughness. Instead, changes in atmospheric circulation may also influence the trends wind speed at these elevated locations. This finding is consistent with Lin et al. (2013) and Guo et al., (2016) on the trend of surface and upper-level wind speed over the Tibetan Plateau. Both of them suggest a distinct feature of elevated regions that these regions are more sensitive to changes in large scale circulation than the non-elevated regions.

(a) Averaged over 200m above the surface

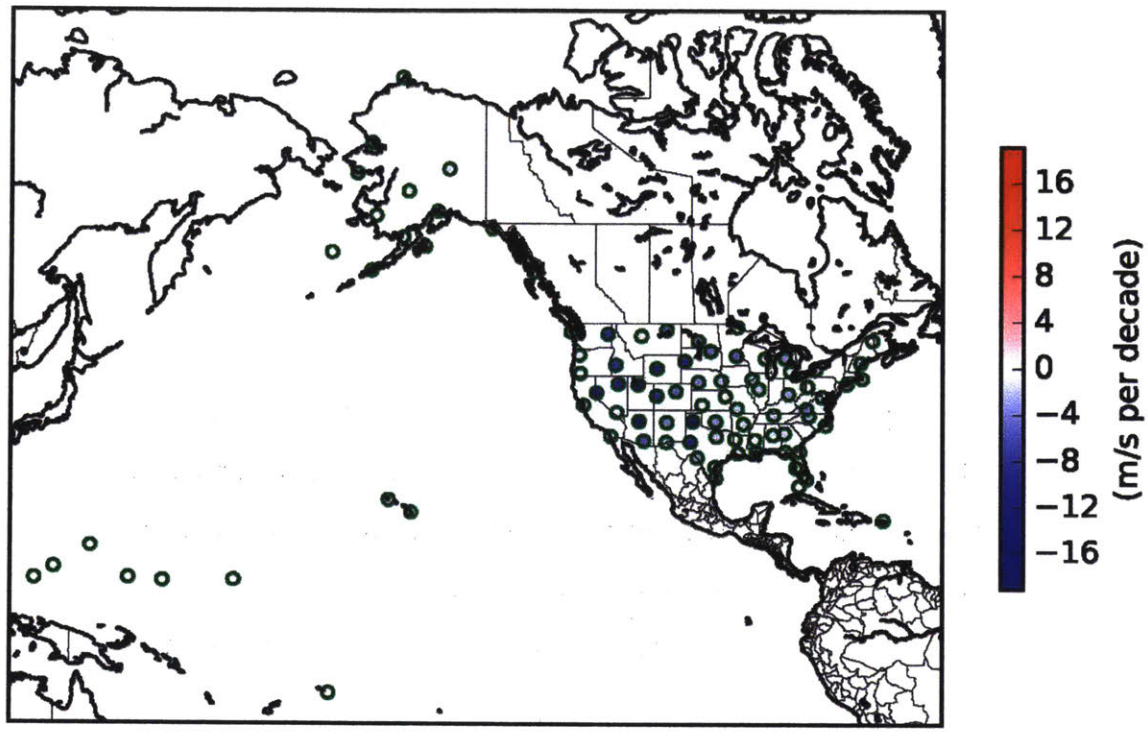

(b) Averaged over 500m above the surface

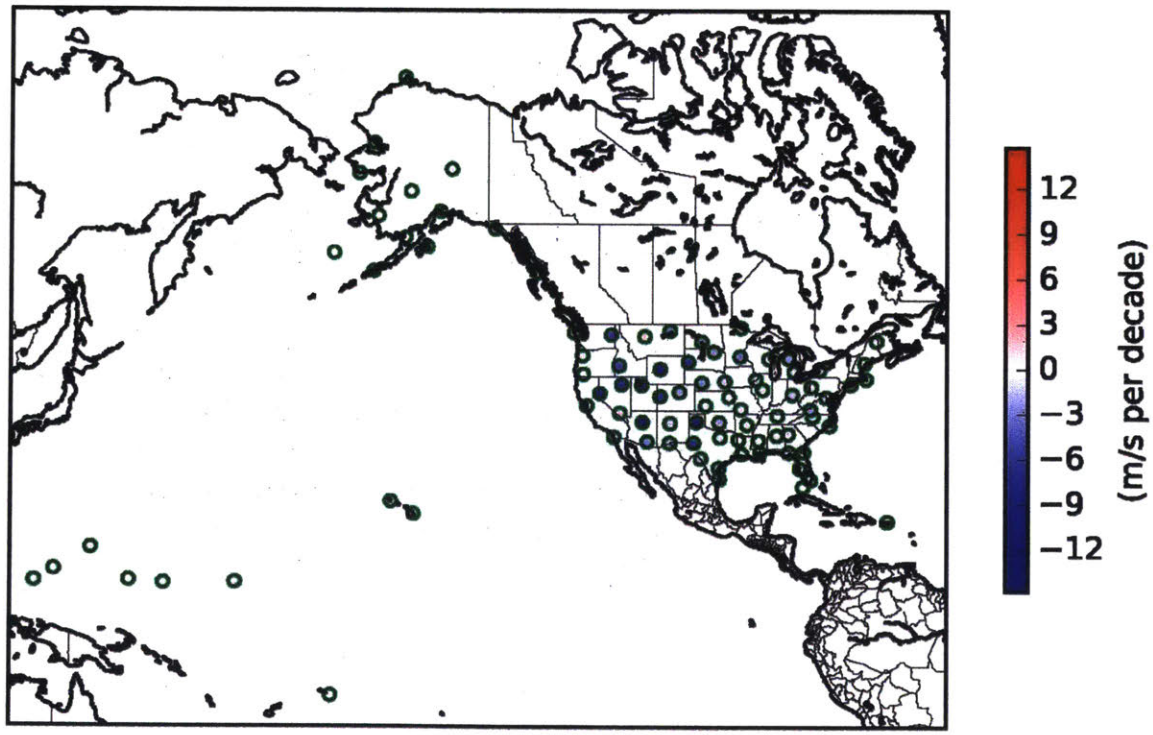

(c) Averaged over 900m above the surface

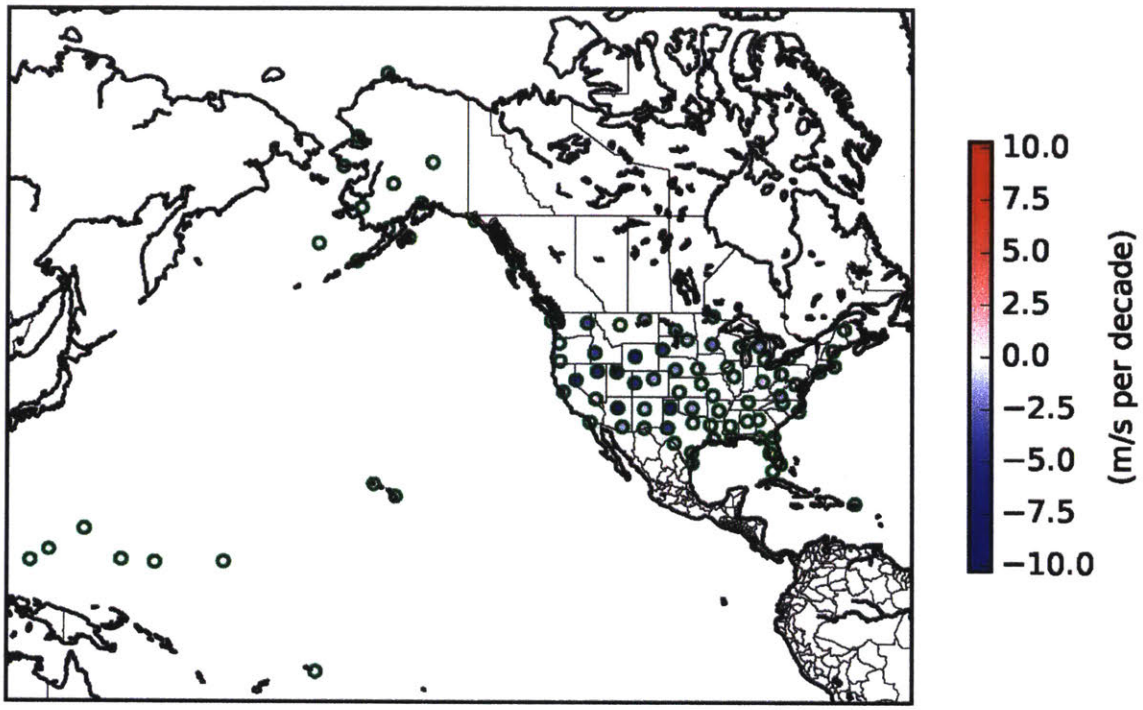

(d) Averaged over 1500m above the surface

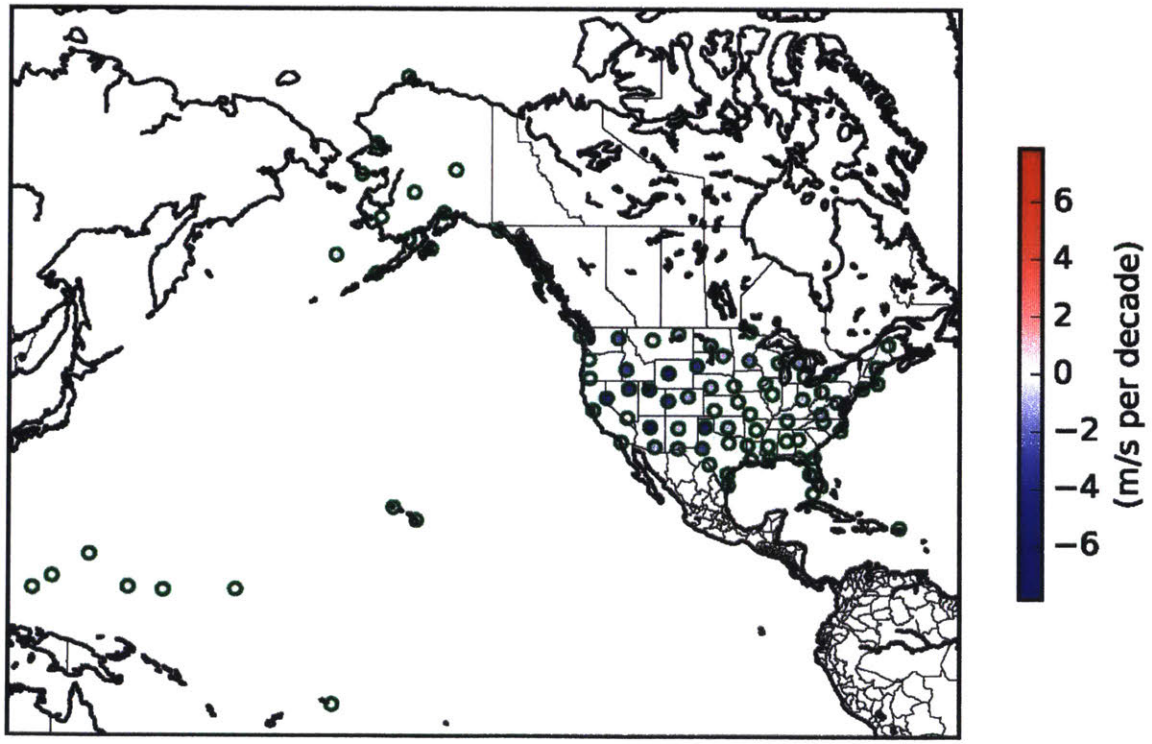

Figure 3-22: Spatial distribution of the trend in wind speed (m/s per decade) at 0 UTC averaged vertically over (a) 200m, (b) 500m, (c) 900m, and (d) 1500m above the surface of each station.

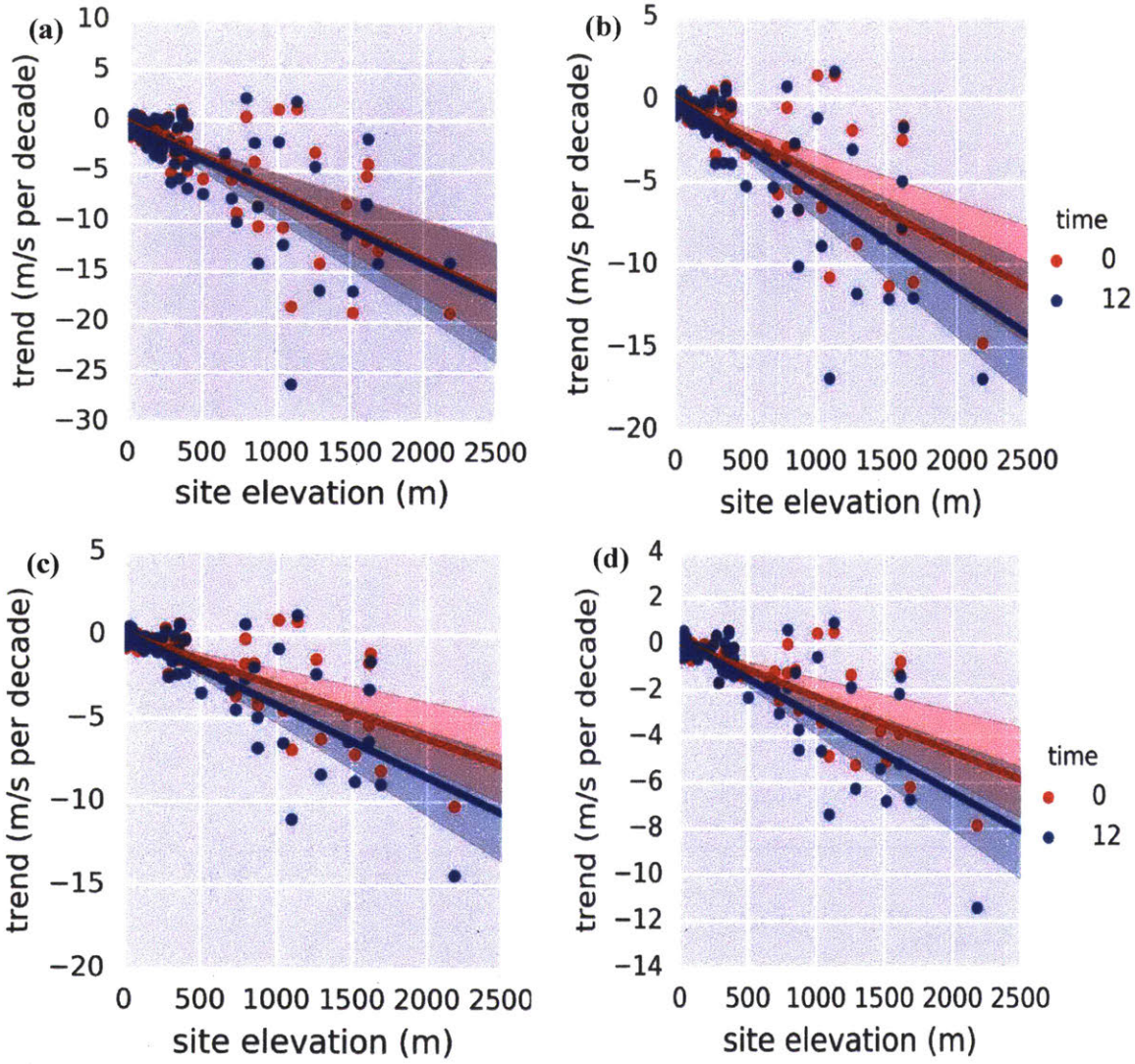

Figure 3-23: Relations between the trends in the wind speed (m/s per decade) averaged vertically over (a) 200m, (b) 500m, (c) 900m, and (d) 1500m above the surface of each station and the elevation of the stations.

(a) Trends at 4800m (A.G.L.)

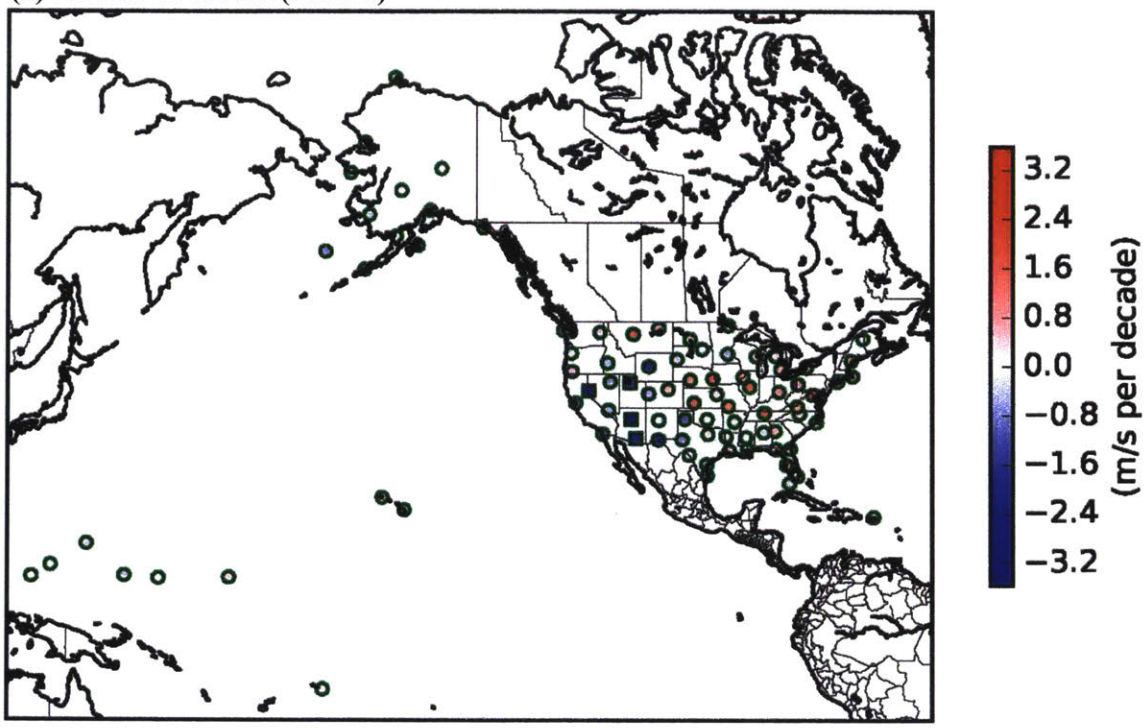

(b) Trends at 6000m (A.G.L.)

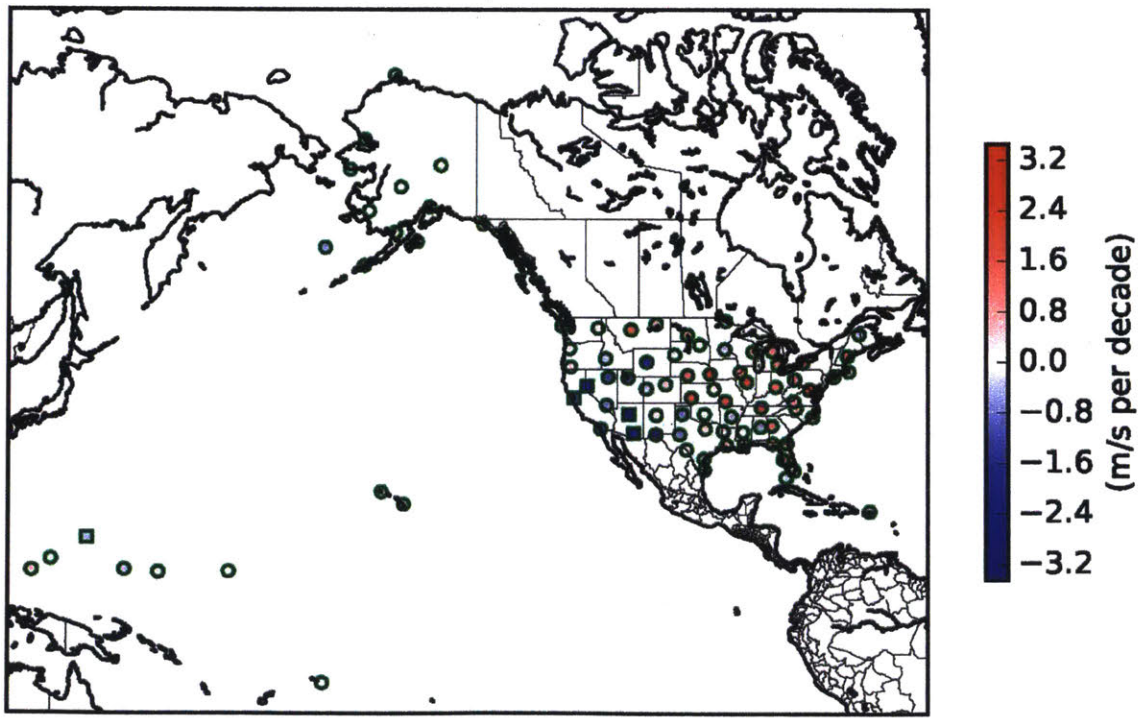

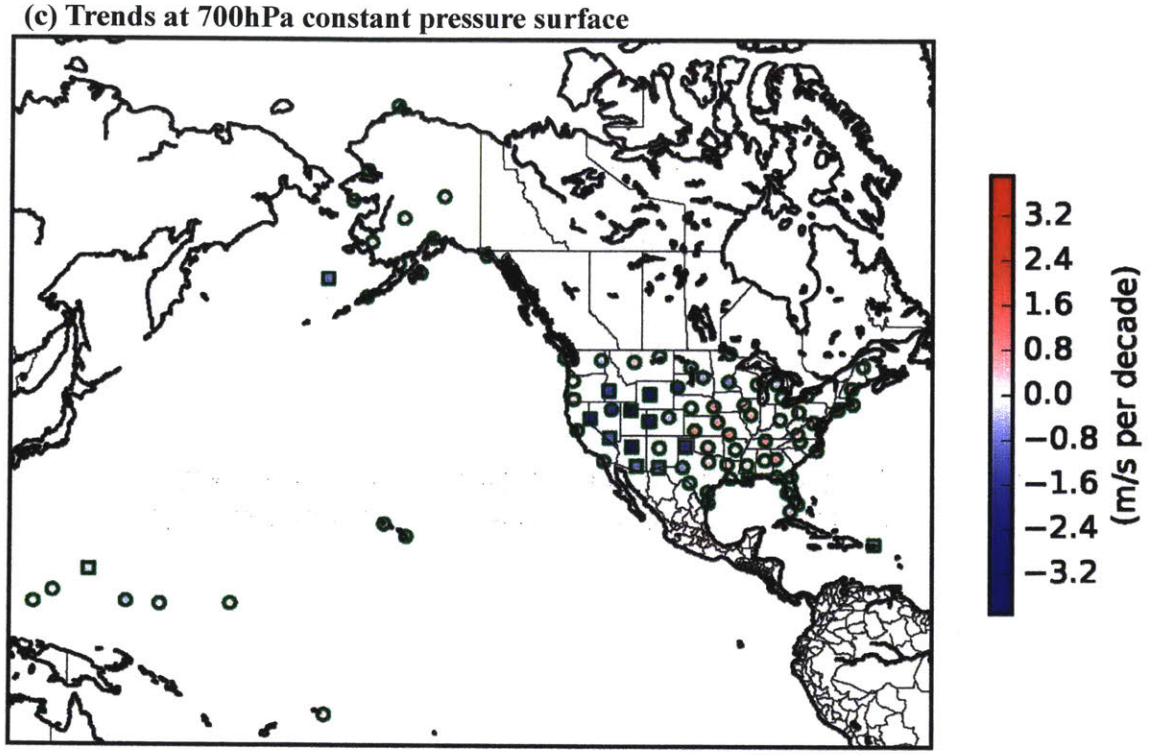

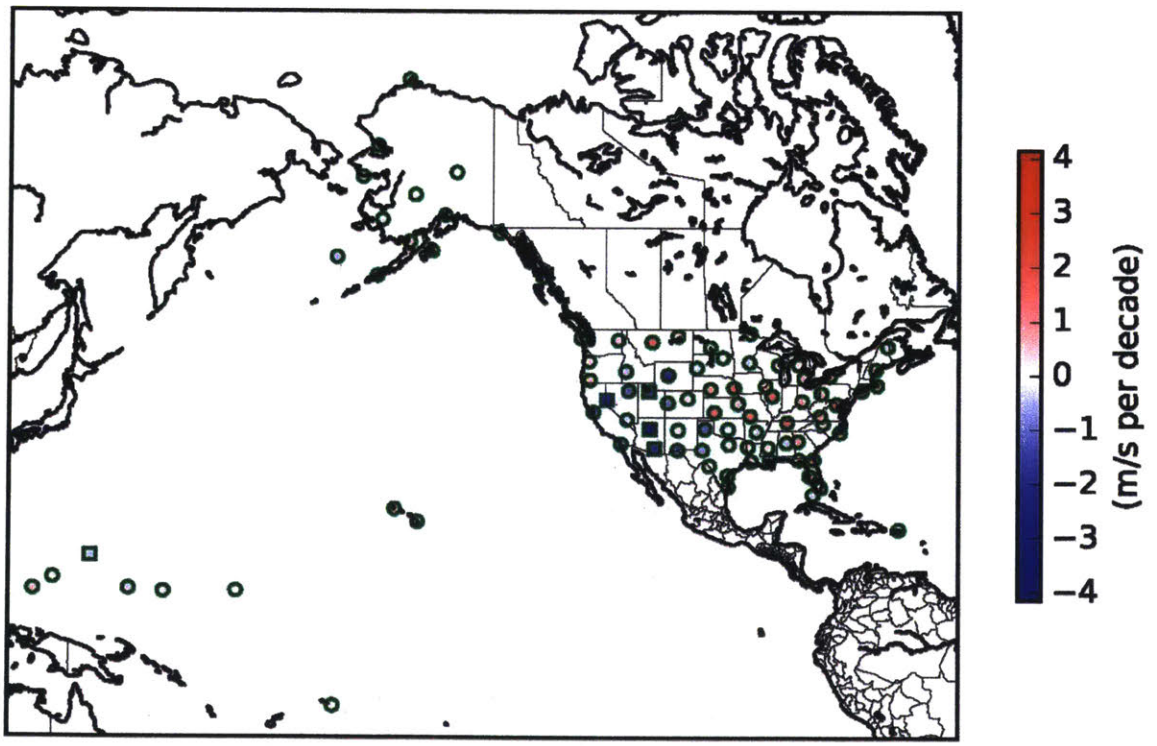

Figure 3-24: Spatial distribution of the trend in wind speed (m/s per decade) at 0 UTC at (a) 4800m A.G.L., (b) 6000m A.G.L., (c) 700hPa constant pressure surface, and (d) 500hPa constant pressure surface. The square denotes the stations with statistically significant (p<0.05) decreasing trend at the corresponding level.

3.5 The influence of changes in measuring frequency on the trends

As discussed in section 2.1 that the dataset used this work spans a period during which NOAA progressively upgraded their upper air stations. As a result, 52 stations out of 89 stations in this dataset experienced a change of vertical measuring frequency from 6 second to 1 second during 2005-2008. Two types of test i.e. checking the distribution of the 1-second data and calculating the mean-to-standard-deviation ratio have been implemented to examine the influence of changes in measuring frequency on the trends. The results of these tests suggest that this change of measuring frequency do not result significant biases in the data. However, these two types of test are not directly related to the calculation of the trends in wind speed. In this section, we examine the influence of such changes on the trends by comparing the results based solely on the 6-second data and the previous results which are based on both data.

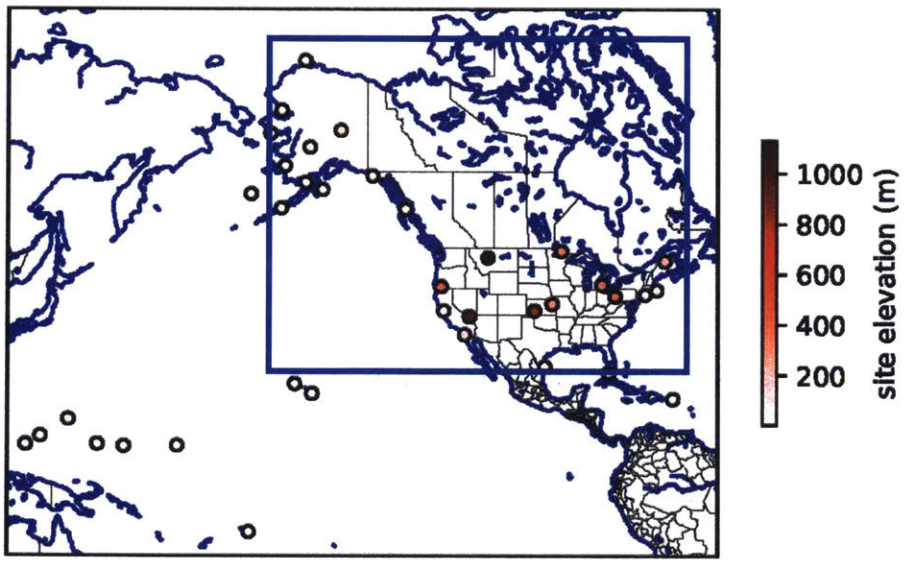

Figure 3-25: 37 stations whose measuring frequency does not change. The color of the dots represents the elevation with darker color indicating higher elevation. Stations in the blue rectangle are included in the calculation of trends.

Figure 3-25 shows the 37 stations whose measuring frequency does not change. In order to compare with the vertical profile of trend in wind speed calculated previously for North America, we only include 26 stations located in North America from them to calculate the trends. The calculation is based on A.G.L. coordinate. The results are shown in **Figure 3-26**. Although the largest negative trend still exists, the magnitude is much smaller than that in **Figure 3-2**. **Figure 3-27** shows the lower part (0m-1000m) of the vertical profile shown in

Figure 3-26. It reads that the largest negative trend is 0.07 per decade which is only 1/8 of the value calculated based on both 1-second and 6-second data as shown in **Figure 3-2**.

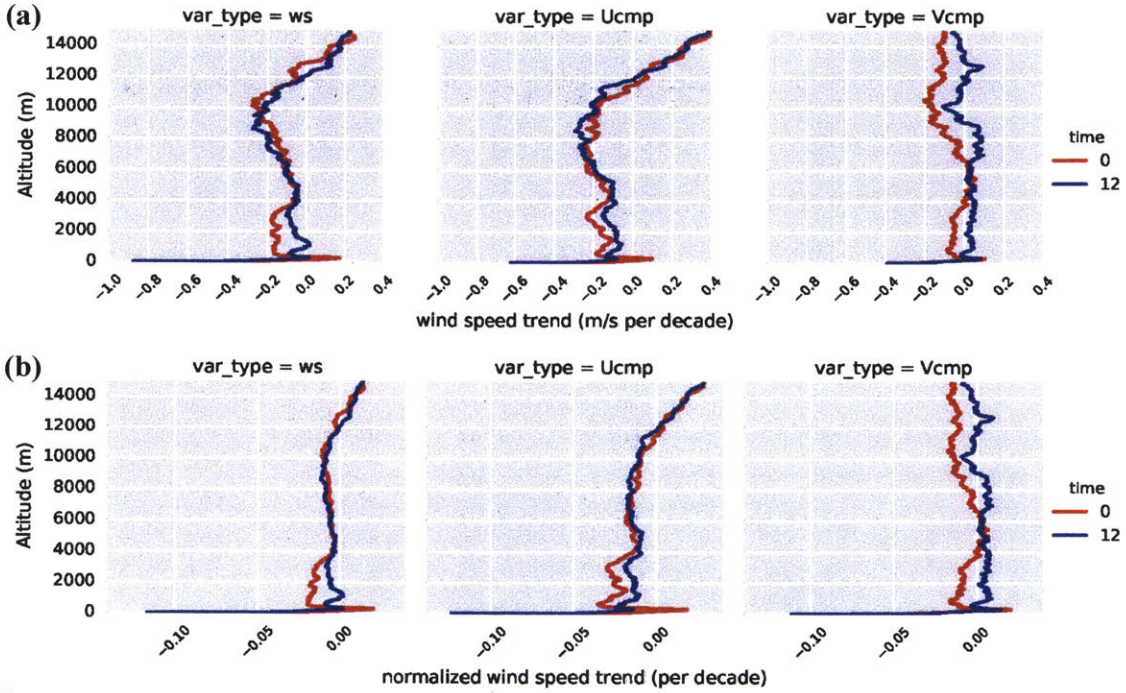

Figure 3-26: For 26 stations whose measuring frequency does not change. Vertical profile of trends in wind speed with A.G.L. vertical coordinate. The upper panel (a) shows the (absolute) trends (m/s per decade) in wind speed (ws), zonal wind (Ucmp), and meridional wind (Vcmp). The lower panel (b) shows the corresponding normalized trends (per decade).

Figure 3-28 shows the stations whose measuring frequency changes during 2005-2008. The vertical profile of the trends in wind speed is shown in **Figure 3-29** and **Figure 3-30** (0m-1000m). They show that the profile of these stations is similar to the previous results in terms of the shape and magnitude of the largest trend. This finding may indicate that the larger magnitude shown in previous results may simply reflect the artifacts of this change of measuring frequency. The difference between the results based on 6-second data and the results based on both 6-second and the 1-second data may also be due to the higher elevation of stations whose measuring frequency changes as shown in **Figure 3-25** and **Figure 3-28**. To further test this hypothesis, we first group the 52 stations whose measuring frequency changes into three based on its elevation i.e. (1) stations with elevation lower than 200m, (2) stations with elevation higher than 1000m, and (3) stations with elevation in between.

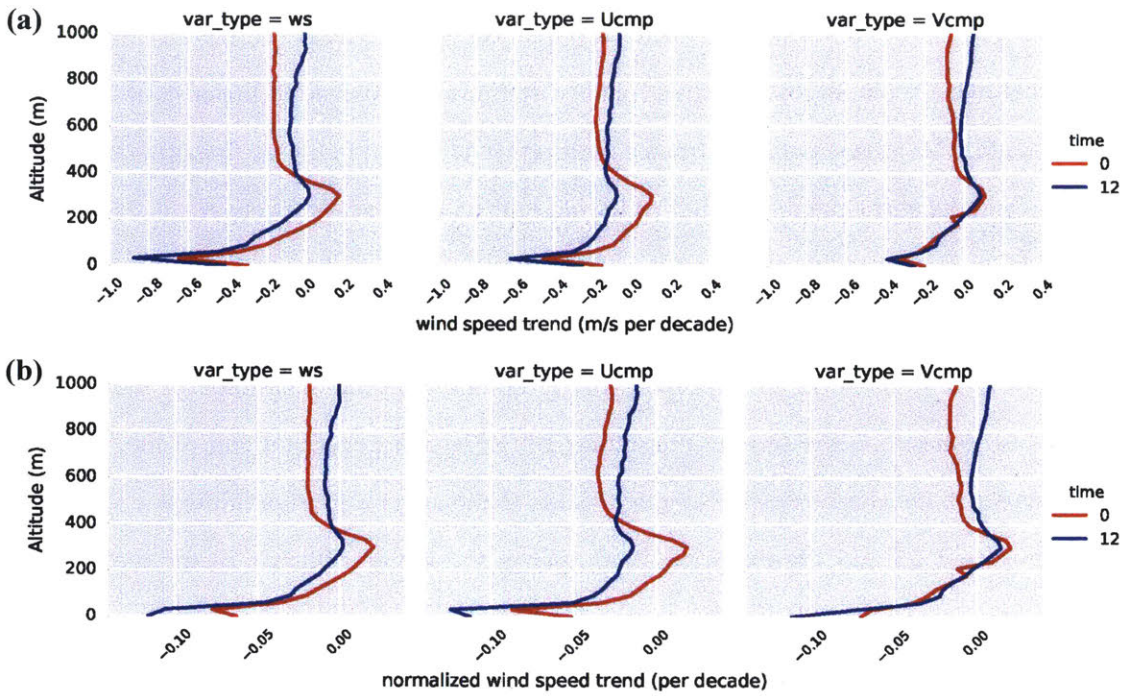

Figure 3-27: For 26 stations whose measuring frequency does not change. Lower part (0m-1000m) of the vertical profile of trends in wind speed with A.G.L. vertical coordinate. Panel (a) shows the (absolute) trends (m/s per decade) in wind speed (ws), zonal wind (Ucmp), and meridional wind (Vcmp). Panel (b) shows the corresponding normalized trends (per decade).

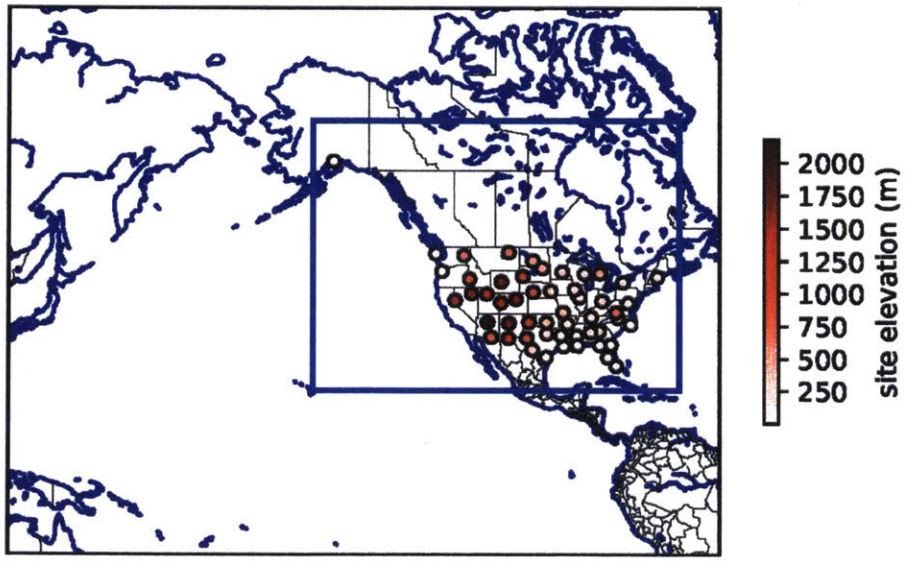

Figure 3-28: 52 stations whose measuring frequency changes. The color of the dots represents the elevation with darker color indicating higher elevation. Stations in the blue rectangle are included in the calculation of trends.

Figure 3-31 to **Figure 3-33** show the trends corresponding to the stations with elevation lower than 200m, elevation higher than 1000m, and elevation in between, respectively. They

shows that the trends at the surface are identical (equals to 0.2 per decade) across all three types of stations. However, the largest negative trend of stations with elevation lower than 200m is 0.33 per decade. The largest negative trend of stations with elevation higher than 1000m is 0.8 per decade. And the corresponding trends of the stations with elevation in between is 0.55. This finding is in consistent with the elevation dependence relation discussed in section 3.4. Moreover, it suggests that even within the 52 stations with changes in measuring frequency, elevation of the stations plays an important role in determining the magnitude of the largest negative trend. Therefore, the smaller magnitude of the largest negative trend of the stations with no changes in measuring frequency may be due to the lower elevation of these stations as shown in **Figure 3-25** and **Figure 3-28**. To further examine the influence of the measuring frequency on the trends, we calculate the trends only using the 6-second data available for those 52 stations described above. The results are shown in **Figure 3-34**.

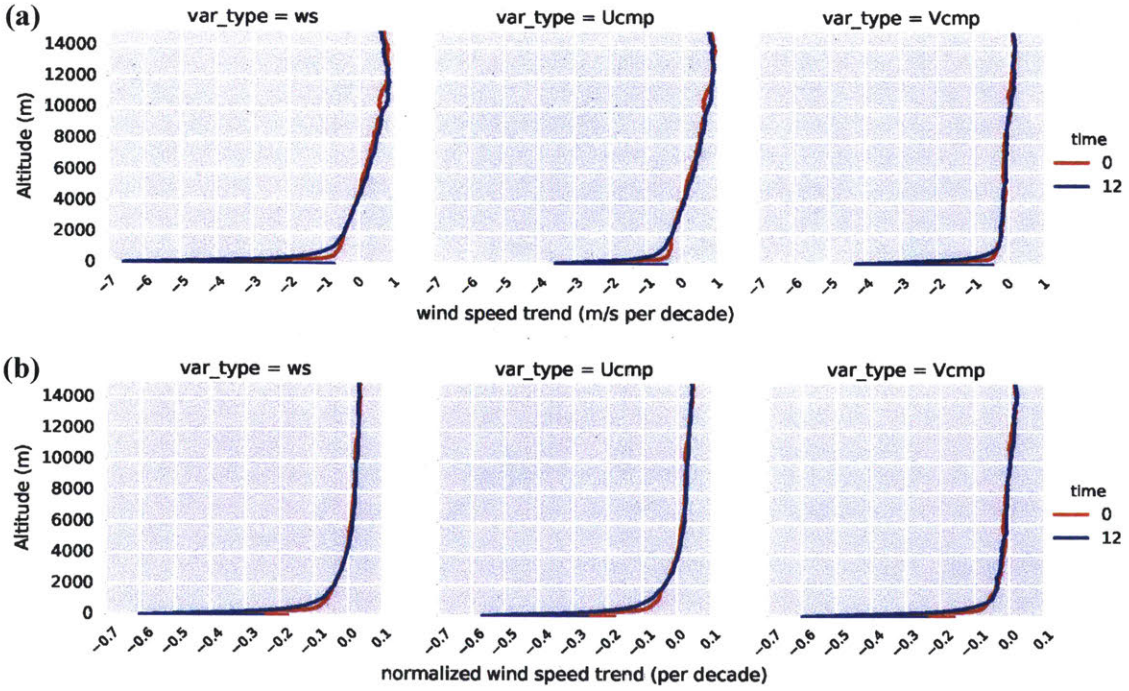

Figure 3-29: For 52 stations whose measuring frequency changes. Vertical profile of trends in wind speed with A.G.L. vertical coordinate. The upper panel (a) shows the (absolute) trends (m/s per decade) in wind speed (ws), zonal wind (Ucmp), and meridional wind (Vcmp). The lower panel (b) shows the corresponding normalized trends (per decade).

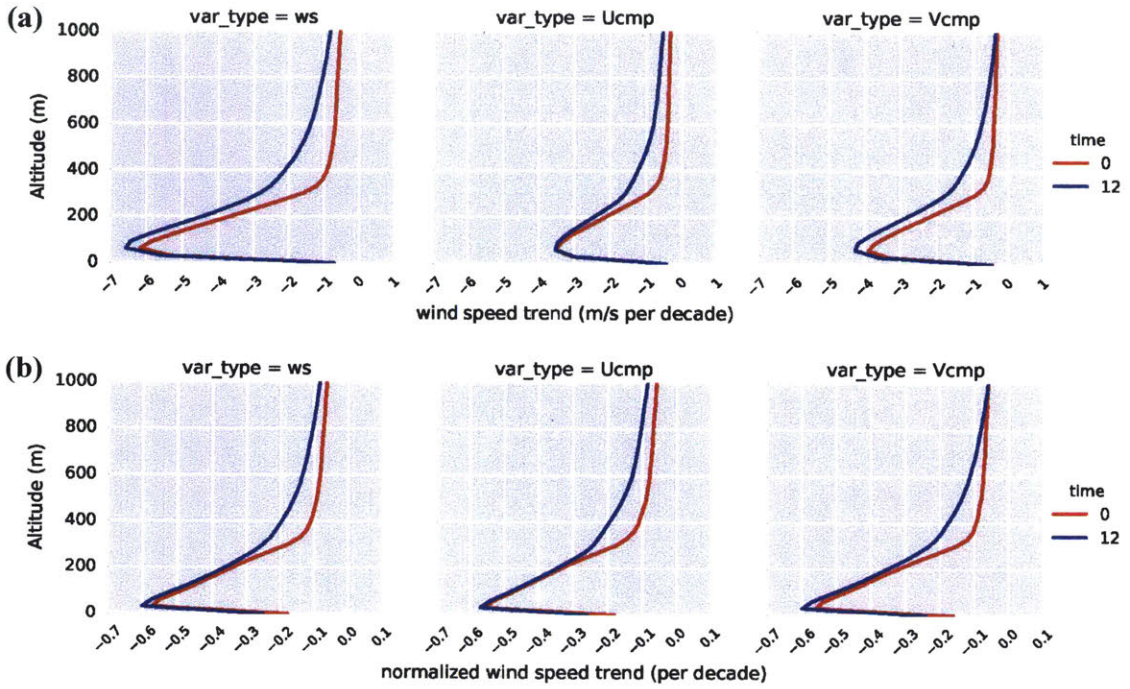

Figure 3-30: For 52 stations whose measuring frequency changes. Lower part (0m-1000m) vertical profile of trends in wind speed with A.G.L. vertical coordinate. Panel (a) shows the (absolute) trends (m/s per decade) in wind speed (ws), zonal wind (Ucmp), and meridional wind (Vcmp). Panel (b) shows the corresponding normalized trends (per decade).

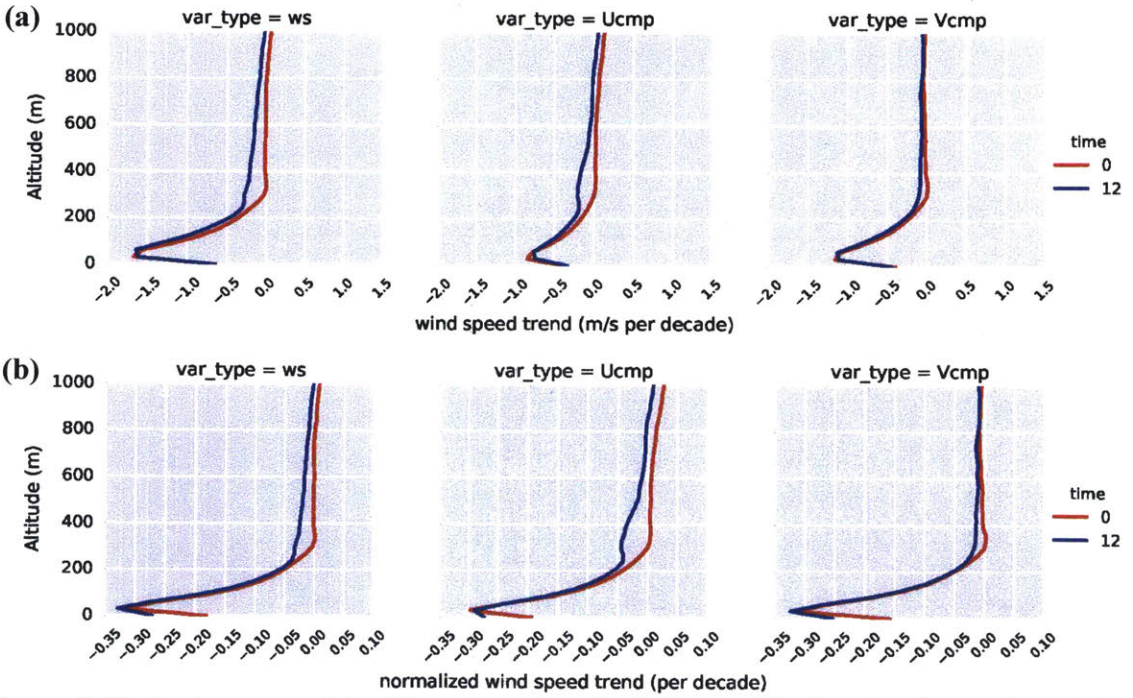

Figure 3-31: Stations out of the 52 stations described above with elevation lower than **200m**. Lower part (0m-1000m) vertical profile of trends in wind speed with A.G.L. vertical coordinate. Panel (a) shows the (absolute) trends (m/s per decade) in wind speed (ws), zonal wind (Ucmp), and meridional wind (Vcmp). Panel (b) shows the corresponding normalized trends (per decade).

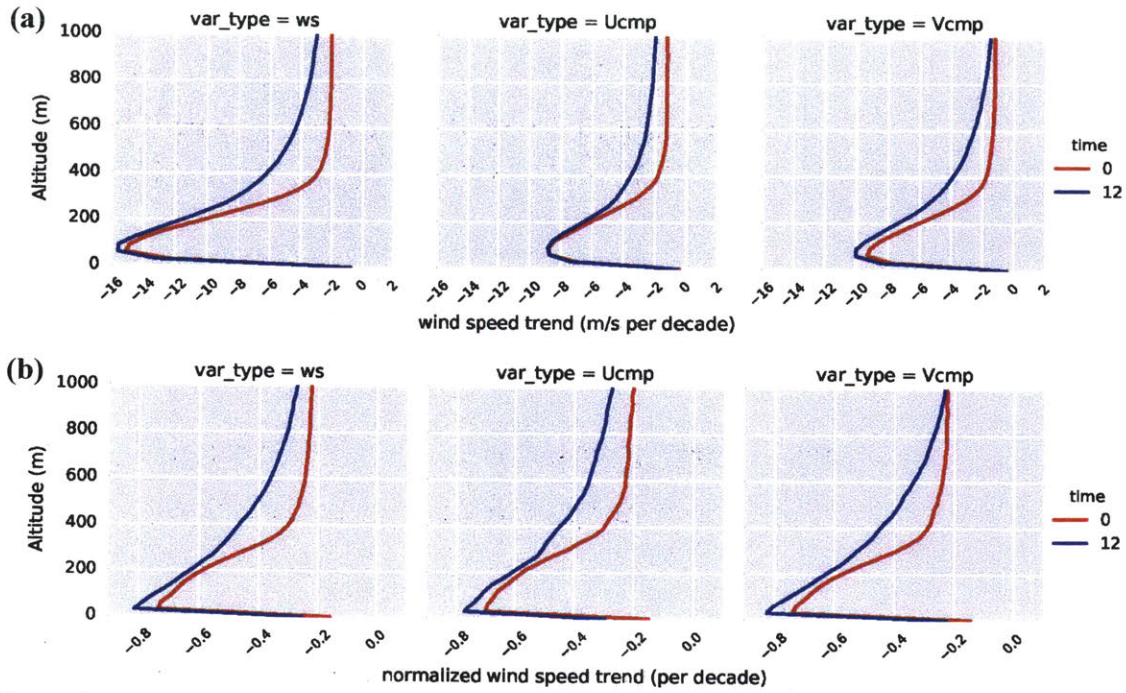

Figure 3-32: Stations among the 52 stations described above with elevation higher than **1000m**. Lower part (0m-1000m) vertical profile of trends in wind speed with A.G.L. vertical coordinate. Panel (a) shows the (absolute) trends (m/s per decade) in wind speed (ws), zonal wind (Ucmp), and meridional wind (Vcmp). Panel (b) shows the corresponding normalized trends (per decade).

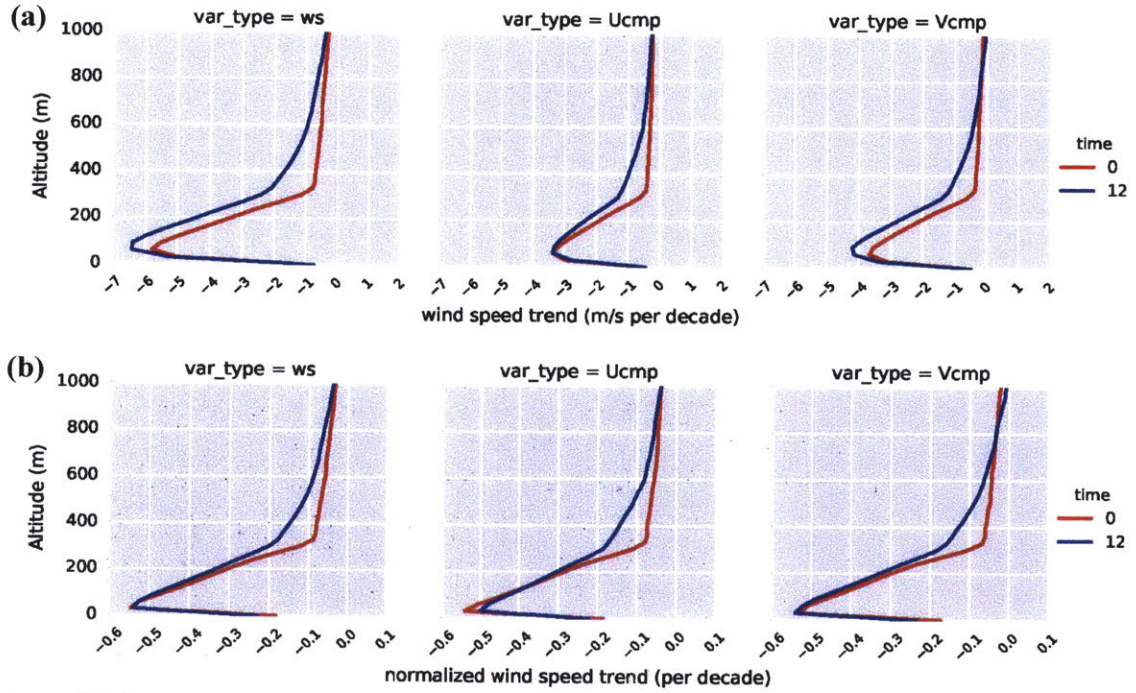

Figure 3-33: Stations among the 52 stations described above with elevation lower than **1000m** but higher than 200m. Lower part (0m-1000m) vertical profile of trends in wind speed with A.G.L. vertical coordinate. Panel (a) shows the (absolute) trends (m/s per decade). Panel (b) shows the normalized trends (per decade).

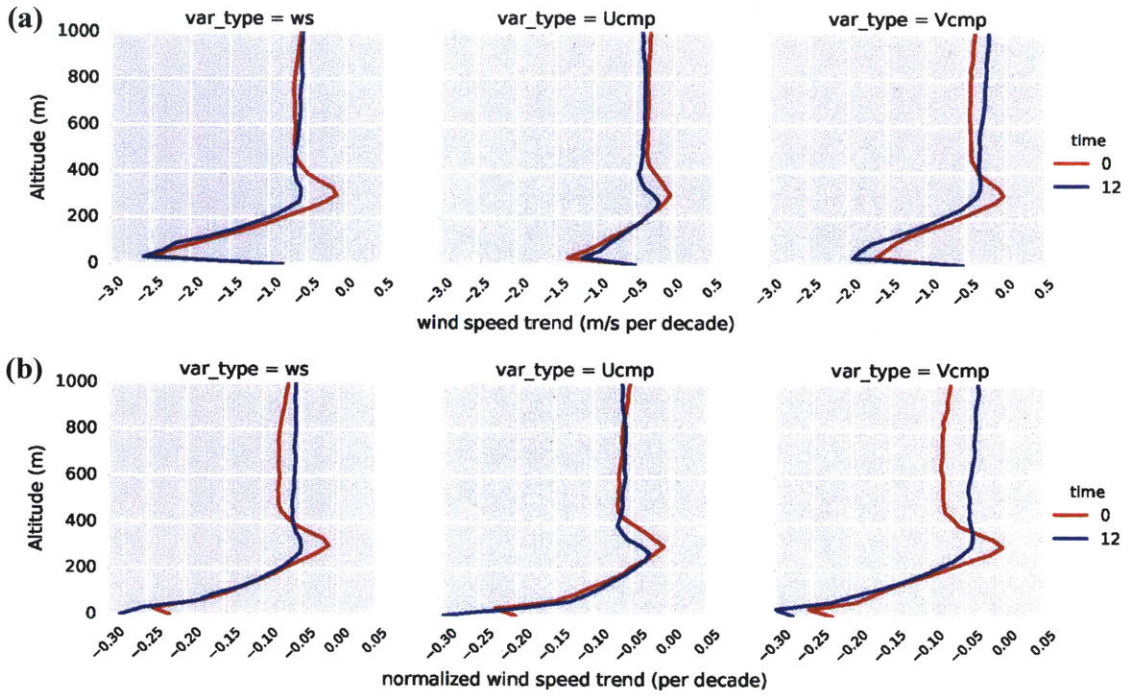

Figure 3-34: For the 52 stations described above, but utilize the 6-second data available at these stations Lower part (0m-1000m) vertical profile of trends in wind speed with A.G.L. vertical coordinate. Panel (a) shows the (absolute) trends (m/s per decade). Panel (b) shows the normalized trends (per decade).

Figure 3-34 shows the trends calculated based only on the 6-second data available at the 52 stations with changes in measuring frequencies. Comparing **Figure 3-34** with **Figure 3-27**, the largest negative trend of the former is still twice of that of the latter, which means that there exists factors other than changes in measuring frequency such as the elevation of the stations that cause the larger magnitude of largest negative trend of the 52 stations, because both **Figure 3-27** and **Figure 3-34** are based on 6-second data. These comparisons suggests that the changes in measuring frequency may cause some biases, but are not the sole cause of the largest negative trend.

Chapter 4

Conclusions and future work

Through the analysis of the high resolution radiosonde measurements over the US, we identified a similar vertical wind speed trend profile to Vautard et al. (2010), with a decreasing trend near the surface and an increasing trend in the upper level. However, the coarse resolution data used in Vautard et al. (2010) did not capture the vertical evolution of the wind speed and lead to missing of important information such as the transition from negative trend to positive trend. By utilizing height above ground as the vertical coordinate, we increased the data points near the surface and therefore obtained a smoother trend profile. It suggests that the decreasing trend of near-surface wind speed is statistically significant ($p<0.05$). However, the statistical significance of the decreasing trend drops with increases in altitude. We used three methods including the bulk Richardson number method, the air parcel method, and the elevated inversion method to estimate the height of planetary boundary layer. The first two methods generate similar estimates while estimates by the last method are much higher than the preceding two. We identified a largest negative trend in wind speed close to the surface (50-80m) for North America. The magnitude of this largest negative trend is up to 15 times of the value reported in the previous studies, which might be due to the higher vertical resolution used in this study, or it may be a result of the shorter record of wind speed in this calculation. By comparing the average trend for daytime and nighttime in wind speed for each time zone, we do not observe significant differences except in the western region of the U.S., which suggests

that the largest negative trend may not be a nighttime phenomenon such as the nocturnal jet.

We found a relationship between the elevation of the sites and trend of near-surface wind and wind aloft. We identified a statistically significant negative association between the average trend in wind speed of the near-surface layers (200m/500m/900m/1500m) and the elevation of the stations, indicating that stations with higher elevation are accompanied with a larger decreasing wind speed trend. For non-elevated sites, decreasing trend is seldom found for wind above the PBL, suggesting the important role of land surface in determining the trend of wind speed. For elevated sites such as those in the mountainous west of the US, decreasing trend is found for both near-surface wind and wind aloft, indicating that the changes in free-tropospheric circulation may also influence the wind speeds. This elevation-dependence relation is consistent with the findings of studies on wind speed over the Tibetan Plateau as discussed above.

Note that both the time period (1998 – 2011) and the geographical range (US) of this study, are covered in Vautard et al. (2010). However, the elevation-dependence relation is not uncovered in that study. Possible explanations is that Vautard et al. [10] utilized pressure rather than A.G.L. as the vertical coordinate. The implication is that height above the ground (A.G.L.) is a useful vertical coordinate for dealing with *in-situ* vertical wind observations. It is especially useful when the locations of the stations are at different levels of elevation and/or the research focus is the influence of surface on layers aloft. Since the largest negative trend is not reported in any previous works on the trends of wind speed, for future work, it is necessary to utilize high-vertical-resolution radiosonde data from other sources to test if this near-surface largest negative trends is statistically robust.

Appendix

A1 Distributions of the 6-Second Data and the 1-Second Data

We plot the distribution (see **Figure A1**) of wind speed measured by the two devices. The distribution is fitted using the kernel density estimation method. There are no significant differences between the distributions of two types of data, so it is unlikely that the instrumental change causes significant measurements biases.

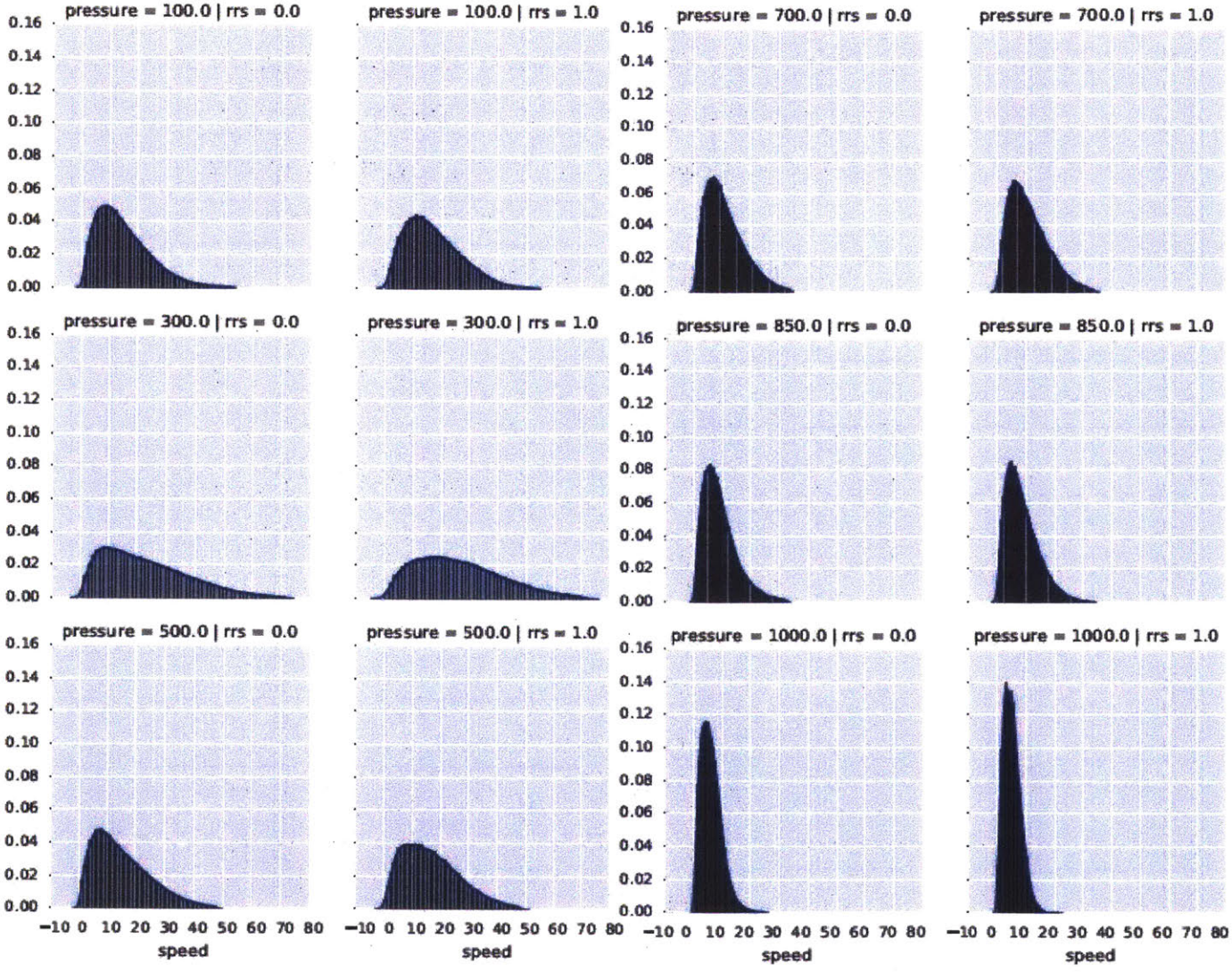

Figure A1: Station Elko, NV. Distribution wind speed data at the selected pressure level. rrs = 0 denotes the distribution of the 6-second data, and rrs = 1 denotes the distribution of the 1-second data. The pressure on the left panel is 100hPa, 300hPa, and 500hPa, and that on the right is 700hPa, 850hPa and 1000hPa.

A2 Ratio between the annual mean to the corresponding standard deviation

We further test the influence of instrumental changes on data quality by calculating the ratio between annual mean wind speed and the corresponding standard deviation (see **Figure A2**). Here we use the site Elko, NV as an example. If there is no significant differences between before and after instrumental changes, then it is not a concern for data consistency. We find that the values of mean/std does not change significantly before and after the instrumental change, so the data measured by these types of devices are consistent.

(a) Pressure level: 100hPa, 300hPa, and 500hPa

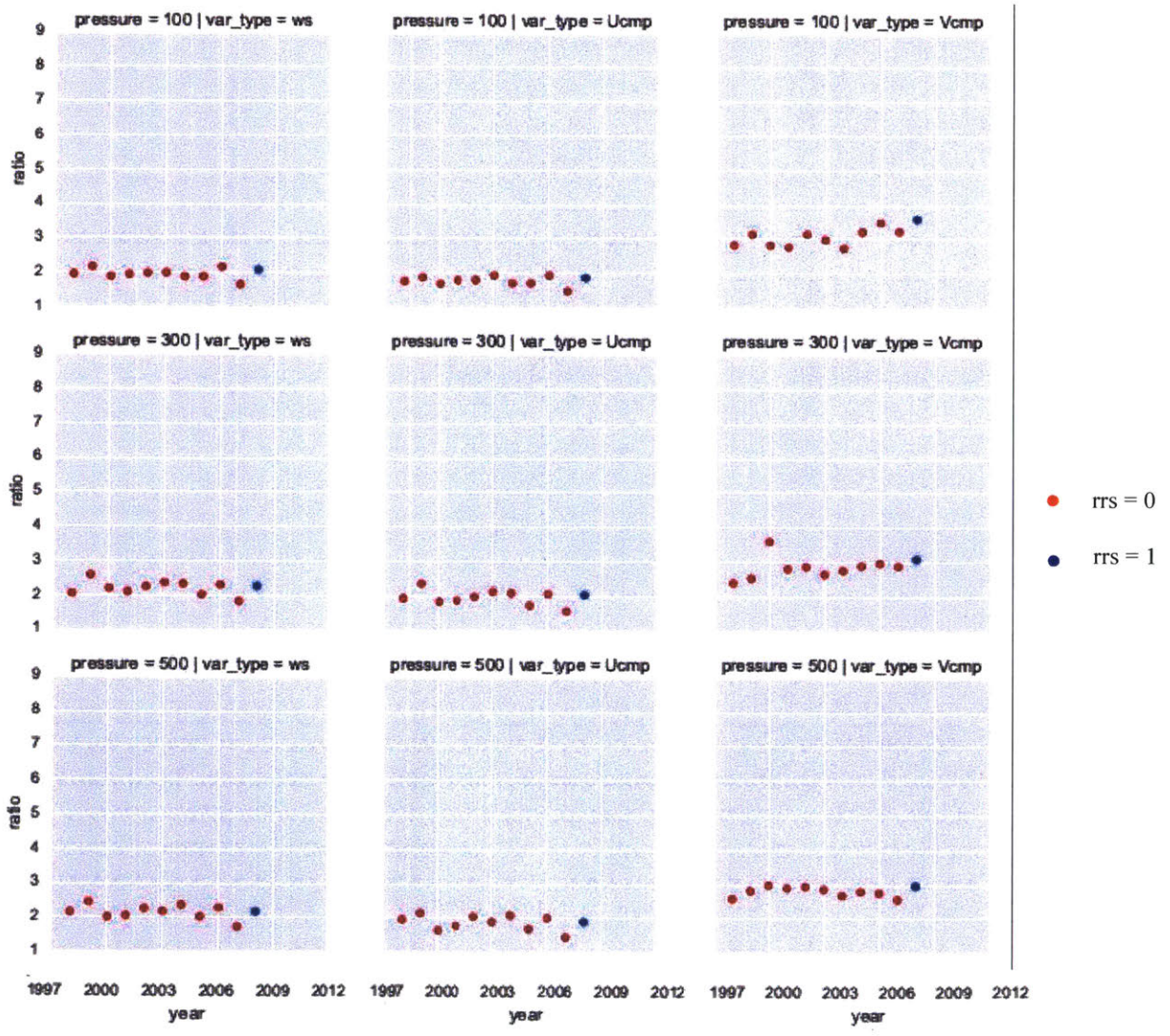

(b) Pressure level: 700hPa, 850hPa, and 1000hPa

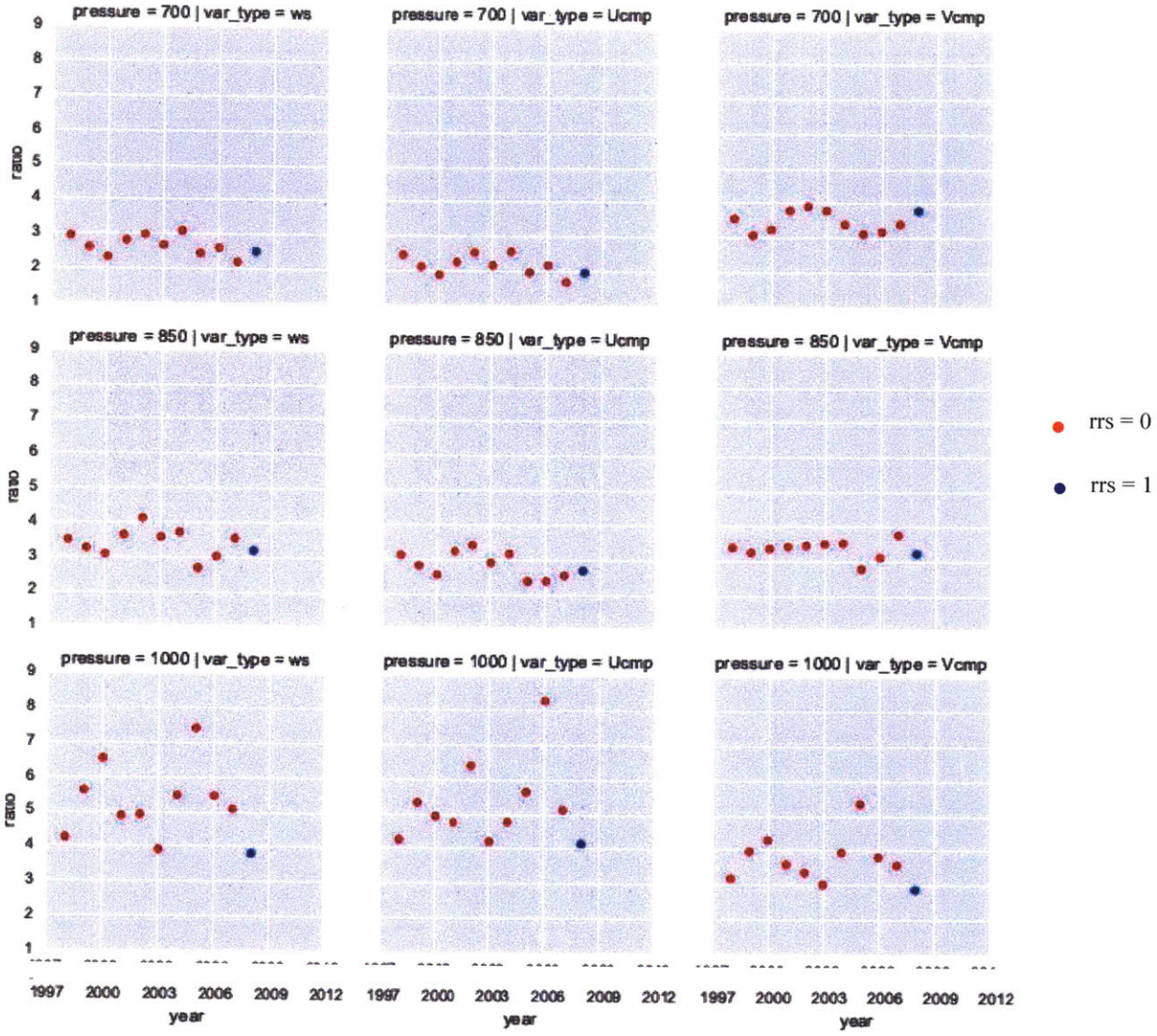

Figure A2: Station Elko, NV. Ratio between annual mean to the corresponding standard deviation of the wind speed data at the selected pressure level. rrs = 0 denotes the ratio corresponding to the 6-second data, and rrs = 1 denotes the ratio corresponding to the 1-second data. The pressure levels are (a) 100hPa, 300 hPa, and 500 hPa; and (b) 700 hPa, 850 hPa and 1000 hPa.

A3 Spatial distribution of the trends in wind speed

As discussed in section 3.4, the trends in wind speed averaged vertical over 200m, 500m, 900m, and 1500m at 12 UTC, are similar to that at 0 UTC (shown in **Figure 3-22**). The results corresponding to 12 UTC are shown in **Figure A3**.

(a) Averaged over 200m above the surface

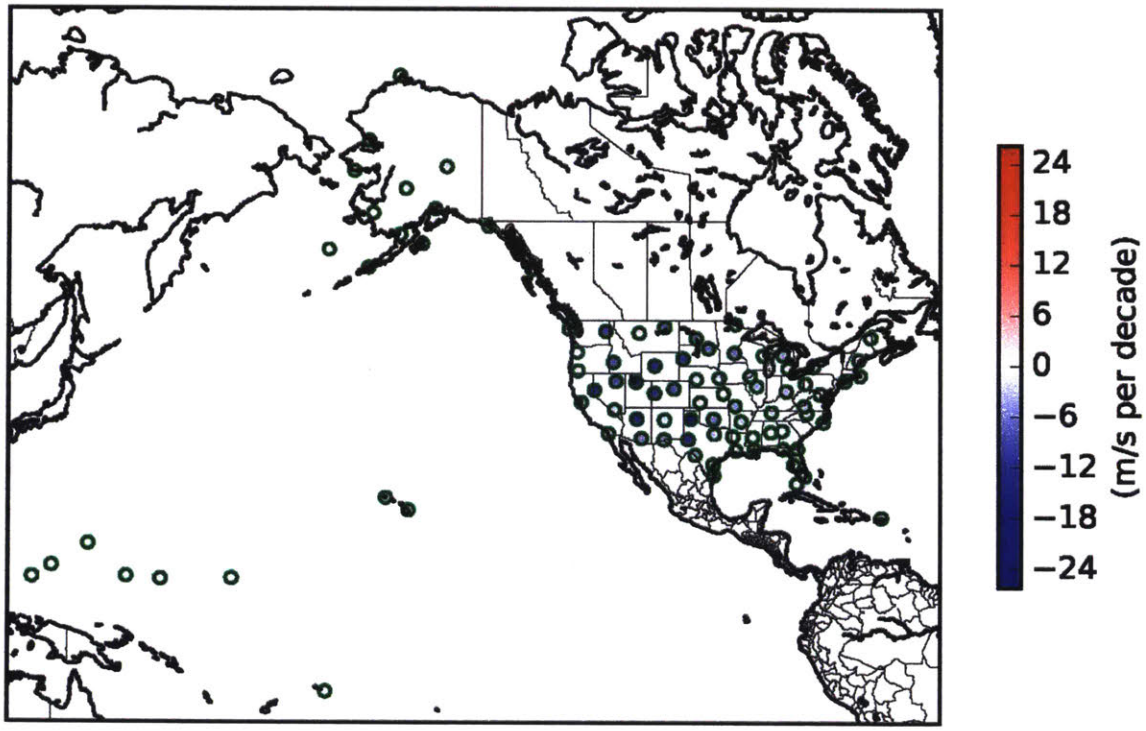

(b) Averaged over 500m above the surface

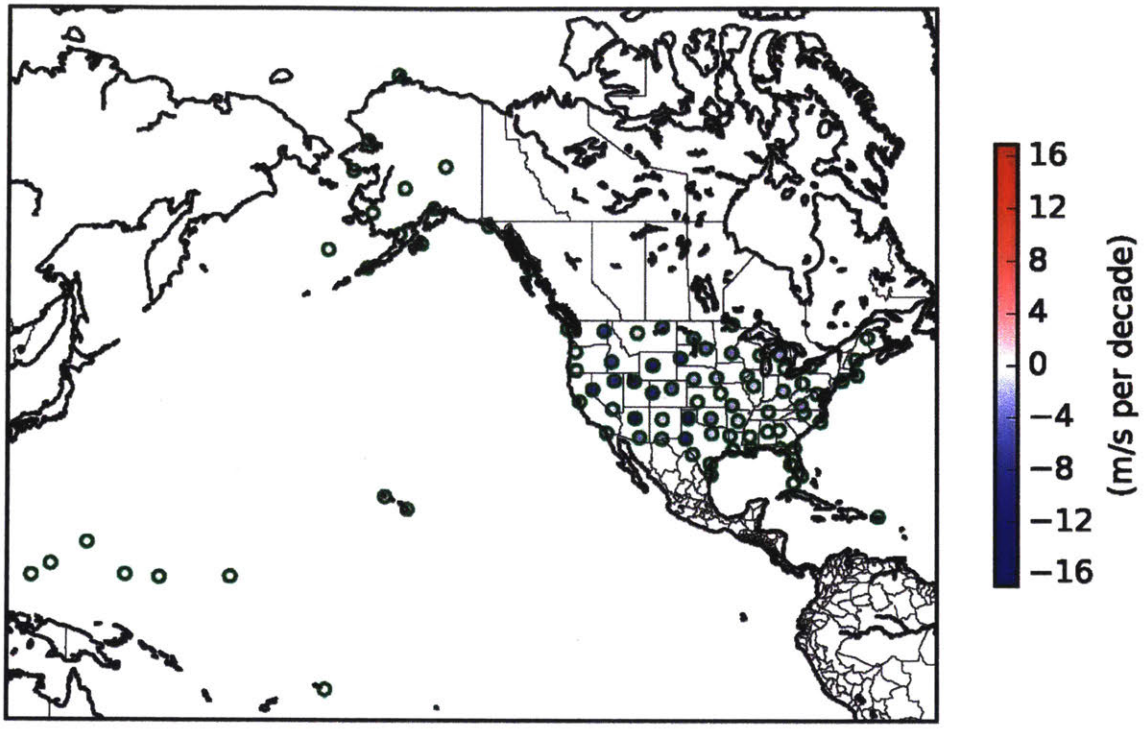

(c) Averaged over 900m above the surface

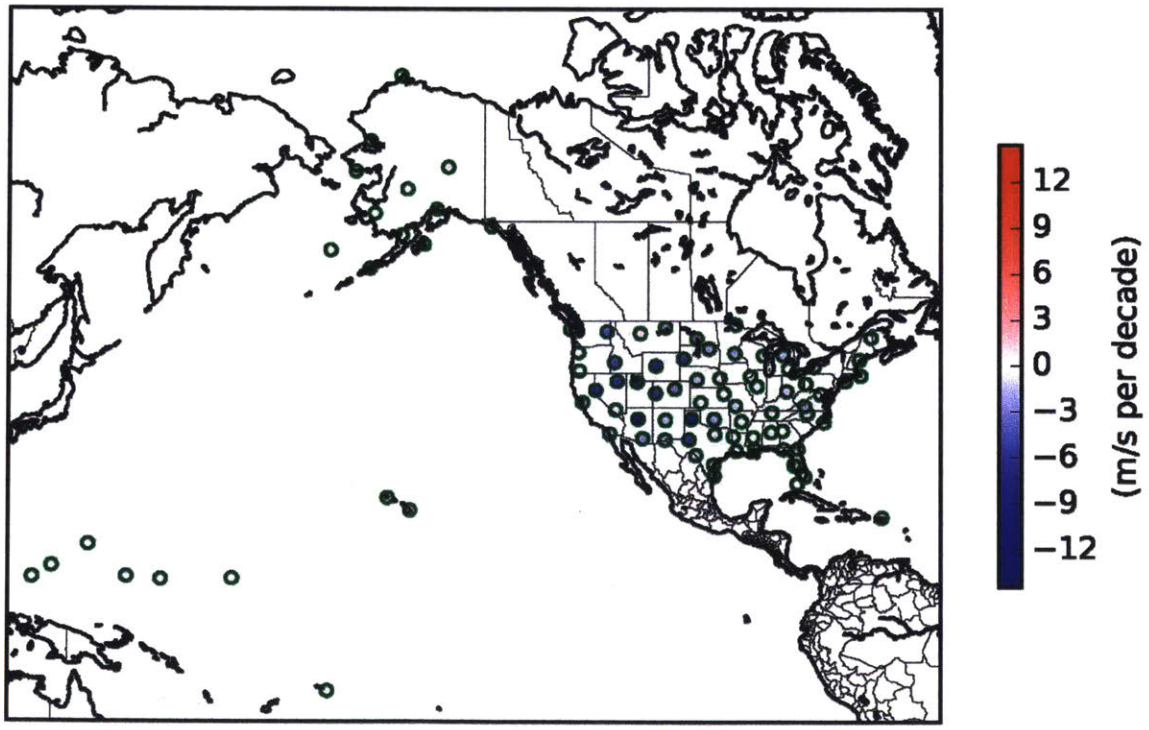

(d) Averaged over 1500m above the surface

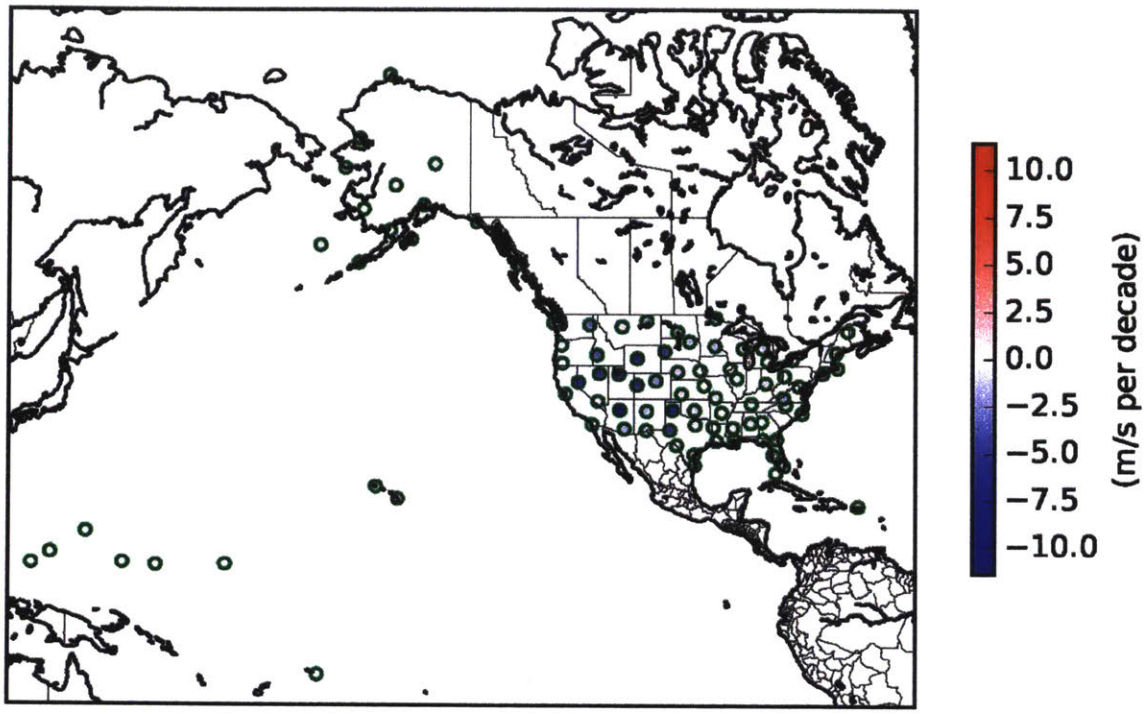

Figure A3: Spatial distribution of the trend in wind speed (m/s per decade) at 12 UTC averaged vertically over (a) 200m, (b) 500m, (c) 900m, and (d) 1500m above the surface of each station.

A 4 Spatial distribution of the trend index

In order to visualize the spatial distribution of the wind speed trend aloft, we calculate the fraction of layers with decreasing trend in all vertical layers above the surface[1], as a trend index between 0 and 1. Trend index equaling to 0 means that there is no vertical layers showing a decreasing trend, and trend index equaling to 1 means that all vertical layers show a decreasing trend. We also evaluate this trend index at different statistical significance and calculate the fraction of layers with statistically significant decreasing trend in terms of 90% confidence level (90% CI), 95% confidence level (95% CI), and 99% confidence level (99% CI).

Figure A4-1 (a) shows the spatial distribution of the trend index at 00:00 UTC. The spatial distribution of the trend index at 12:00 UTC is almost identical to that at 00:00. It suggests that the sites that contains smaller fraction of vertical layers with decreasing trend are concentrated in the eastern part of the US. Sites in the western US especially those located in the mountainous region contain a much larger fraction of layers with decreasing trend. **Figure A4-1 (b) – (d)** show the spatial distribution of the sites that contain vertical layers with statistically significant decreasing trend. We found that the fraction of layers with statistically significant decreasing trend decreases with the increase in confidence level, however, the sites located in the mountainous region still have higher fraction of layers with decreasing trend than those in eastern US, especially for Flagstaff (AZ) and Reno (NV).

Figure A4-2 shows the relations between the trend index corresponding to 90% CI, 95% CI, and 99% CI with elevation of the station. It suggests that the trend index corresponding to 90% CI, 95% CI, and 99% CI are all positively associated with the elevation of the stations and the positive associations are statistically significant (the band of the fitted curve represents 95% confidence interval of the slope). This relation indicates that stations with higher elevation are accompanied with more vertical layers with statistically significant decreasing trend. This finding is in support of the preceding elevation-dependent of relation.

To further detect if this elevation-dependence is a result of surface influence e.g. changes in land roughness, we calculate the trend index for the layers below the nocturnal PBL height

[1] There are 451 vertical layers in the pressure coordinate system, and 500 layers in the A.G.L. system. For details, refer to the supplementary materials.

and that above PBL height. Here we use the nocturnal PBL height calculated based on the bulk *Ri* method because it represents the influence of surface friction on wind as discussed above. Comparing between **Figure A4-3 (a)** and **(b)**, we found that the fraction of decreasing trending layers does not change much between above and below PBL for the mountainous sites. In contrast, this fraction drops to close 0 for the non-elevated sites. The fraction in terms of 90% statistical significance shows similar pattern (see **Figure A4-3 (c)** and **(d)**). This comparison suggests a distinct difference between elevated sites and non-elevated sites. For non-elevated sites such as those located in the eastern region of US, the decreasing trend mainly occurs in the (nocturnal) boundary layer, while layers aloft do not show significant decreasing trend. This difference indicates that the decreasing trend of near-surface winds can be mainly attributed to the effect of land surface e.g. increases in land roughness. For elevated sites such as those located in the mountainous region of US, the decreasing trend occurs for both PBL and layers aloft.

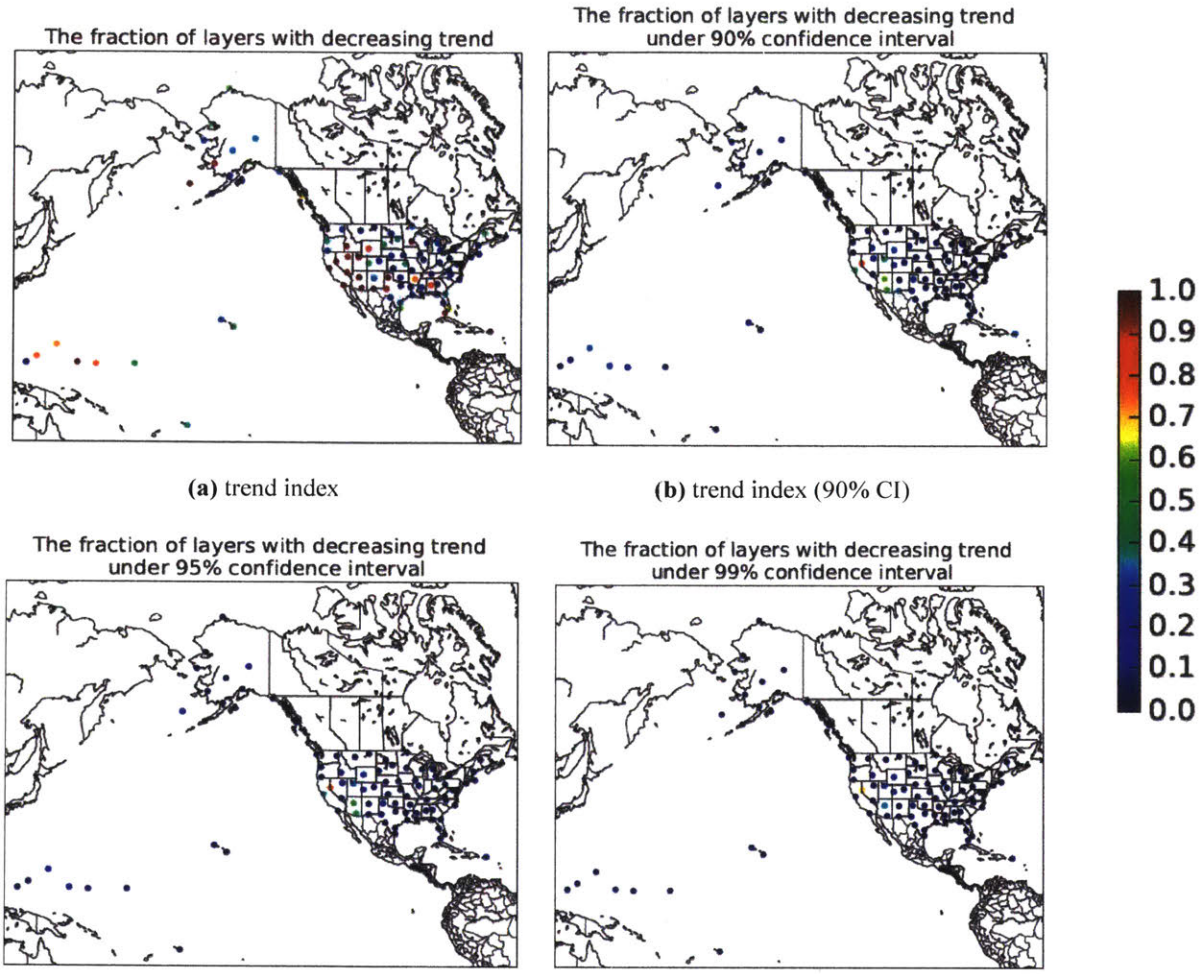

(a) trend index

(b) trend index (90% CI)

(c) trend index (95% CI)

(d) trend index (99% CI)

Figure A4-1 Trend index at 00:00 UTC

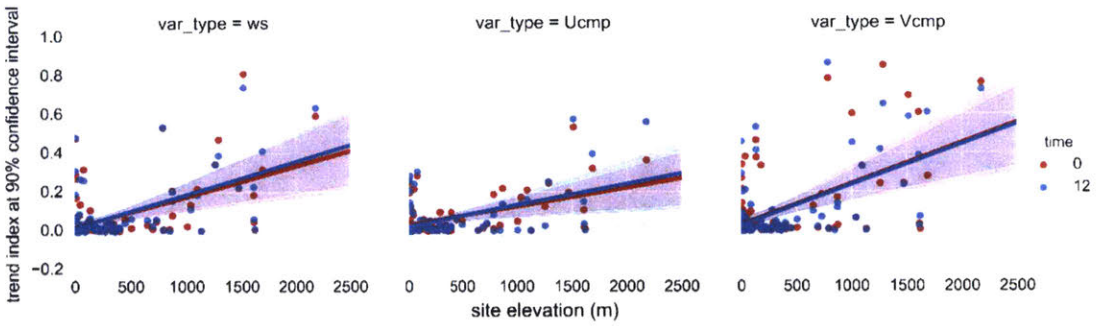

(a) trend index corresponding to the fraction of layers with statistically significant decreasing trend at 90% CI

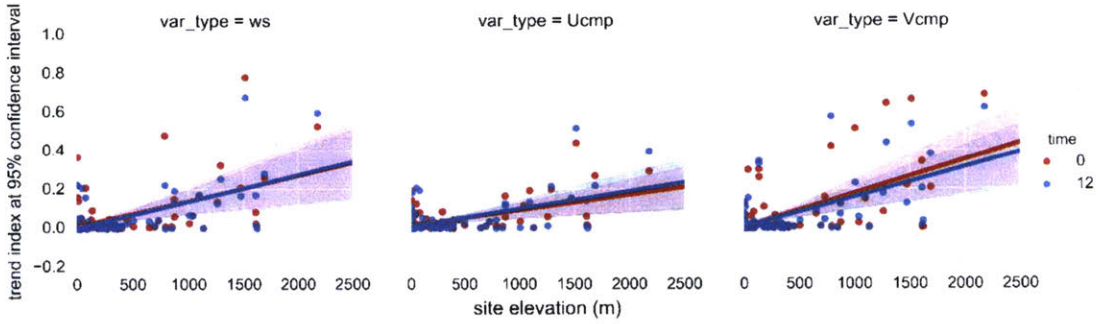

(b) trend index corresponding to the fraction of layers with statistically significant decreasing trend at 95% CI

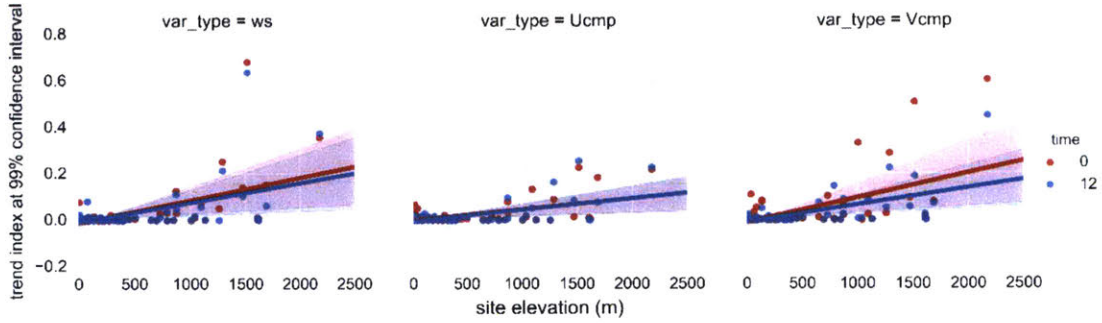

(c) trend index corresponding to the fraction of layers with statistically significant decreasing trend at 99% CI

Figure A4-2 Relations between the trend index and the elevation of stations (the band of the fitted curve represents the 95% confidence interval of the slope)

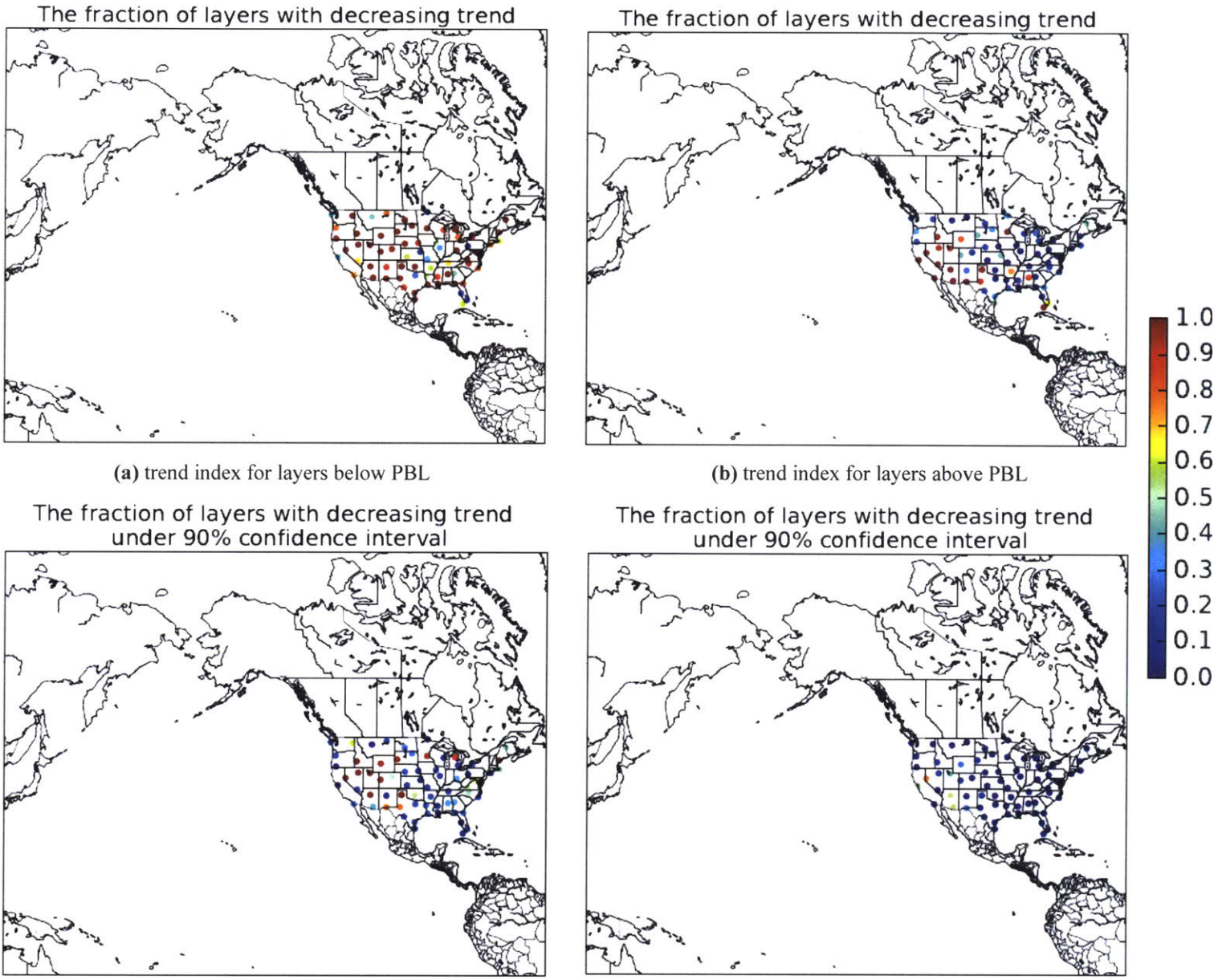

(a) trend index for layers below PBL

(b) trend index for layers above PBL

(c) trend index(90% CI) for layers below PBL

(d) trend index (90% CI) for layers below PBL

Figure A4-3 Trend index for layers below PBL and layers above PBL

Bibliography

Cardone V J, Greenwood J G, Cane M A. On trends in historical marine wind data [J]. Journal of Climate, 1990, 3(1): 113-127.

Coumou D, Lehmann J, Beckmann J. The weakening summer circulation in the Northern Hemisphere mid-latitudes [J]. Science, 2015, 348(6232): 324-327.

Flohn H, Kapala A. Changes of tropical sea-air interaction processes over a 30-year period [J]. Nature, 1989, 338(6212): 244-246.

Griffin B J, Kohfeld K E, Cooper A B, et al. Importance of location for describing typical and extreme wind speed behavior [J]. Geophysical Research Letters, 2010, 37(22).

Guo, X., Wang, L., Tian, L., & Li, X. Elevation - dependent reductions in wind speed over and around the Tibetan Plateau[J]. International Journal of Climatology [J], 2017, 37(2), 1117-1126.

Guo S, Hu M, Zamora M L, et al. Elucidating severe urban haze formation in China[J]. Proceedings of the National Academy of Sciences, 2014, 111(49): 17373-17378.

Liang X, Zou T, Guo B, et al. Assessing Beijing's PM2. 5 pollution: severity, weather impact, APEC and winter heating[C]//Proc. R. Soc. A. The Royal Society, 2015, 471(2182): 20150257.

Lin, Changgui, et al. Observed coherent trends of surface and upper-air wind speed over China since 1960 [J]. Journal of Climate, 2013, 26(9): 2891-2903.

McVicar T R, Roderick M L, Donohue R J, et al. Global review and synthesis of trends in observed terrestrial near-surface wind speeds: Implications for evaporation [J]. Journal of Hydrology, 2012, 416: 182-205.

McVicar, Tim R., et al. Observational evidence from two mountainous regions that near - surface wind speeds are declining more rapidly at higher elevations than lower elevations: 1960–2006 [J]. Geophysical Research Letters, 2010, 37(6).

McVicar T R, Van Niel T G, Li L T, et al. Wind speed climatology and trends for Australia, 1975–2006: Capturing the stilling phenomenon and comparison with near - surface reanalysis output [J]. Geophysical Research Letters, 2008, 35(20)

Pryor S C, Barthelmie R J, Young D T, et al. Wind speed trends over the contiguous United States [J]. Journal of Geophysical Research: Atmospheres, 2009, 114(D14).

Roderick M L, Rotstayn L D, Farquhar G D, et al. On the attribution of changing pan evaporation [J]. Geophysical research letters, 2007, 34(17).

Seidel, Dian J., et al. Climatology of the planetary boundary layer over the continental United States and Europe [J]. Journal of Geophysical Research: Atmospheres, 2012, 117(D17).

Seidel, Dian J., Chi O. Ao, and Kun Li. Estimating climatological planetary boundary layer heights from radiosonde observations: Comparison of methods and uncertainty analysis [J]. Journal of Geophysical Research: Atmospheres, 2010, 115(D16).

Smits, A. A. K. T., A. M. G. Klein Tank, and G. P. Können. Trends in storminess over the Netherlands, 1962–2002 [J]. International Journal of Climatology, 2005, 25(10): 1331-1344.

Thomas B R, Kent E C, Swail V R, et al. Trends in ship wind speeds adjusted for observation method and height [J]. International Journal of Climatology, 2008, 28(6): 747-763.

Verkaik, J. W. Evaluation of two gustiness models for exposure correction calculations [J]. Journal of Applied Meteorology, 2000, 39(9): 1613-1626.

Vautard, R., Cattiaux, J., Yiou, P., Thépaut, J. N., & Ciais, P. Northern Hemisphere atmospheric stilling partly attributed to an increase in surface roughness [J]. Nature geoscience, 3(11): 756,

Vogelezang, D. HP, and A. AM Holtslag. Evaluation and model impacts of alternative boundary-layer height formulations [J]. Boundary-Layer Meteorology, 1996, 81(3): 245-269.

Wang, Ling, and Marvin A. Geller. Morphology of gravity - wave energy as observed from 4 years (1998–2001) of high vertical resolution US radiosonde data [J]. Journal of Geophysical Research: Atmospheres, 2003, 108(D16).

Wu Z, Hu M, Liu S, et al. New particle formation in Beijing, China: Statistical analysis of a 1 - year data set[J]. Journal of Geophysical Research: Atmospheres, 2007, 112(D9).

Xu M, Chang C P, Fu C, et al. Steady decline of east Asian monsoon winds, 1969–2000: Evidence from direct ground measurements of wind speed [J]. Journal of Geophysical Research: Atmospheres, 2006, 111(D24).

Young I R, Zieger S, Babanin A V. Global trends in wind speed and wave height [J]. Science, 2011, 332(6028): 451-455.